Molecular and cellular mechanisms of collagen degradation in the foreign body reaction

Ye, Qingsong

Molecular and cellular mechanisms of collagen degradation in the foreign body reaction

Qingsong Ye

The research described in this thesis was carried out and supported by:

University Medical Center Groningen (UMCG), Faculty of Medical Sciences, University of Groningen, Stem Cells & Tissue Engineering Group, Section of Medical Biology; Department of Orthodontics, Groningen, The Netherlands.

The print of this thesis is partly sponsored by 3M Unitek

rijksuniversiteit
groningen

Molecular and cellular mechanisms of collagen degradation in the foreign body reaction

ISBN: 978-90-367-6016-4

Lay-out & Cover: I. Harris & Y. He
Printed by Off Page, Amsterdam, NL. www.offpage.nl

rijksuniversiteit
groningen

Molecular and cellular mechanisms of collagen degradation in the foreign body reaction

Proefschrift

ter verkrijging van het doctoraat in de
Medische Wetenschappen
aan de Rijksuniversiteit Groningen
op gezag van de
Rector Magnificus, dr. E. Sterken,
in het openbaar te verdedigen op
woensdag 10 april 2013
om 11.00 uur

door
Qingsong Ye
geboren op 7 maart 1981
te Zhejiang, China

Promotores:	Prof. dr. Y. Ren Prof. dr. R.A. Bank
Beoordelingscommissie:	Prof. dr. ir. H. J. Busscher Prof. dr. G. Molema Prof. dr. R.R.M. Bos

Paranimfen: Drs. Arjen Grotenhuis
Drs. Ee-Soo Lee

CONTENTS

CHAPTER 1

Introduction and scope of the thesis

General introduction

1 Biomaterials in tissue engineering and regenerative medicine

Regenerative medicine is an innovative scientific field in which the problems and problem-solving approaches of clinical medicine are integrated into the natural and engineering sciences. In the broadest sense, regenerative medicine is concerned with the restoration of function to cells, tissues, and organs either by biological replacement, such as with tissues cultured in vitro, or by stimulating the body's own reparative and regenerative mechanisms. The focus of this field extends beyond the replacement of organs and tissues (tissue engineering) to encompass both innovation and advancement in classical transplantation medicine and cell therapy, including stem cell technologies and pharmacological approaches to targeted stimulation of tissue regeneration *in vivo*. The goal of regenerative medicine is to translate research findings into the development and establishment of therapeutic options in clinical medicine.

Due to the morbidity shift over the past few decades, clinical medicine today is increasingly concerned with diseases that bring about a gradual decline in the function of vital cell and organ systems. It is expected that the solutions offered by regenerative medicine to replace destroyed or degenerating tissues with functional substitutes will prove to be the curative therapy that could obviate symptomatic treatment. Regenerative medicine often makes use of implantable biomaterials. The development of successful therapies for regenerative medicine is currently evolving towards the paradigm that the opportunities for biomimetic or bioartificial materials significantly exceed those of existing prosthetic implants. It was a widely held belief that prostheses must be biologically inert, i.e., that they must not interact with the surrounding cells and tissues. Recently, a more advanced view has emerged that is based on the principle of the

construction of materials that most closely imitate the tissue in which they are implanted and that actively interact with cells. Presumably, the materials used in the construction of biomimetic implants must possess proper physical (strength, elasticity, texture, etc.) and chemical (non-inflammatory and non-toxic) characteristics. These materials must furnish the cells with a hospitable environment that provides all of the major signals to direct cell physiology and metabolism to enhance tissue repair.

The progress of biomaterials during the past 50 years can be understood in terms of three different generations: a first generation (bioinert materials), a second generation (bioactive and biodegradable materials), and a third generation (biomaterials designed to stimulate specific cellular responses at the molecular level). It is worth noting that this classification of the materials used for biomedical purposes does not imply that a new generation of materials excludes the use of preceding ones. Indeed, first-generation biomaterials are still successfully used for a wide range of applications.

The progress in biomaterials has resulted from the continuous addition of new demands to the list of required properties. New biomaterials have been developed in response to these demands to address new needs in the field. Concepts such as the foreign body reaction (FBR), stress shielding, biocompatibility, biodegradability, bioactivity and osteoinduction are some of the demands that have guided the search for new biomaterials. In the beginning, the main concern was to develop or select materials that combined the necessary physical properties for the devices in which they were used to match the functionality of the substituted tissue, with minimal toxicity to the host. Consequently, the first generation of biomaterials mainly comprised inert materials.

Inertness reduces the toxicity to the host; however, it does not eliminate the FBR and the formation of a fibrous layer that envelopes the implant or device, thereby preventing direct contact between the surface of the material and the surrounding tissue. Second-generation biomaterials are characterised by the development of materials that overcome the formation of the fibrous layer that hinders the surface/tissue interaction. This goal was achieved by two different means: (a) by

promoting a specific biological response and (b) by using biodegradable materials that progressively degrade as the new tissue is regenerated. This was the generation of "bioactive materials" and "biodegradable materials". Biomaterials developed during the third generation were designed to trigger specific cellular responses at the molecular level. During this generation, the biodegradability and bioactivity concepts were combined to generate biomaterials that were both degradable and bioactive. In addition to these two properties, materials that had the ability to stimulate specific cellular events and behaviours, depending on their final application, were also sought.

Without discounting the advances in the field, the utility and potential application of a biomaterial can be determined only after an assessment of its biocompatibility. The first step in this usually long-term process is the in vitro culturing of the appropriate cells on the surface of the material followed by the assessment of the behaviour of the cells. The capacity of a biomaterial to provide cells with the correct adhesivity and to ensure proliferation and formation of an extracellular matrix (features that are essential for successful implantation in a living organism) is evaluated through diverse cell and molecular biology methods. After a series of *in vitro* assays, a material must also be implanted in vivo to study the performance of the material in the context of the host.

Once a biomaterial is implanted *in vivo*, it directly contacts the physiological environment, which consists of a highly corrosive aqueous medium containing various ions, molecules such as proteins, polysaccharides and enzymes, and different types of cells (non-adherent as well as adherent). The initial events that occur on the surface of biomaterial after implantation will strongly influence the lifespan of the implant.

The cascade of reactions by the host to the implanted material is called the tissue response or FBR. The FBR is essentially an inflammatory response that persists as long as there is a foreign body (implanted material) present. The reaction is characterised by the presence of inflammatory cells, especially macrophages, at the implant surface and a walling-off by a capsule that is arranged parallel to the implant surface. Interactions between implanted materials and the host tissue are of

great importance for the fate of the implanted scaffold. The interactions affect both the healing response and the long-term organisation of the surrounding tissues.

Although a wide variety of biomaterials has been developed for regenerative medicine, few have been systematically investigated with respect to their effect on the FBR. Consequently, we can make few predictions about the fate of a biomaterial once it is implanted into the body. Collagen, a natural polymer, is one biomaterial that is widely used for a variety of applications. Part of our research has focused on the FBR that is elicited by collagen and by gelatin, a collagen derivative.

Collagen is a major component of mammalian connective tissues. Currently, over 20 different types of collagen have been described, among which type-I collagen is the most abundant. Collagen is composed of three polypeptide chains that intertwine to form a triple helix. The polypeptide chains consist of repeated sequences of Gly-X-Y, in which X and Y are most frequently proline and hydroxyproline. The presence of adhesion domains allows collagen to present an attractive surface for cell attachment. Collagen is enzymatically biodegradable and has a tendency to degrade quickly, limiting its mechanical properties. Cross-linking collagen with chemical compounds such as glutaraldehyde or hexamethylenediisocyanate decreases its degradation rate. Gelatin is a collagen derivative acquired by denaturing (via heating) the triple helix structure of collagen into single-stranded molecules. It is water-soluble and entangles easily to form a gel by lowering the denaturation temperature. Gelatin is broken down enzymatically by numerous enzymes (e.g., the gelatinases MMP-2 and MMP-9), whereas native (triple helical) collagen can be degraded by only a few enzymes (e.g., the collagenases MMP-1, MMP-8, MMP-13 and MMP-14, and cathepsin K).

Collagen products are supplied in various physical forms, including powders, solutions, gels, sponges, fibres and membranes. Furthermore, the biodegradability of collagen allows for its replacement by newly synthesised tissue. As a naturally derived scaffolding biomaterial for tissue engineering and regenerative medicine, extensive studies have been conducted on the architecture, surface characteristics and biomechanical properties of collagen scaffolds. However, few studies have been published

on the biodegradability of collagen scaffolds. Therefore, the precise *in vivo* molecular and cellular mechanisms involved in the degradation of implanted collagen scaffolds remain largely unknown.

2 The foreign body reaction to collagen scaffolds

Implantation of any type of medical device or tissue-engineered construct, including collagen scaffolds, will provoke an inflammatory reaction known as the FBR. The FBR is a complex interaction between the host and the implanted biomaterial. Our previous studies have shown that, with respect to collagen scaffolds, the FBR depends on the physicochemical state of the scaffold, the animal species, and the location where the collagen scaffold is implanted, among other factors. A short overview of our previous findings follows.

- ***The FBR is biomaterial-dependent***

  The FBR to different types of biomaterials, including the non-degradable biomaterial Dacron, the synthetic biomaterial PCLdiUPy and hexamethylenediisocyanate cross-linked dermal sheep collagen (HDSC), has been previously investigated in rats. These three biomaterials exhibited completely different types of tissue responses with respect to the morphology and biological behaviours of foreign body giant cells (fused macrophages), which play a crucial role in the FBR. For Dacron, small giant cells (with 3-7 nuclei) formed and surrounded the Dacron fibres. For PCLdiUPy, the biomaterial was degraded by phagocytosis by giant cells, which were large with a regular shape (with greater than 10 nuclei). In HDSC, degradation occurred in association with the formation of large and irregular giant cells (with greater than 10 nuclei), which engulfed and phagocytosed the HDSC

bundles. These observations indicate that the giant cells in the FBR may differ depending on the implanted biomaterial.

- ***The FBR is species-dependent***

Previous studies have shown that the FBR differs between species. HDSC disks were implanted subcutaneously in fiverat strains (AO, BN, F344, LEW and PVG) and three mouse strains (129 SVEV, BALB/c and C57BL/6), which resulted in distinct tissue responses towards the implanted biomaterial between mice and rats, but only negligible differences were observed among strains within the same species. Mice showed a less pronounced inflammatory response than rats towards the implant.

- ***The FBR is implantation site-dependent***

Although no significant differences exist in the FBR to subcutaneously implanted collagen among mouse strains, it has been noted that the FBR does differ markedly between subcutaneous and epicardial implantation of collagen scaffolds in mice. The activity of matrix metalloproteinases, a family of enzymes that is strongly correlated with collagen degradation, was high in epicardial implants and low or nearly absent in subcutaneous implants. As a result, the collagen disks were degraded epicardially within 4 weeks, whereas subcutaneous implants remained largely intact.

- ***Intracellular and/or extracellular degradation of collagen***

There are two major pathways for collagen degradation: (a) phagocytosis of collagen bundles by surrounding inflammatory cells, i.e., macrophages and giant cells (fused macrophages), and (b) enzymatic degradation by secreted enzymes such as matrix metalloproteinases (MMPs). We previously showed that in rats, subcutaneously implanted collagen disks were degraded via phagocytosis by giant cells. Despite the presence of giant cells

in subcutaneous collagen implants in mice, phagocytosis was not observed. In contrast, when the same collagen disks were epicardially implanted in mice, they were degraded rapidly through the enzymatic degradation pathway (MMP activity). The exact cellular and molecular mechanisms underlying this phenomenon are not fully understood.

3 The FBR MICRO-ENVIRONMENT

The FBR involves a complex cascade of spatiotemporally regulated and interconnected processes, including infiltration and activation of inflammatory cells, angiogenesis, enzymatic activity and phagocytosis, which ultimately resolves after the degradation of scaffolds.

During the FBR, neutrophils are the first cells that arrive at the implant site and produce chemokines, including CCL2/MCP-1 and CCL3/MIP-1α, which are macrophage chemoattractants. Normally, neutrophils disappear quickly after the recruitment of macrophages. However, we have previously shown that the degradation of collagen disks implanted epicardially correlates with the presence of a second wave of neutrophils, which suggests that neutrophils may play an important role in the degradation of collagen scaffolds. Generally, there are two ways to activate the recruited macrophages depending on the different mediators present in the micro-environment. In the presence of pro-inflammatory IFN-γ, macrophages are activated in a classical way. The classically activated macrophages (M1 macrophages) promote the expression of MMPs and pro-inflammatory cytokines such as IL-1 and IL-6 but reduce the expression of TIMPs and anti-inflammatory factors such as IL-10 and TGF-β. In contrast, in the presence of IL-4 and/or IL-13, alternatively activated macrophages (M2 macrophages) are generated. M2 macrophages can upregulate TIMPs and anti-inflammatory cytokines and downregulate MMPs and pro-inflammatory factors (Lacraz et al. 1995). In addition, IL-4 and IL-13 are also involved in the fusion of macrophages into giant cells *in vitro*. The roles of lymphocytes and

fibroblasts (primarily located in the capsules of implants) in the FBR are unclear.

In general, chemokines (e.g., MIP-1α and MCP-1) are involved in the recruitment of inflammatory macrophages, and cytokines (e.g., IL-1, IL-4, IL-6, IL-10, IL-13, IFN-γ and TGF-β) determine the behaviours of macrophages through different pathways of activation. The cytokines IL-4 and IL-13 can induce multiple fusogenic effects and result in membrane fusion and giant cell formation. However, it is unknown whether these general principles regarding the roles of these inflammatory mediators, which are mostly derived from wound-healing studies, are also applicable to the particular situation described in this thesis, i.e., the FBR to a collagen scaffold.

Cell-matrix interactions rely on cell surface receptors that bridge the signal exchange between the intercellular and extracellular environment. In the context of collagen scaffolds, in addition to the well-known integrins that act with collagen (α1β1, α2β1, α10β1 and α11β1), several other types of collagen receptors may play an important role in the cell-matrix interaction in the tissue response towards collagen scaffolds. These collagen receptors include mannose receptors (Endo180, PLA2R and MR), discoidin domain receptors (DDR-1 and DDR-2) and the leukocyte-associated IG-like receptor (LAIR-1). The collagen receptor Endo180 binds a range of collagens and gelatin via its fibronectin type-II-like domain. After it binds to Endo180, collagen is efficiently internalised and transported to lysosomal compartments for degradation (Rivera-Calzada et al., 2003). Discoidin domain receptor 2 (DDR-2) is expressed on a wide range of adult cells, including fibroblasts and smooth muscle cells, and is involved in activating many biological processes, such as the expression of MMP-13. Thus far, nothing is known about the role of the collagen receptors Endo180 and DDR-2 in the FBR to collagen implants.

Scope of this thesis

The mechanisms involved in the degradation of collagen scaffolds during the FBR are not well characterised. A better understanding of these mechanisms is a prerequisite for modulating the rate of collagen scaffold degradation (to match the degradation rate to tissue regeneration). The overall objective of this thesis is to gain further insight into the molecular and cellular mechanisms of the degradation of collagen scaffolds and to provide indications and clues to improve future therapies in regenerative medicine in which the regulated degradation of collagen scaffolds is required. In pursuit of this overall objective, this thesis will focus on the following four sub-objectives:

Sub-objective 1: To gain further insight into the roles of proteinases in the degradation of collagen scaffolds.

a) To reveal the roles of the MMP/TIMP proteolytic network in the degradation of the collagen scaffold and its regulatory mechanisms;
b) To investigate the involvement of cathepsin K in collagen degradation.

Sub-objective 2: To gain further insight into the roles of infiltrating inflammatory cells during the degradation of collagen scaffolds.

a) To study the roles of neutrophils, macrophages and giant cells in the FBR to the collagen scaffold;
b) To characterise the mechanisms of phagocytosis and the different sub-types of macrophages/giant cells in the FBR.

Sub-objective 3: To gain further insight into the correlation

between the micro-environment and the degradation of collagen scaffolds.

a) To study the involvement of cytokines (IL-4, IL-10, IL-13, TNF-α and IFN-β) and chemokines (CCL-2 and CCL-3) in the regulation of proteolytic activities and cellular phagocytosis;
b) To study the involvement of collagen receptors (Endo180 and DDR-2) in the degradation of collagen scaffolds.

Sub-objective 4: To gain further insight into the correlation of the physical status or chemical cross-linking of collagen scaffolds and their degradation.

a) To study the differences in the FBR to different chemically cross-linked collagen scaffolds;
b) To study the differences in the FBR to different physical forms of collagen scaffolds (native or gelatin).

The following experimental models have been established to facilitate the aforementioned investigation of the molecular and cellular mechanisms of degradation of the collagen scaffold in the FBR:

1) The following collagen disks with different chemical and physical properties were implanted in experimental animals:

Chemical status:
- Non-cross-linked dermal sheep collagen (NDSC);
- Glutaraldehyde cross-linked dermal sheep collagen (GDSC);
- Hexamethylenediisocyanate cross-linked DSC (HDSC);
- Hexamethylenediisocyanate cross-linked bovine type-I collagen (Col-I).

Physical status:
- Non-cross-linked dermal sheep collagen (NDSC);
- Non-cross-linked gelatin.

2) The following experimental models were used (Figure 1.1.):
In vivo animal models: Male C57BL/6 mice (Harlan, Horst, The Netherlands)
- Subcutaneous implantation;
- Supra-epicardial implantation.

In vitro experiments: culture of the murine monocyte/macrophage cell line RAW 264.7 on plates or wells with or without a collagen coating in the presence of different cytokines (IFN-γ, IFN-γ + IL-10, IL-1β or TNF-α) (Figure 1.2).

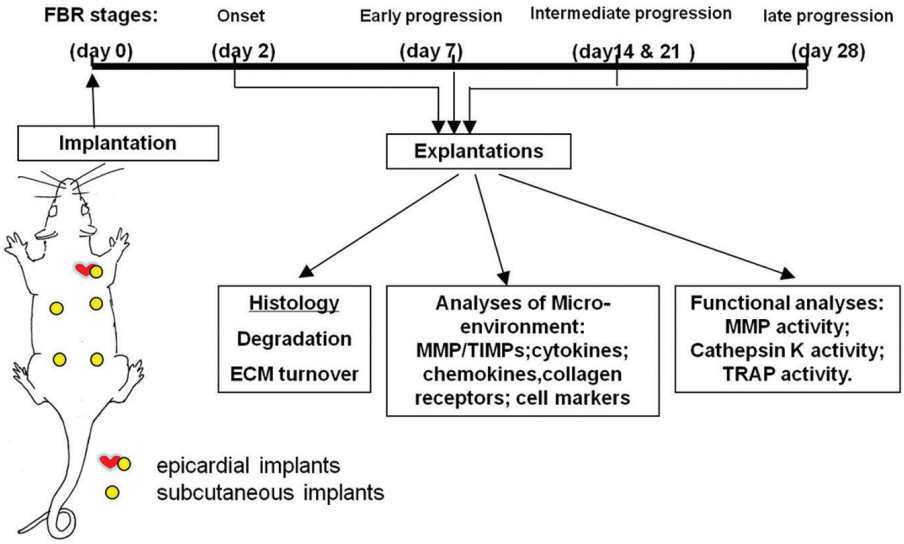

Figure 1.1: Schematic illustration of the design of animal experiments (ECM: extracellular matrix; MMP: matrix mattelloproteinase; TIMP: tissue inhibitor of mattelloproteinase; TRAP: tartrate-resistant acid phosphate)

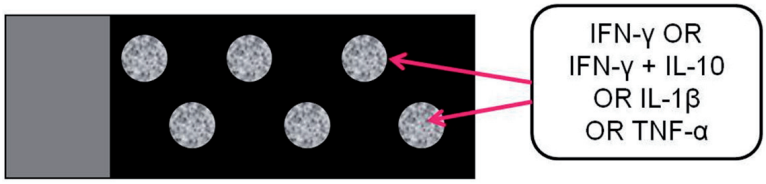

Figure 1.2: Schematic illustration of the design of ***in vitro*** experiments (culture on plates)

CHAPTER 2

Site-specific tissue inhibitor of metalloproteinase-1 governs the matrix metalloproteinases-dependent degradation of crosslinked collagen scaffolds and is correlated with interleukin-10

Qingsong Ye [1,2]
Machteld J. van Amerongen [1]
Andrew Sandham [3]
Ruud A. Bank [1]
Marja J. A. van Luyn [1]
Martin C. Harmsen [1]

[1] Stem Cell and Tissue Engineering Research Group, Department of Pathology and Medical Biology, University of Groningen, The Netherlands

[2] Department of Orthodontics, University Medical Centre Groningen, University of Groningen, The Netherlands

[3] School of Medicine and Dentistry, James Cook University, Cairns, Australia

J Tissue Eng Regen Med 2011; 5: 264-274

Abstract

We have previously shown that the foreign body reaction (FBR) against crosslinked collagen type I (Col-I) differs between subcutaneous and epicardial implantation sites; Col-I was quickly degraded epicardially, whereas degradation was attenuated subcutaneously. The current study set out to dissect the nature and regulation of the MMP-based degradation of implanted Col-I in mice during the FBR. Immunohistochemistry showed that MMP-2, MMP-8 and MMP-13 were present in subcutaneous and epicardial implants, whereas only MMP-9 was also present epicardially. Western blotting showed that MMP-8 and MMP-9 were mainly present in their inactive proform. In contrast, collagenase MMP-13 and gelatinase MMP-2 were the predominant active MMPs at both sites. Interestingly, the major MMP inhibitor TIMP-1 was solely observed in subcutaneous implants, which is why MMP-13 and MMP-2 are not able to degrade the collagen scaffold at the subcutaneous implantation site. Interleukin 10 (IL-10), a potent inducer of TIMP-1 expression, was also mainly detected subcutaneously; giant cells were the main source. Therefore, we surmise that IL-10, through regulation of the balance between MMPs and TIMP-1, suppresses the FBR against implanted biomaterials. Together, our findings would provide cues and clues to improve future therapies in regenerative medicine that are based on the tuned regulation of the degradation of biomaterial scaffolds.

1. Introduction

Tissue engineering is a promising discipline that aims at the functional regeneration of damaged or otherwise impaired tissues and organs (Paquette *et al*., 2004; Rivron *et al*., 2008). In this approach, biomaterial scaffolds are often applied to provide transient support and instruction to achieve functional regeneration (Hedrick and Daniels, 2003; Mather *et al*., 2007; Mason, 2007; Petersen and Niklason, 2007; Munirah *et al*., 2008). An ideal scaffold should feature the right porosity, appropriate surface chemistry, suitable mechanical properties and, above all, proper biocompatibility and controllable biodegradability (Hutmacher *et al*., 2001; Tai *et al*., 2007). As a naturally derived scaffold in tissue engineering, collagen has been frequently studied (Cummings *et al*., 2004; Daamen *et al*., 2005; Sachlos *et al*., 2006; Wahl *et al*., 2007). The majority of studies focus on the threedimensional (3D) architecture, surface characteristics and biomechanical properties of collagen scaffolds (Sachlos and Czernuszka, 2003; Sachlos *et al*., 2006), while few studies engage in the in vivo molecular and cellular mechanism of collagen scaffold degradation (Khouw *et al*., 1998, 2000; Luttikhuizen *et al*., 2007). In general, the degradation of collagen is influenced by a number of related proteolytic pathways, such as MMPs, ADAMs, serine proteinases and cysteine proteinases (Brinckerhoff and Matrisian, 2002; Jones and Riley, 2005; Mohamed and Sloane, 2006). Our previous studies showed that the degradation of crosslinked collagen type I (Col-I) in mice relies on the activity of matrix metalloproteinases (MMPs) (van Amerongen et al., 2006; Luttikhuizen et al., 2006b), yet the precise molecular nature and regulation of the MMP-based proteolytic network in the degradation process remains largely unknown.

MMPs participate in the physiological turnover of the extracellular matrix (ECM) through degradation of its major components, including collagens. Thus, MMPs are also actively involved in the regulation of many general (patho)physiological processes, such as wound healing,

immunity, cancer and inflammation (Nagase and Woessner, 1999; Kyriakides and Bornstein, 2003). In tissue-engineered biomaterial implants, such as collagen type I, inflammation and scaffold degradation are orchestrated by the foreign body reaction (FBR) (Kyriakides *et al*., 2004; Luttikhuizen *et al*., 2006a). Collagen type I is also one of the major constituents of ECM. In general, degradation of collagen is achieved by the interplay between active collagenases and active gelatinases (Nagase and Woessner, 1999; Brinckerhoff and Matrisian, 2002). The first step of the degradation of collagen is cleavage of its triple helix by collagenases (MMP-8 and -13 in mice). Next, the cleaved collagen spontaneously denatures into gelatin at body temperature. Gelatinases (MMP-2 and -9) further degrade the gelatin into breakdown products that are easily disposed of by the lymphatic system (Brinckerhoff and Matrisian, 2002).

Cardiac tissue engineering requires the application of biomaterials on or in themyocardium. By themselves, biomaterials affect wound-healing processes, as they induce a FBR (van Amerongen *et al*., 2006). Generally, the FBR is assessed through subcutaneous implantation in rodents, but we noted that the FBR differs markedly between subcutaneous and epicardial implantation (Luttikhuizen *et al*., 2006b). We observed that the subcutaneously implanted scaffolds remained largely intact after 4 weeks, and that the MMP activity was low or nearly absent. In contrast, epicardially implanted Col-I scaffolds were degraded within 4 weeks, associated with high MMP activity that co-localized with the presence of collagenase MMP-8. Furthermore, gene expression of gelatinase MMP-9 was upregulated in epicardial Col-I implants but absent in subcutaneous Col-I implants (van Amerongen *et al*., 2006; Luttikhuizen *et al*., 2006b). This observation led us to reason that MMP-8 and MMP-9 were responsible for the degradation of Col-I during the FBR in mice. However, in our previous studies we did not measure the molecular variants of MMP-8 and MMP-9 (latent or activated) or the other MMPs, neither were the tissue inhibitors of MMP (TIMP) protein expression dynamics determined. We postulate that the difference in the degradation in subcutaneous and epicardial Col-I implants is due to the tissue-specific MMP-based proteolytic microenvironment. Additionally, it has been shown that the expression of MMPs and their inhibitors

TIMPs is strongly regulated by inflammatory mediators, of which the immunosuppressive cytokine IL-10 is a key player (Lacraz *et al*., 1995; Sternlicht and Werb, 2001). Thus, we also investigated the correlation between MMP proteolytic activity and IL-10.

The above findings have consequences for the development of cardiac tissue-engineering constructs. Our study set out to perform a fundamental investigation on the MMP-based proteolytic degradation of a model scaffold, i.e. crosslinked collagen, epicardially and subcutaneously.

2. Materials and methods

2.1 Animals and scaffolds

Male C57BL/6 mice (10 weeks old; Harlan, Horst, the Netherlands) were housed individually under standard conditions with food and water ad libitum. A hexamethylenediisocyanate-crosslinked, degradable, bovine collagen type I matrix (Biomaterial Research, Vaals, The Netherlands) was used in the experiment and is referred to as Col-I. The Col-I disks were punched at 6 mm in diameter and 0.75 mm in thickness and then sterilized with ethylene oxide (ETO). The LAL method (Cambrex, LAL kinetic-QCL®) was used to measure the endotoxin content of the Col-I disks. Endotoxin levels were <0.25 EU/ml.

2.2 Surgical procedures

All procedures performed on animals were approved by the local committee for care and use of laboratory animals of the University of Groningen and were performed according to international and governmental guidelines on animal experimentation and also in line with the *Ethical Principles and Guidelines for Scientific Experiments on Animals of the Swiss Academy of Medical Sciences.*

2.2.1 Implantation

The Col-I disks were implanted following a standard procedure, as described previously (Luttikhuizen *et al*., 2006b). Briefly, the mice were anaesthetized with 4% isoflurane and maintained by 2% isoflurane inhalation in combination with a mixture of equal volumes of N2O and O2. For the subcutaneous implantations, the back was shaved and disinfected. The scaffolds were implanted in subcutaneous pockets 1

cm away from the incision site, minimizing the effect of wound healing on the inflammatory reaction. For epicardial implantations, the mice were intubated and ventilated with anaesthetics in combination with subcutaneous injections of the analgesic drug buprenorfine (0.03 mg/kg). The heart was exposed via a left lateral thoracotomy. A Col-I disk was sutured onto the left ventricular epicardium with one suture (6- 0 non-absorbable Prolene suture) in the middle of the Col-I disk. From our previous work (van Amerongen *et al*., 2006), we noted that the suture is immediately encapsulated by a few layers of fibroblasts. As a result, the suture does not participate or interfere in the tissue response against collagen. The intercostal space and skin were closed with sutures. The mice received pure oxygen until they awoke, after which the endotracheal tubes were taken out.

2.2.2. Explantation

The Col-I disks were explanted at the following time points after implantation that were related to the distinct phases of the FBR in mice: two days (day 2, onset), one week (week 1, early progression), two weeks (week 2, intermediate progression) and one month (month 1, late progression), n = 6/time point. At all time points, we explanted the disks together with excess surrounding tissue. Since the epicardially implanted disks were largely degraded after 21 days, we first explanted the entire heart together with disk and excess surroundings then prepared the scaffold from it for analyses. In this case, the encapsulated suture was used as a reference to determine the implant site and the remaining collagen scaffold. The disks were cut in half after explantation. One half was snap-frozen in liquid nitrogen immediately, and the other half was immersed in 2% glutaraldehyde (Merck, Darmstadt, Germany) in 10 mM phosphate buffer, pH 7.4, for plastic embedding.

2.3. Histology

Our previous research showed that the newly deposited collagen bundles are in the nanometer size range, while the implanted scaffolds comprise

microsize-range bundles. Thus, the new bundles are invisible as distinct structures with the light microscope (van Amerongen *et al.*, 2006). Implanted and newly formed collagen can be differentiated through a histochemical staining procedure. Tissue sections (2 μm) of T 7100 (Heraeus Kulzer, Wehrheim, Germany) embedded explants were stained with toluidine blue (Fluka Chemie, Buchs, Switzerland) and mounted in Permount (Fisher, NJ, USA). The sections were analysed by light microscopy.

2.4. Immunohistochemical staining

Tissue expression of *in situ* localization of collagenases (MMP-8, MMP-13), gelatinases (MMP-2, MMP-9), Membrane-type metalloproteinase (MT1-MMP or MMP- 14), TIMPs (TIMP-1, TIMP-2) and cytokine IL-10 was examined with immunohistochemistry (IHC) on explants of 2 weeks.

Tissue sections (5 μm) were mounted on silane-coated slides. Cryo-sections were fixed with 2% paraformaldehyde (PFA) in phosphate-buffered saline (PBS) at room temperature for 30 min, followed by rehydration (1× PBS, 10 min), and subsequent incubation with 0.5% Triton X-100 in PBS (10 min).

The antibodies were purchased from commercial suppliers and their specificity was validated before use. Information on the optimization of all primary antibodies used is detailed in Table 2.1. For MMP-2, -8, -9 and - 14, TIMP-1 and IL-10, the sections were washed in PBS and pre-incubated in 2% normal goat or rabbit serum (depending on the producer of secondary antibody) for 10 min. The sections were incubated with primary antibody in PBS with 2% normal goat or rabbit serum for 1 h. Thereafter, the sections were washed in 0.05% Tween PBS (three times, 5 min) and endogenous peroxidase was blocked with 0.1% H2O2 in PBS (10min in the dark). Endogenous avidin and biotin were blocked with the avidin/biotin kit according to the manufacturer's instructions (Biotin Blocking System, Dako Cytomation, Denmark). The slides were incubatedwith goat anti-rabbit (Dako) or rabbit anti-goat (Southern Biotech) biotinylated secondary antibody as appropriate (secondary

antibody in PBS with 2% normal mouse serum, 30 min). Dilutions that were used were 1 : 150 for MMP-9 and 1 : 100 for the rest, followed by incubation of streptavidin conjugated to peroxidase (Strep-PO, 1 : 100, 30 min). For MMP-13, TIMP-2 detection, sections were pre-incubated in PBS with 2% donkey serum for 10 min and then incubated in the primary antibodies for 1 h. After washing (0.05% Tween PBS, 5 min, three times) and blocking of endogenous perioxidase (0.1% H2O2

Antibodies	Host Species	IHC	WB	Sources
MMP-2	Rabbit	1 : 200	1: 500	Ab37150, Abcam, Cambridge, UK
MMP-8	Rabbit	1 : 100	1: 500	SA-370, BIOMOL, USA
MMP-9	Rabbit	1 : 1000	1 : 1000	Ab38898, Abcam, Cambridge, UK
MMP-13	Sheep	1 : 20	1: 500	Ab35320, Abcam, Cambridge, UK
MMP-14	Rabbit	1: 50	1 : 2000	2010-1, Epitomics Inc., CA, USA
TIMP-1	Goat	1: 50	1: 500	AF980, RnDSystems, Minneapolis, MO, USA
TIMP-2	Sheep	1 : 10	1: 500	9013-2609, AbD Seroter, Oxford, UK
IL-10	Rabbit	1 : 125	Not done	AAM32, AbD Serotec, Oxford UK

Table 2.1. Characteristics of the primary antibodies used for immunohistochemical staining (IHC) and western blotting (WB) of MMPs, TIMPs and IL-10

in PBS, 10 min in the dark), the primary antibody was detected using donkey anti-sheep IgG H&L (HRP, 1 : 100; ab6900, Abcam, Cambridge, UK) and streptavidin conjugated to peroxidase (Strep-PO, 1 : 100, 30 min). The procedures were the same for all negative controls, except that the primary antibody was omitted or replaced with the same dilution of its host serum (i.e. sheep or rabbit) according to Table 2.1 (to exclude the background staining from the host serum).

Colour development was done with 3-amino-9-ethylcarbazole (AEC, Sigma, Steinheim, Germany) and finally the sections were counterstained with haematoxylin (Fluka Chemie).

2.5. Image analysis

The quantification of MMP/TIMPs expressing cells was performed by

counting the number of positive cells in micrographs (×400) taken in six areas equally distributed in the scaffold of each disk. Disks from four different animals (n = 4) of each time point were used to calculate the mean values. All analyses and determinations were repeated at least three times by two independent investigators on blinded samples. In addition, the fraction of cells that adhered to collagen bundles and expressed MMPs was quantified by morphometry of the area of positive staining (ImageJ 1.38, NIH).

2.6. Western blotting

Proteins were isolated from the frozen explants of the two sites at all time points. Sections of explants from four mice (five sections of 10 μm fromeach mouse) were pooled to minimize the individual variation. Samples (10 μg) of each protein was separated in a 10% sodium dodecyl sulphate–polyacrylamide gel. Then the proteins were transferred by electro-blotting (1.5 h, 100 V) to a PROTRAN membrane, which was blocked with 3% BSA (shaking for 1 h).

The primary antibodies used for the western blots were the same as those for immunohistochemistry. The concentrations of all primary antibodies used are shown in Table 2.1. β-Actin (1 : 2000, mouse monocolonal antibody, sc-47778; Santa Cruz Biotechnology) was used as a control for equal loading of the protein samples. The membranes were incubated with primary antibodies at 4 ◦C overnight, then washed three times with 1% Tween in PBS and incubated with secondary antibodies (for MMP-2, -8, -9 and -14, goat anti-rabbit AP, 1 : 1000, Jackson Immunoresearch; for TIMP-1, rabbit anti-goat AP, 1 : 1000, Zymax; for MMP-13 and TIMP-2, donkey antisheep HRPO, 1 : 1000, Abcam) and again washed with 1% Tween PBS three times. Antibody binding was visualized by either NBT/BCIP (for AP) or DAB (for HRPO).

Computerized densitometry was used to measure the intensity of the bands and the relative intensity (relative units) was determined through the ratio of the intensity of MMP:β-actin (ImageJ 1.38, NIH).

3. Results

3.1. Degradation of Col-I scaffolds

The course of the FBR against Col-I scaffolds differed between the subcutaneous and epicardial implants as showed in the histochemical staining on plastic embedded sections (Figure 2.1). The degradation of Col-I bundles was only minor or virtually absent in subcutaneous implants during the one month analysis period (Figure 2.1E). In contrast, epicardially the degradation of Col-I had commenced at week 1, although only few cells had infiltrated (Figure 2.1B). The degradation had advanced at week 2 and was characterized with increased cellular influx surrounding the Col-I bundles (Figure 2.1D). Within 1 month, the majority of Col-I had been degraded (Figure 2.1F). Significantly more giant cells were formed subcutaneously than epicardially from day 14 on (Figure 2.1C, D). Yet phagocytosis (as revealed by light microscopy) was never observed during the whole time course of the FBR in either subcutaneous or epicardial implants.

Based on the histological results, primarily the presence of numerous inflammatory cells and presence of Col- I bundles at both sites, week 2 (Figure 2.1C, D) was selected for the *in situ* detection and characterization of the MMP-based proteolytic network and IL-10 by immunohistochemistry.

3.2. Distribution and status of collagenases and gelatinases

The presence of active or inactive (i.e. latent proform) of collagenases and gelatinases was assessed by western blotting for the whole time course of the experiment (day 2, week 1, week 2 and month 1). For collagenases, the active form of both collagenases (MMP-8, -13) was detected (Figure 2.3) in subcutaneous implants throughout the time course. Epicardially,

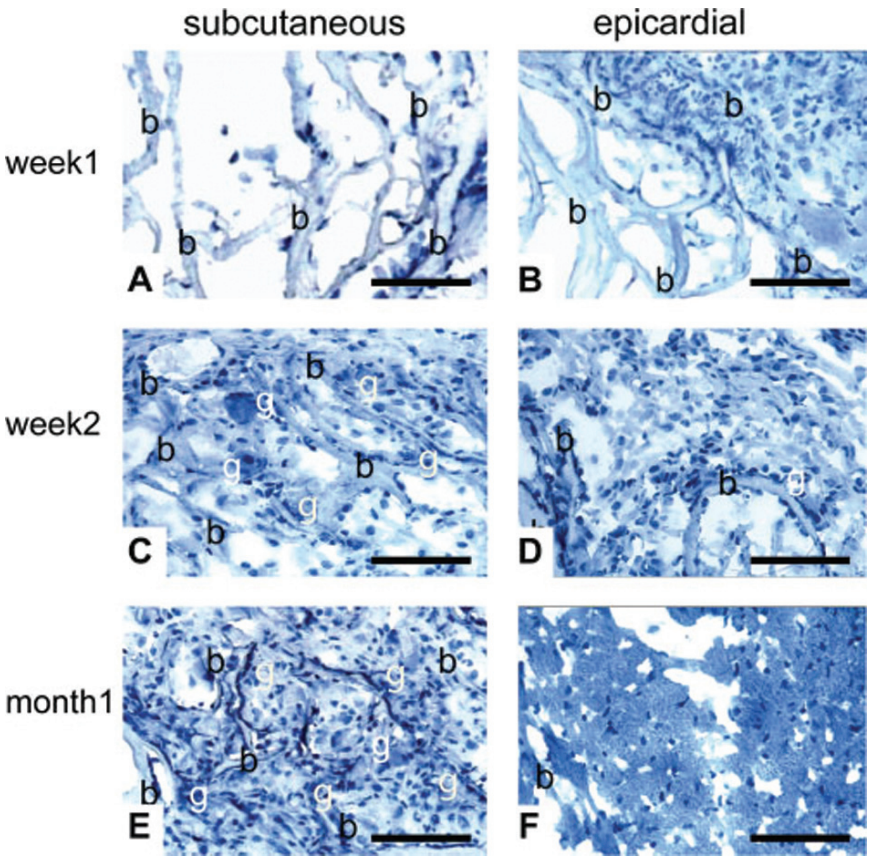

Figure 2.1. Comparison of cellular infiltration and degradation in subcutaneously and epicardially implanted Col-I scaffolds at week 1 (A, B), week 2 (C, D) and month 1 (E, F). Subcutaneously, the number of cells increased with time (A, C and E) and giant cells (g) were observed from week 2 on. The majority of Col-I bundles (b) remained intact until 1 month (E). Epicardially, the number of cells increased with time (B and D). At week 2, the infiltrating cells had adhered to most of the Col-I bundles. Far fewer giant cells were observed compared to that in subcutaneous implants (D). The number of Col-I bundles decreased from week 2 on and the Col-I had almost completely degraded after 1 month (F). All scale bars represent 20 µm

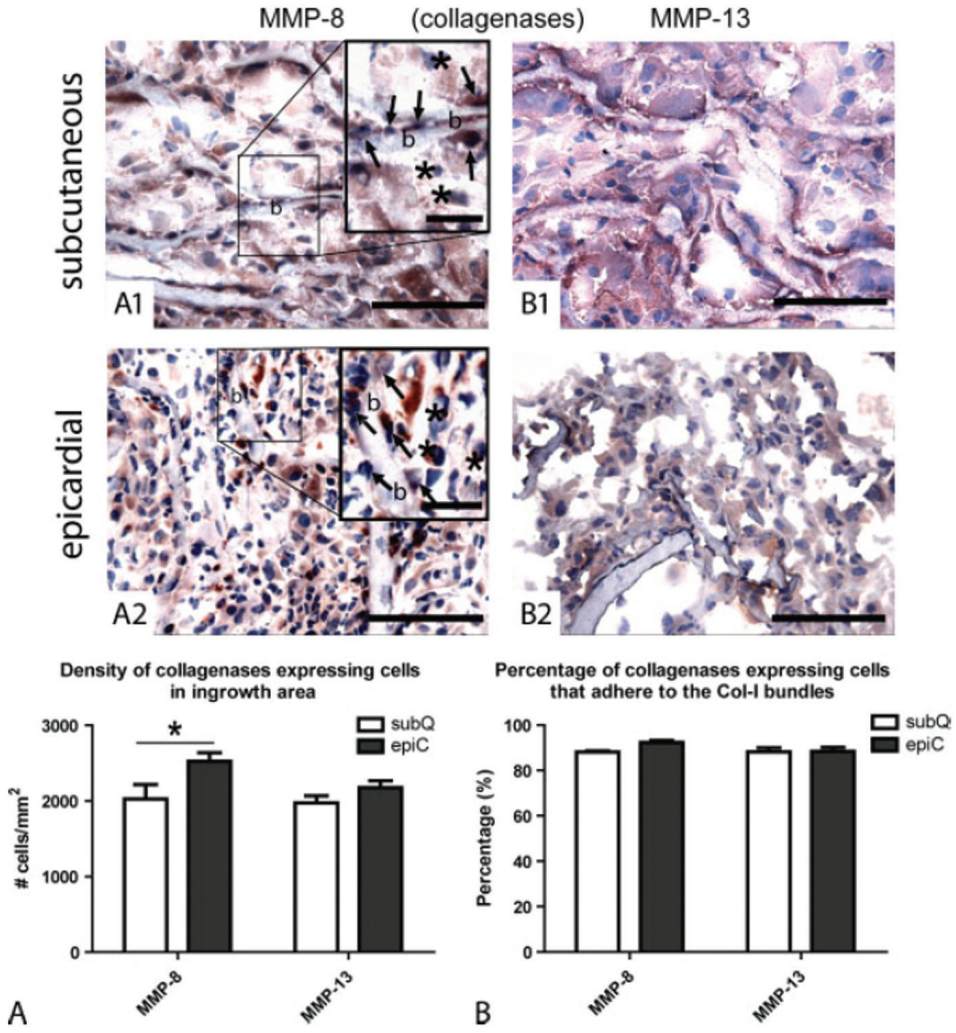

Figure 2.2. Collagenase protein analyses by immunohistochemistry. Light micrographs show the presence of MMP-8 and -13 in subcutaneously (A1, B1) and epicardially (A2, B2) implanted disks at week 2. The inserts of A1 and A2 show that cells adhered to (arrows) or were apart from (asterisks) the Col-I bundles (b). Scale bar represents 5 μm for the inserts (A1 and A2) and 20 μm for the rest. The number of positive-stained cells was counted (A), and their distribution patterns were determined through the percentage of positive-staining cells that adhered to Col-I bundles (B); Values are depicted as mean ± SD. $*p < 0.05$

the latent form of both collagenases (proMMP-8, 13) was always present, yet only MMP-13 was also present in its active form during the whole time course (Figure 2.3). For the gelatinases, subcutaneously both active and latent forms of MMP- 2 were present during the progression of the FBR, while MMP-9 was only present at day 2 and in the latent proform (Figure 2.5). Epicardially, MMP-2, mainly in its active form,and MMP-9, mainly in its latent proform, were present (Figure 2.5). This indicates that the main collagenase and gelatinase that were active in epicardial Col-I implants were MMP-13 and MMP-2, respectively.

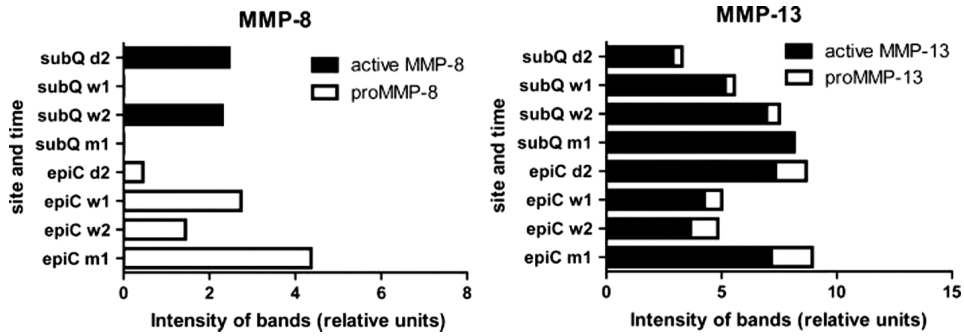

Figure 2.3. Collagenase protein analyses by western blotting at the time points of 2 days (d2), 1 week (w1), 2 weeks (w2) and 1 month (m1) after implantation. Protein samples from explants of four mice were pooled and the proteolytic activation of MMP-8 and -13 was determined by virtue of significant differences in molecular weight between active form and proform. Computerized densitometry was used to measure the intensity of the bands and the relative intensity (relative units) was determined through ratio of the intensity of MMP/β-actin. Subcutaneously, both MMP-8 and MMP-13 were present and active. Epicardially, MMP-13 was the only active collagenase throughout the time course, whereas the present MMP-8 was in its proform

3.3. Presence of activators and inhibitors of MMPs

Collagenases and gelatinases are secreted as their inactive proforms. The MMP activity is regulated extracellularly by at least two mechanisms.

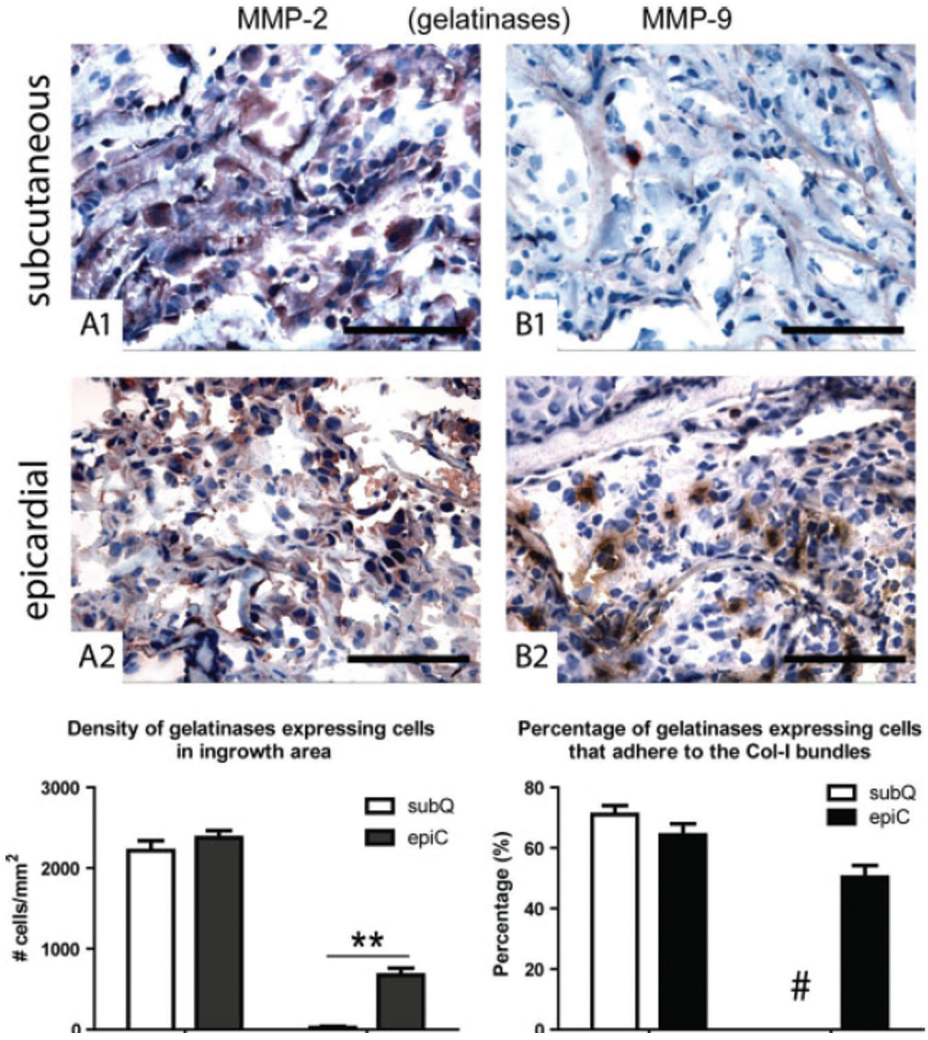

Figure 2.4. Gelatinase protein analyses by immunohistochemistry. Light micrographs show the positive staining of MMP-2 and -9 in subcutaneously (A1, B1) and epicardially (A2, B2) implanted disks at week 2. All scale bars represent 20 µm. The number of positive-stained cells was counted (A) and their distribution patterns were determined through the percentage of positive cells that adhered to Col-I bundles (B). Values are depicted as mean ± SD. **p < 0.01. # Percentage could not be calculated (no positive cells present)

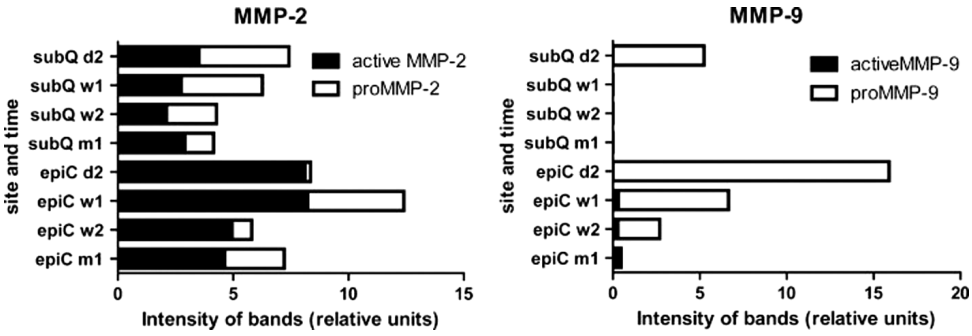

Figure 2.5. Gelatinase protein analyses by western blotting at d2, w1, w2 and m1. Protein samples from explants of four mice were pooled and the status of MMP-2 and MMP-9 were determined by virtue of significant differences in molecular weight between active form and proform. Computerized densitometry was used to measure the intensity of the bands and the relative intensity (relative units) was determined through ratio of the intensity of MMP/β-actin. Subcutaneously MMP-2 was present and active, whereas MMP-9 was present only at day 2. Epicardially both gelatinases were present but MMP-9 was mainly present in proform; in contrast, MMP-2 was mainly in active form

One is the proteolytic activation of the secreted MMPs by MMP-14 (together with the co-activator TIMP-2) and the other is the inhibition of MMP activity by TIMPs. Therefore, we determined the spatiotemporal expression of the main MMP activators (MMP-14, TIMP-2) and inhibitors (TIMP- 1, TIMP-2) by immunohistochemistry and western blotting. Immunohistochemistry showed that at week 2 all the investigated activators and inhibitors were present at both implant sites (Figure 2.6) except for TIMP-1, which was absent epicardially (Figure 2.6, C2). Neither the number nor the distribution pattern of MMP-14- expressing cells differed between the two implant sites (Figure 2.6A, B), although more TIMP-2-expressing cells were present in epicardial implants than in subcutaneous implants (Figure 2.6A) and in general TIMP-2-expressing cells were more associated with Col-I bundles epicardially (Figure 2.6B). Irrespective of the implant sites, western blotting showed that MMP-14 and TIMP-2 were detected throughout the whole time course (Figure 2.7). MMP-14 was only present in its 'proform', which, remarkably, is the

known conformation required for activating other MMPs, such as MMP-2. In contrast to the continuous expression of TIMP-2 at both implant sites, TIMP-1 was exclusively expressed in subcutaneous implants at all time points (Figure 2.7). Moreover, the average expression of TIMP-2 levels was lower subcutaneously than epicardially during the progression of the FBR (Figure 2.7).

3.4. Presence of IL-10

Immunohistochemical staining showed that IL-10- producing cells were present in subcutaneous Col-I implants at week 2 (Figure 2.8A). In contrast, only few IL-10-producing cells were present in epicardial Col-I implants and these cells produced less IL-10 compared to subcutaneous implants (Figure 2.8B). Subcutaneously, the majority of IL-10-expressing cells appeared to be giant cells (Figure 2.8A). Since few giant cells were observed in epicardial implants, this explains why only low levels of IL-10 were present in the epicardial scaffold microenvironment.

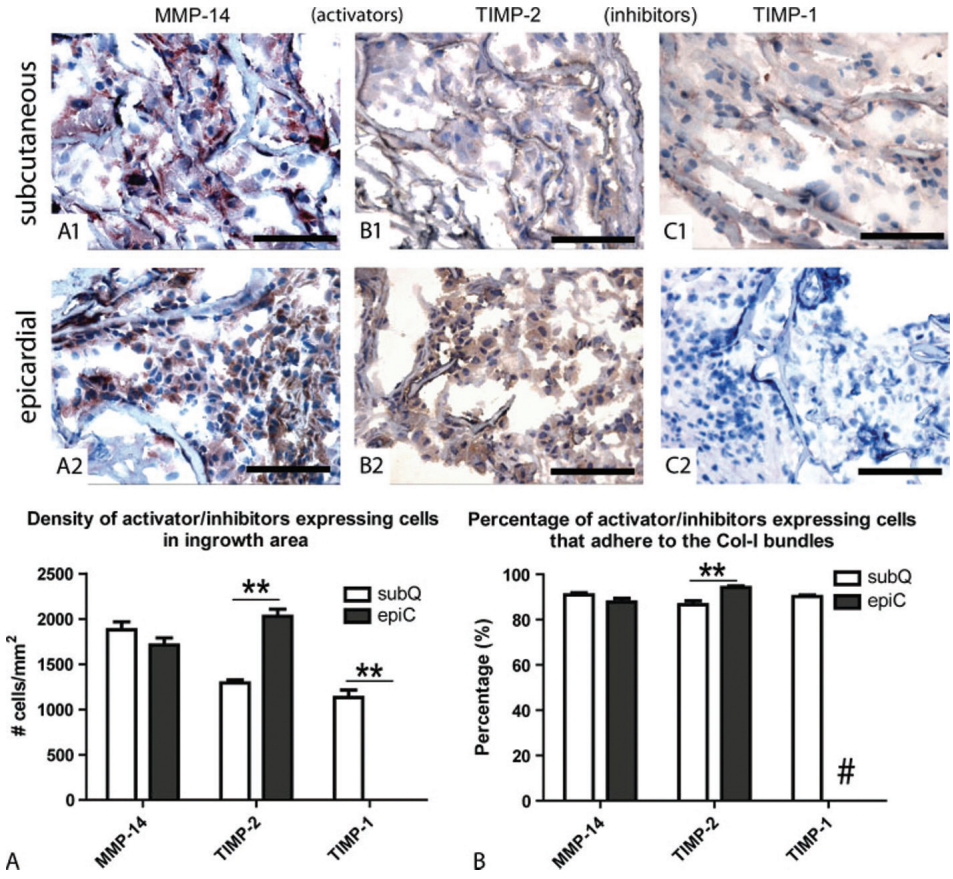

Figure 2.6. Protein analyses of MMP activators and inhibitors by immunohistochemistry. Light micrographs show the presence of MMP-14, TIMP-2 and TIMP-1 in subcutaneously (A1–C1) and epicardially (A2–C2) implanted disks at week 2. All scale bars represent 20 µm. The number of positive-stained cells was counted (A) and their distribution patterns were determined through the percentage of positive cells that adhered to Col-I bundles (B). Values are depicted as mean ± SD. $^{**}p < 0.01$. # Percentage could not be calculated (no positive cells present)

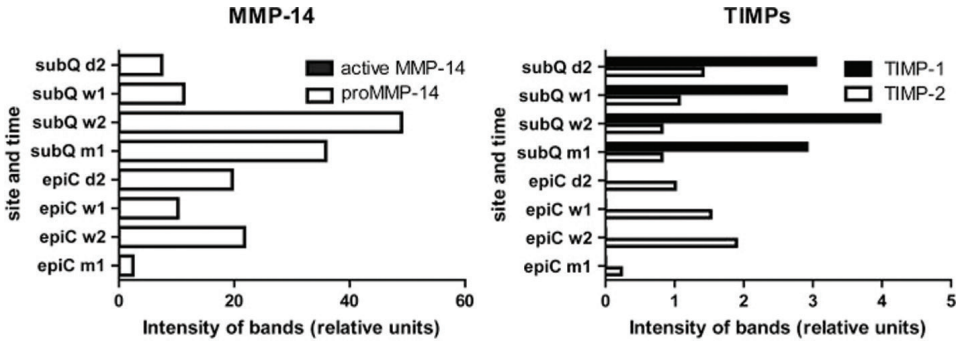

Figure 2.7. Protein analyses of MMP activators and inhibitors by western blotting at d2, w1, w2 and m1. Protein samples from explants of 4 mice were pooled and then detected the presence of MMP-14, TIMP-1 and -2 by western blotting. Computerized densitometry was used to measure the intensity of the bands and the relative intensity (relative units) was determined through ratio of the intensity of (MMP or TIMP)/β-actin. Irrespective of the implant sites, both activators were detected. In contrast, TIMP-1 was only detected in subcutaneous explants during the entire time course

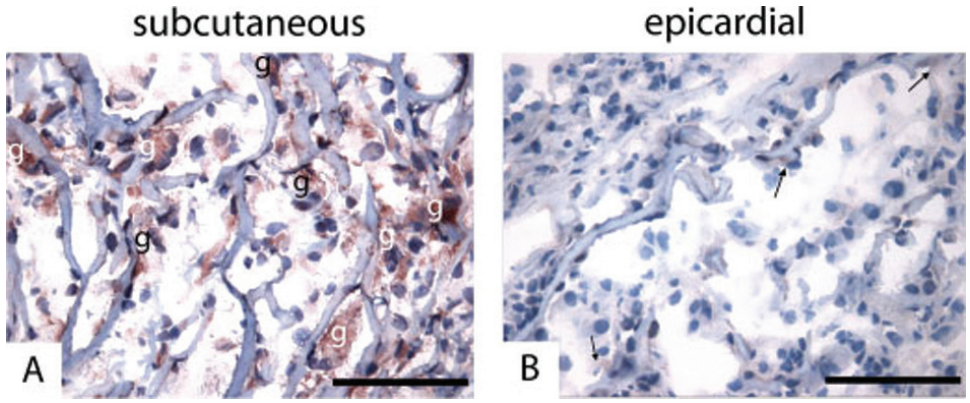

Figure 2.8. Light micrographs of immunohistochemical analysis of cytokine IL-10 (week 2). Representative images show strongly positive staining associated with the presence of giant cells (g) in subcutaneous implants (A). In contrast, only slight staining was shown in epicardial implants (B, arrows). All scale bars represent 20 μm

4. Discussion

MMPs are produced and secreted as zymogens (proMMPs). To degrade collagen, MMPs need to be activated. MMP-2 is among the first MMPs to be activated in the MMP proteolytic network. Activation of proMMP-2 is achieved through a trimolecular complex at the cell surface, comprising proMMP-14, TIMP-2 and proMMP-2 (Strongin *et al.*, 1995; Cao *et al.*, 2005).Of note, proMMP- 14, but not its furin-activated form, converts proMMP-2 into its activated form (Cao *et al.*, 1998; Cao et al., 1999). After liberation of active MMP-2, this enzyme is able to activate both proMMP-13 and proMMP-9, which can further activate the other MMPs in the extracellular proteolytic network.

In the current study, we investigated the molecular mechanisms and regulation of the MMP-based proteolytic network during the FBR against Col-I in mice. We show that epicardially implanted collagen scaffolds were degraded during the FBR, whereas there was hardly any degradation of the subcutaneously implanted scaffold.

Our data showed the presence of proMMP-14 and TIMP-2 at both implant sites during the whole time course. This likely leads to the activation of MMP-2, whose presence was confirmed at both implant sites. MMP-13, as shown by Western blotting, was present in its activated form at both implant sites, most likely due to the activation of MMP-2. Interestingly, the MMP-9 present in the epicardial implants remained largely in its proform. Thus, MMP-9, although it is exclusively seen in epicardial implants, can not be responsible for the high degradation rate of the scaffold. In addition, we here show that the MMP-8 present in the epicardial implants is also only present in its latent proform. Although the above findings do not contradict our previous observations that MMP-8 protein and MMP-9 mRNA are highly present in epicardial Col-I implants, we now believe that the role of MMP-8 and MMP-9 during the FBR is negligible, because both enzymes were largely inactive. In the current study it turned out that the MMPs in the epicardial implants are

present in an activated form are MMP-2 and MMP- 13. Therefore, the collagenase MMP-13 and the gelatinase MMP-2 seem to be the effective MMPs that are responsible for the degradation of epicardial Col-I implants.

On the other hand, the activated forms of MMP-2 and MMP-13 were also found in the subcutaneously implanted scaffolds, as well as MMP-8. Surprisingly, Col-I scaffolds were not degraded at this implant site. In general, the proteolytic activity of MMPs depends not only upon the presence of the activated form of MMPs but also upon the stoichiometric balance between TIMPs and the activated form of MMPs (Nagase and Woessner, 1999). Higher molar levels of TIMPs than active MMPs will put the proteolytic network in an 'off mode'. Therefore, the apparent contradiction between the presence of activated MMPs and the absence of Col-I degradation in subcutaneous implants may be due to TIMPs. Among the four members of the TIMP family, only TIMP-1 and TIMP-2 were found to participate in the FBR against biomaterials *in vitro* (Jones *et al*., 2008). Generally, TIMP-1 acts as an unconditional MMP inhibitor of MMP activity, whereas TIMP-2 can act as either an activator or an inhibitor, according to the protein level of TIMP-2. Low-to-moderate TIMP-2 levels induce the activation of MMPs, while higher levels lead to inhibition (Sternlicht and Werb, 2001). Here we show that the TIMP-2 protein expression levels at both implant sites are relatively low, and during the progression of the FBR (weeks 1 and 2), TIMP-2 protein levels are lower subcutaneously than epicardially. Therefore, the low TIMP-2 levels would seem to suffice for MMP activition in complex with proMMP-14, yet TIMP-2 levels are too low to inhibit MMP activity in degrading the extracellular matrix and the Col-I bundles. The only limiting factor for the Col-I degradation subcutaneously thus remains TIMP- 1. Indeed, although TIMP-1 was absent in epicardial scaffolds, it was readily detected subcutaneously at all time points. The ratio of MMPs and TIMP-1 in favour of TIMP-1 likely results in the inhibition of MMP-2, -8 and -13 activity at the subcutaneous implant site.

The balance of the MMP/TIMP network is affected by inflammatory mediators. In particular, the expression of TIMP-1 protein is upregulated by the immunosuppressive cytokine IL-10 (Lacraz *et al.*, 1995; Sternlicht

and Werb, 2001). *In vitro* studies have shown that IL-10 is a dose-dependent stimulator for the transcription of TIMP- 1 mRNA (Lacraz et al., 1995; Mostafa et al., 2001). We wondered whether the presence of TIMP-1 in subcutaneous implants and the absence of TIMP-1 in epicardial implants is due to high and low levels of IL-10, respectively. This was indeed the case. Here we show that TIMP-1 and IL-10 are correlated and co-localized, suggesting that also *in vivo*, in the FBR, IL-10 regulates TIMP-1 protein expression. Furthermore, the current results show that IL-10 protein seems to be produced mainly by the giant cells. Together with our previous findings that significantly more giant cells are formed in subcutaneous implants than in epicardial implants (Luttikhuizen *et al.*, 2006b), this would explain the higher subcutaneous IL-10 expression during the FBR. Together, the current data indicate that the presence of the high IL- 10 level secreted by giant cells in subcutaneous implants may have promoted the synthesis of TIMP-1 protein and hence downregulated the extracellular MMP activity. Interestingly, IL-10 has also been shown to downregulate the level of MMP-9 gene expression (Mostafa *et al.*, 2001; Tziakas *et al.*, 2003; Popi et al., 2004), which would explain our observation of the near absence of MMP-9 in subcutaneous explants. Further studies are needed to dissect the role of potential therapeutic candidate IL-10 in the FBR, via IL-10 deficient mice.

In summary, in subcutaneously implanted scaffolds the high number of IL-10-producing giant cells may have created a different inflammatory microenvironment that resulted in: (a) decreased MMP-9 levels; and (b) increased TIMP-1 levels that effectively dampened the degradation of the scaffolds by inhibiting MMP-13 and MMP-2. Our data provide basic knowledge of the MMPbased proteolytic activity against crosslinked collagen in mice, and hold promise for the development of future therapeutic modalities in cardiac tissue engineering. Based on these results, modulation of the FBR via MMP network is feasible through several routes. One is to regulate the expression of TIMP-1, while the regulation of cytokines, e.g. by IL-10, might also be effective.

Acknowledgements

This study was supported by RuG Jan Kornelis de Cock-Stiching for Q. Ye (Grant No. De-Cock-08-69). The authors wish to acknowledge the excellent technical support of Dr Ben Stulp, Mrs Marja Brinker, Mrs Linda Brouwer and Mr Xavier Gallego y van Seijen.

References

Brinckerhoff CE,Matrisian LM. 2002; Matrix metalloproteinases: a tail of a frog that became a prince. *Nat Rev Mol Cell Biol* **3**(3): 207–214.

Cao J, Drews M, Lee HM, *et al.* 1998; The propeptide domain of membrane type 1 matrix metalloproteinase is required for binding of tissue inhibitor of metalloproteinases and for activation of pro-gelatinase A. *J Biol Chem* **273**(52): 34745–34752.

Cao J, Drews M, Lee HM, *et al.* 1999; The 9 kDa N-terminal propeptide domain of MT1-MMP is required for the activation of progelatinase A. *Ann N Y Acad Sci* **878**: 710–712.

Cao J, Rehemtulla A, Pavlaki M, *et al.* 2005; Furin directly cleaves proMMP-2 in the trans-Golgi network resulting in a nonfunctioning proteinase. *J Biol Chem* **280**(12): 10974–10980.

Cummings CL, Gawlitta D, Nerem RM, *et al.* 2004; Properties of engineered vascular constructs made from collagen, fibrin, and collagen-fibrin mixtures. *Biomaterials* **25**(17): 3699–3706.

Daamen WF, Nillesen ST, Hafmans T, *et al.* 2005; Tissue response of defined collagen–elastin scaffolds in young and adult rats with special attention to calcification. *Biomaterials* **26**(1): 81–92.

Hedrick MH, Daniels EJ. 2003; The use of adult stem cells in regenerative medicine. *Clin Plast Surg* **30**(4): 499–505.

Hutmacher DW, Schantz T, Zein I, *et al.* 2001; Mechanical properties and cell cultural response of polycaprolactone scaffolds designed and fabricated via fused deposition modeling. *J Biomed Mater Res* **55**(2): 203–216.

Jones G, Riley G. 2005; ADAMTS proteinases: a multi-domain, multi-functional family with roles in extracellular matrix turnover and arthritis. *Arthritis Res Therapy* **7**(4): 160–169.

Jones JA, McNally AK, Chang DT, *et al.* 2008; Matrix metalloproteinases and theirinhibitors in the foreign body reaction on biomaterials. *J Biomed Mater Res A* **84**(1): 158–166.

Khouw IM, vanWachem PB, de Leij LF, *et al.* 1998; Inhibition of the tissue reaction to a biodegradable biomaterial by monoclonal antibodies to IFN-γ. *J Biomed Mater Res* **41**(2): 202–210.

Khouw IM, van Wachem PB, van der Worp RJ, *et al.* 2000; Systemic anti-IFN-γ treatment and role of macrophage subsets in the foreign body reaction to dermal sheep collagen in rats. *J BiomedMater Res* **49**(3): 297–304.

Kyriakides TR, Bornstein P. 2003; Matricellular proteins as modulators of wound healing and the foreign body response. *Thromb Haemost* **90**(6): 986–992.

Kyriakides TR, Foster MJ, Keeney GE, *et al.* 2004; The CC chemokine ligand, CCL2/MCP1, participates in macrophage fusion and foreign body giant cell formation. *Am J Pathol* **165**(6): 2157–2166.

Lacraz S, Nicod LP, Chicheportiche R, *et al.* 1995; IL-10 inhibits metalloproteinase and stimulates TIMP-1 production in human mononuclear phagocytes. *J Clin Invest* **96**(5): 2304–2310.

Luttikhuizen DT, Harmsen MC, van Luyn MJ. 2006a; Cellular and molecular dynamics in the foreign body reaction. *Tissue Eng* **12**(7): 1955–1970.

Luttikhuizen DT, Harmsen MC, van Luyn MJ. 2007; Cytokine and chemokine dynamics differ between rats and mice after collagen implantation. *J Tissue Eng Regen Med* **1**(5): 398–405.

Luttikhuizen DT, van Amerongen MJ, de Feijter PC, *et al.* 2006b; The correlation

between difference in foreign body reaction between implant locations and cytokine and MMP expression. *Biomaterials* **27**(34): 5763–5770.

Mason C. 2007; Regenerative medicine. The industry comes of age. *Med Device Technol* **18**(2): 25–30.

Mather ML, Morgan SP, Crowe JA. 2007; Meeting the needs of monitoring in tissue engineering. *Regen Med* **2**(2): 145–160.

Mohamed MM, Sloane BF. 2006; Cysteine cathepsins: multifunctional enzymes in cancer. *Nat Rev Cancer* **6**(10): 764–775.

Mostafa ME, Chollet-Martin S, Oudghiri M, *et al*. 2001; Effects of interleukin-10 on monocyte/endothelial cell adhesion and MMP-9/TIMP-1 secretion. *Cardiovasc Res* **49**(4): 882–890.

Munirah S, KimSH, Ruszymah BH, *et al*. 2008; The use of fibrin and poly(lactic-coglycolic acid) hybrid scaffold for articular cartilage tissue engineering: an *in vivo* analysis. *Eur Cell Mater* **15**: 41–52.

Nagase H, Woessner JF Jr. 1999; Matrix metalloproteinases. *J Biol Chem* **274**(31): 21491–21494.

Nuttall RK, Sampieri CL, Pennington CJ, *et al*. 2004; Expression analysis of the entire *MMP* and *TIMP* gene families during mouse tissue development. *FEBS Lett* **563**(1–3): 129–134.

PaquetteJS, MoulinV, TremblayP, *et al*. 2004; Tissue-engineered human asthmatic bronchial equivalents. *Eur Cell Mater* **7**: 1–11.

Petersen T, Niklason L. 2007; Cellular lifespan and regenerative medicine. *Biomaterials* **28**(26): 3751–3756.

Popi AF, Lopes JD, Mariano M. 2004; Interleukin-10 secreted by B-1 cells modulates the phagocytic activity of murine macrophages *in vitro*. *Immunology* **113**(3):

348–354.

Rivron NC, Liu JJ, Rouwkema J, *et al*. 2008; Engineering vascularised tissues *in vitro*. *Eur Cell Mater* **15**: 27–40.

Sachlos E, Czernuszka JT. 2003; Making tissue engineering scaffolds work. Review: the application of solid freeform fabrication technoogy to the production of tissue engineering scaffolds. *Eur Cell Mater* **5**: 29–39.

Sachlos E, Gotora D, Czernuszka JT. 2006; Collagen scaffolds reinforced with biomimetic composite nano-sized carbonate-substituted hydroxyapatite crystals and shaped by rapid prototyping to contain internal microchannels. *Tissue Eng* **12**(9): 2479–2487.

Sternlicht MD, Werb Z. 2001; How matrix metalloproteinases regulate cell behavior. *Annu Rev Cell Dev Biol* **17**: 463–516.

Strongin AY, Collier I, Bannikov G, *et al*. 1995; Mechanism of cell surface activation of 72-kDa type IV collagenase. Isolation of the activated form of the membrane metalloprotease. *J Biol Chem* **270**(10): 5331–5338.

Tai H, Mather ML, Howard D, *et al*. 2007; Control of pore size and structure of tissue engineering scaffolds produced by supercritical fluid processing. *Eur Cell Mater* **14**: 64–77.

Tziakas DN, Chalikias GK, Hatzinikolaou HI, *et al*. 2003; Anti-inflammatory cytokine profile in acute coronary syndromes: behavior of interleukin-10 in association with serum metalloproteinases and proinflammatory cytokines. *Int J Cardiol* **92**(2–3): 169–175.

van Amerongen MJ, Harmsen MC, Petersen AH, *et al*. 2006; The enzymatic degradation of scaffolds and their replacement by vascularized extracellular matrix in the murine myocardium. *Biomaterials* **27**(10): 2247–2257.

Wahl DA, Sachlos E, Liu C, Czernuszka JT. 2007; Controlling the processing of

collagen–hydroxyapatite scaffolds for bone tissue engineering. *J Mater Sci Mater Med* **18**(2): 201–209

CHAPTER 3

The relationship between collagen scaffold cross-linking agents and neutrophils in the foreign body reaction

Qingsong Ye [1,2,3,4]
Martin C. Harmsen [1]
Marja J.A. van Luyn [1]
Ruud A. Bank [1]

[1] Stem Cell and Tissue Engineering Research Group, Department of Pathology and Medical Biology, University of Groningen, The Netherlands

[2] West China College of Stomatology, the State Key Laboratory of Oral Diseases, Sichuan University, Chengdu, China

[3] Department of Orthodontics, University Medical Centre Groningen, University of Groningen, The Netherlands

[4] School of Medicine and Dentistry, James Cook University, Cairns, Australia

Biomaterials 31 (2010) 9192-9201

Abstract

In order to get more insight into the role of neutrophils on the micro-environment and consequently on macrophages in the foreign body reaction in mice, we investigated the fate of the two differently cross-linked dermal sheep collagen disks (glutaraldehyde = GDSC, hexamethylenediisocyanate = HDSC) in mice implanted in one anatomical location, namely subcutaneously. In GDSC massive infiltration of neutrophils is seen at day 2 and day 21, whereas in HDSC only minor infiltration is seen at day 2. The presence of neutrophils coincided with high levels of IFN-γ, a cytokine that activates macrophages. Major differences were seen in degradation rate of the two disks: GDSC was almost completely degraded after 28 days, whereas HDSC remained intact. Degradation of GDSC occurred through collagenolytic activity and phagocytosis by macrophages. Phagocytosis was observed at day 2 and day 21. IL-13 was only observed in HDSC, and this resulted in the presence of giant cells in HDSC. These giant cells produced IL-10, that promoted TIMP-1 expression and that inhibits collagenolytic and phagocytic activity. We conclude that the function of macrophages in mice is largely influenced by differences in micro-environment induced by GDSC and HDSC and that the presence/absence of neutrophils play a major role in the shaping of this micro-environment.

1. Introduction

In regenerative medicine, biomaterial scaffolds are extensively investigated for their support of attachment, proliferation and differentiation of transplanted or local cells [1], [2] and [3]. As such, biomaterial scaffolds provide novel clinical modalities that aid in the regeneration or repair of damaged tissues [4] and [5]. Yet, the application of biomaterial scaffolds interacts with the physiological tissue repair process [1], [6] and [7]. The foreign body reaction (FBR) is an inflammatory local tissue response induced by both the surgical trauma of implantation and the presence of the biomaterial scaffold in the body [8], [9] and [10]. The FBR may favor or adversely affect the tissue repair process. An important part of the FBR is the degradation of the implanted biomaterial scaffold and therefore it is important to get an insight in the processes that govern and result in scaffold degradation [11] and [12].

The FBR involves a complex cascade of spatiotemporally regulated and interconnected processes that include cellular activation, fluxes of inflammatory cells, angiogenesis, extravasation, migration, phagocytosis, which finally resolve after the degradation of the implant [9], [10] and [13]. Similar to inflammation, the FBR is mediated by soluble mediators such as growth factors, cytokines, chemokines and matrix metalloproteinases (MMPs) and their inhibitors (TIMPs) [14] and [15]. These mediators are produced and secreted locally by cells in the surrounding tissue and by infiltrated cells inside the biomaterial. The nature of these host reactions is to a large extent tissue-, organ- and species-dependent [11], [16], [17] and [18].

We have previously investigated the fate of chemically cross-linked collagen disks, i.e. biomaterials scaffolds, in mice and rats [11], [16], [17] and [18]. Subcutaneously implanted hexamethylenediisocyanate cross-linked bovine collagen type I disks in mice are virtually not degraded after 4 weeks due to the very limited proteolytic response of the host. Although activated MMP-2, -8, -13 and -14 were present, their action

was inhibited by high levels of TIMP-1. In spite of large numbers of giant cells inside the collagen disks, these giant cells did not phagocytose the disk. Instead these giant cells produced IL-10, a cytokine that increases the expression level of TIMP-1 mRNA and protein. Interestingly, similar collagen disks were almost completely degraded in mice upon epicardial implantation. Epicardially, TIMP-1 was not expressed and therefore the degradation was promoted by the active forms of MMP-2 and -13 that were present. The degradation was predominantly caused by extracellular proteolysis, because phagocytosis was absent. Moreover, less giant cells were seen and consequently only low levels of IL-10 were observed. Thus, marked tissue-specific differences were observed, indicating that the micro-environment of the location influenced the fate of the implanted biomaterial [11].

An obvious difference between subcutaneously and epicardially implanted hexamethylenediisocyanate cross-linked bovine collagen type I disks in mice was the continuous presence of neutrophils until day 21 (with peaks at the start and at day 14) in epicardially implanted scaffolds, whereas in subcutaneously implanted scaffolds neutrophils were hardly detected after 2 days of implantation [11] and [12]. The neutrophils might account for the previously indicated difference in micro-environment, resulting in differences in degradation rates of the scaffold between both tissues. With another scaffold placed in another animal species, namely glutaraldehyde cross-linked dermal sheep collagen (GDSC) subcutaneously implanted in rats, we have observed degradation rates of the GDSC scaffolds that is comparable with that of epicardially implanted hexamethylenediisocyanate cross-linked bovine collagen type I disks in mice [11] and [19]. Interestingly, the continuous presence of neutrophils was a common denominator in both models. However, from these anecdotal data it is difficult to draw conclusions about the interrelationship between neutrophil infiltration and scaffold degradation, as the experiments were carried out in two animal models, and in each animal model with a different biomaterial. As stated before, large differences exist in the FBR between animal species, such as rats and mice.

In order to get more insight into the role of neutrophils in the FBR,

we investigated the fate of the two differently cross-linked dermal sheep collagen disks (GDSC, HDSC) in mice implanted in one anatomical location, namely subcutaneously. By doing so, we ruled out differences in tissue type and animal species. In this experimental setup, differences in the FBR of the two biomaterials are primarily dictated by the nature of the scaffold itself, as the micro-environment at the start of the experiment is the same. If a change is seen in the micro-environment, then this change is primarily triggered by the biochemical make-up of the scaffold. Here we hypothesize that the GDSC will create part of the epicardial micro-environment via attraction of neutrophils, followed by an enhanced degradation.

2. Materials and methods

2.1. Animals and biomaterials

Male C57BL/6 mice (10 weeks old, Harlan, Horst, the Netherlands) were housed individually under conventional conditions with food and water *ad libitum*.

Non-cross-linked dermal sheep collagen (DSC), processed from sheep skin [14], was obtained from the Zuid Nederlandse Zeemlederfabriek (Oosterhout, the Netherlands). DSC was cross-linked with either glutaraldehyde (henceforth referred to as GDSC) or hexamethylenediisocyanate (henceforth referred to as HDSC), according to protocols described previously [19] and [20]. Disks (6 mm in diameter, 0.75 mm in thickness) were punched from pieces of HDSC and GDSC from the same batch, and sterilized with ethylene oxide. Surface-associated endotoxin levels were below 0.25 EU/ml.

2.2. Operating procedures

All procedures performed on animals were approved by the local committee for care and use of laboratory animals of the University of Groningen and were performed according to international and governmental guidelines on animal experimentation.

Implantation: mice were anesthetized with 4% isoflurane and maintained by 2% isoflurane inhalation in combination with a mixture of equal volumes of N_2O and O_2. The back was shaved and disinfected with chlorhexidine, two incisions were made and subcutaneous pockets were created on both sides. The HDSC or GDSC disks were implanted about 1 cm away from the incision site, thus minimizing the effect of wound healing on the inflammatory reaction. The incisions were closed with 6–0 non-absorbable Prolene sutures. Finally, mice received pure oxygen until awakening.

Explantation: the Col-I disks were removed at the following time points after implantation (related to the different phases of the FBR in mice): 2 days (onset), 7 days (early progression), 14 and 21 days (intermediate progression), and 28 days (late progression), $n = 6$ per time point. The disks were snap-frozen in liquid nitrogen immediately after explantation.

2.3. Histological techniques

Tissue sections (2 μm in thickness) of T 7100 (Heraeus Kulzer, Wehrheim, Germany) embedded explants were stained with toluidine blue (Fluka Chemie, Buchs, Switzerland) and mounted in Permount (Fisher, New Jersey, USA). Sections were analyzed by light microscopy. The number of giant cells per square millimeter inside implant on blinded samples was counted independently by two investigators. The degradation of the scaffold was determined by image analysis as the percentage of the size of remained disk as compared with the original size (before implantation). The cellular ingrowth inside the disk was evaluated by image analysis as percentage of the entire cross-sectional area, as described in our previous study [16].

2.4. Gene expression analysis

Total RNA was extracted from snap-frozen explants as described previously [14]. One microgram of total RNA was used to generate the first strand cDNA synthesis using M-MuLV reverse transcriptase (MBI Fermentas, St. Leon-Rot, Germany) and random hexamer primers, according to the manufacturer's protocol. Ten nanogram of a cDNA mixture from 5 mice was pooled per time point for each reaction. The PCR reaction of 35 cycles was performed using primers of interleukins (IL-4, IL-6, IL-10, IL-13), interferon-gamma (IFN-γ), transforming growth factor beta (TGF-β), monocyte chemoattractant protein 1 (MCP-1/CCL-2), macrophage inflammatory protein 1α (MIP-1α/CCL-3) and the control gene β-actin (Table 3.1). Amplimers were separated in 2% agarose gels.

Mediators	Forward	Reverse	Anneal
IL-4	ATGGGTCTCAACCCCCAGCTAGT	GCTCTTTAGGCTTTCCAGGAAGTC	60 ° c
IL-6	AAATCGTGGAAATGAGAAA	AGATGAATTGGATGGTCTTG	60 ° c
IL-10	CCCAGAAATCAAGGAGCATTTG	CATGTATGCTTCTATGCAGTTG	55 ° c
IL-13	ATGGCGCTCTGGGTGACTGCAGTCC	GAAGGGGCCGTGGCGAAACAGTTGC	67 ° c
TGF-β	CGGAAGCGCATCGAAGCCATCC	GCAAGCGCAGCTCTGCACGG	59 ° c
IFN-γ	TGGAGGAACTGGCAAAAGGATGGT	TTGGGACAATCTCTTCCCCAC	56 ° c
MIP-1α	CCCTTTTCTGTTCTGCTGACAAG	GAAGAGTCCCTCGATGTGGCTA	60 ° c
MCP-1	TCTCTTCCTCCACCACCATGCaG	GGAAAAATGGATCCACACCTTGC	60 ° c
β-actin	GTGAAAAGATGACCCAGATCAT	GCTTCTCTTTGATGTCACGCACGAT	60 ° c

Table 3.1. PCR primers of inflammatory mediators and the control gene

2.5. Immunohistochemistry

Tissue expression was verified by means of *in situ* immunohistochemistry staining (IHC) on explants of the two biomaterials at all time points. Tissue sections (5 μm) were mounted on silane-coated slides. Cryosections were fixed with 2% paraformaldehyde (PFA) in 1x phosphate-buffered saline (PBS) at room temperature for 30 min, followed by rehydration (1x PBS, 10 min), and subsequent incubation with 0.5% Triton X-100 in PBS (10 min). Sections were washed in PBS and pre-incubated in 2% normal goat serum for 10 min. Sections were incubated with 1:125 diluted rabbit-anti-mouse IL-10 antibody (AAM32, AbD Serotec, Oxford, UK) in PBS with 2% normal goat serum for 1h. Thereafter, sections were washed in 0.05% Tween PBS (5 min, 3 times), and endogenous peroxidase was blocked with 0.1% H_2O_2 in PBS (10 min, in dark). Endogenous avidin and biotin were blocked with the avidin/biotin kit according to the manufacturer's protocol (Biotin Blocking System, DakoCytomation, Denmark). The slides were incubated with goat anti-rabbit biotinylated secondary antibody (1:100, Dako, Carpineteria, USA) with 2% normal mouse serum for 30 min, followed by incubation of streptavidin conjugated to peroxidase (Strep-PO, 1:100, 30 min). The same procedures were performed for all negative controls except that the primary antibody was omitted. Color development was done with 3-amino-9-ethyl-carbazole (AEC, Sigma,

Steinheim, Germany), and finally the sections were counterstained with hematoxylin (Fluka Chemie, Buchs, Switzerland).

To determine the inflammatory cell infiltration during the time course, sections were stained for neutrophils (monoclonal rat anti-mouse neutrophils, Serotec Ltd. Oxford, UK), macrophages (rat anti-mouse F4/80, Serotec Ltd. Oxford, UK) and lymphocytes (polyclonal hamster anti-mouse CD3ε, BD Pharmingen, USA), as described previously by our lab [11] and [12].

2.6. In situ zymography (ISZ) and double-staining for TIMP-1

Cryosections (5 μm, $n = 3$ per time point) on glass slides were covered with DQ™ collagen type I from bovine skin conjugated to fluorescein (Invitrogen, Breda, the Netherlands) as a substrate. The fluorescence of this substrate is fully quenched. Upon cleavage by active MMPs, the substrate is dequenched and starts to fluoresce (excitation 495 nm/ emission 515 nm). The substrate was diluted to 100 μg/ml in 50 mm Tris–HCl (pH 7.4), containing 16 mm $CaCl_2$, 0.05% Brij 35 (all obtained from Sigma–Aldrich, Zwijndrecht, the Netherlands) in the presence of the serine-protease inhibitor PMSF (5 mmol/l (Fluka Chemie, Buchs, Switzerland). The slides were incubated in a humified chamber in the dark at 37 °C for 2 h. After incubation, unbound substrate was washed off with distilled water, followed by incubation with 1% Triton X-100 for 10 min. Next, the slides were incubated with 4′,6-diamidino-2-phenylindole (DAPI) (Sigma–Aldrich, Zwijndrecht, the Netherlands) to stain cell nuclei and mounted in Citifluor (Agar Scientific, Stansted, UK) and examined under a fluorescence microscope. As a negative control the substrate was omitted to determine the autofluorescence of the sections. Other negative control slides were pre-incubated with the general MMP inhibitor 10-phenanthroline monohydrate (Sigma–Aldrich, Zwijndrecht, the Netherlands) at a concentration of 20 μg/ml in 50 mm Tris–HCl (pH 7.4). Each section was viewed using a Leica fluorescent microscope with FITC filter (Leica Microsystems, Rijswijk, the Netherlands), fitted with a Leica DC350 FX high resolution fluorescence digital camera and Leica

Qwin Pro image analysis software (Leica Microsystems, Rijswijk, the Netherlands).

For combining ISZ with staining for TIMP-1, sections were stained as described above, except that the PO-conjugated antibodies were replaced by antibodies conjugated with Cy3 (Zymed Laboratories Inc., San Francisco, USA). Subsequently, ISZ was performed as described.

2.7. Quantification of TIMP-1 expression and MMP activity

GDSC and HDSC sections showed distinct patterns in the TIMP-1 expression and MMP activity. To further quantify the number of cells that associated to TIMP-1 expression and MMP activity, three representative images (magnification: 40×) of each tissue section were analyzed with a Tissue-Quest® 2.2 software, Zeiss AxioImager Z1 Microscope System (Tissue-Gnostics GmbH, Vienna, Austria). Single cells were identified by their nuclei (DAPI staining). This identification mask was then applied to determine gray values in the two corresponding channels (TIMP-1 and ISZ) of each object in all images. The percentage of cells that associated with TIMP-1 expression and MMP activity was determined and depicted as scattergrams respectively. Each scattergram represents average values calculated from analysis of all three images of one entire tissue section. Pictures were digitalized, analyzed, and protein expression was quantified.

2.8. Statistical analyses

All quantitative data are presented as mean ± SD. The data were analyzed using statistical software (GraphPad Prism, GraphPad Software Inc.). Differences within groups were analyzed by two-way ANOVA followed by Tukey's *post hoc* test. Differences between groups were analyzed by one-way ANOVA and Student's *t*-test. A difference of $p < 0.05$ was considered statistically significant.

3. Results

3.1. Degradation, cellular ingrowth and cell infiltration

The FBR against the subcutaneously implanted disks differed between GDSC and HDSC. During the 28 day course of the investigation, degradation took place only in GDSC disks but not

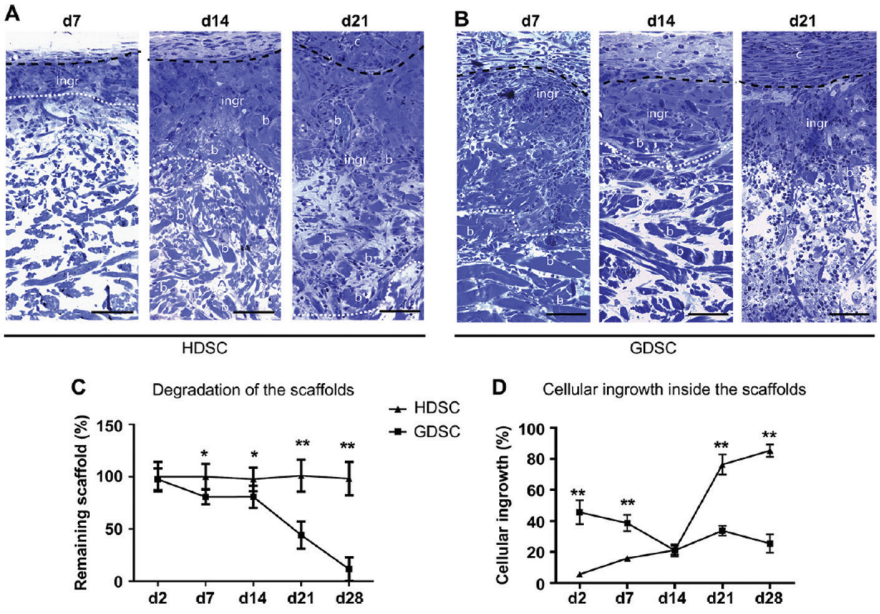

Figure 3.1. Comparison of degradation and cellular ingrowth between HDSC and GDSC disks in the foreign body reaction. The upper panel shows the fate of HDSC (A) and GDSC (B) at day 7, day 14 and day 21 (staining by means of toluidine blue; scale bar ¼ 50 mm). The lower panel shows the quantification of degradation (C) and cellular ingrowth (D) in HDSC and GDSC throughout the time course. Values are depicted as mean S.D. (n : 5 for each group). * : $p < 0.05$; ** : $p < 0.01$.

in HDSC disks. The average size of GDSC disks had decreased by around 20% at day 7, and did not change until day 14. Between day 14 and day 28, more than 90% of the GDSC disks had degraded (Fig. 3.1A, C). In contrast, the size of the HDSC disks remained unchanged throughout the time course (Fig. 3.1B, C).

The process of cellular ingrowth also differed between GDSC and HDSC. In GDSC, cellular ingrowth was higher at day 2 and 7 than in HDSC (≥40% in GDSC and <20% in HDSC), whereas cellular ingrowth in HDSC (≥70%) was at least twice as high at day 21 and 28 than in GDSC due to a steep increase in cellular ingrowth in the HDSC disk after day 14 (Fig. 3.1A, B, D). At day 28, almost the whole HDSC disk (>80%) had filled with infiltrated inflammatory cells and stroma deposition (Fig. 3.1B, D).

To determine the quality and quantity of cells involved in the FBR, we assessed numbers of neutrophils, macrophages, foreign body giant cells and lymphocytes. Inside the HDSC disks only low numbers of neutrophils were observed at day 2 which rapidly disappeared (Fig. 3.2A). The number of neutrophils was much higher (>10 fold) in GDSC than in HDSC during the whole process of the FBR. In the GDSC implants, neutrophils were always present and their numbers varied during the entire time course, peaking at day 2 and day 21 with a dip at day 14 (Fig. 3.2A). This bimodal distribution is indicative for the appearance of two waves of neutrophils. The presence of macrophages gradually increased at both materials and their numbers did not differ between GDSC and HDSC during the whole time course except at day 28, at which 80% less macrophages were present in GDSC which correlates with the high degradation of the GDSC (Fig. 3.2B). Giant cells were first observed at day 7 in both biomaterials. The number of giant cells in GDSC remained at relatively low or near absent levels after day 7, while in HDSC, the number of giant cells rapidly increased, and reached a maximum after day 21 (Fig. 3.2C). Lymphocytes were only sporadically present (<1% of the cell population) during the entire FBR in both biomaterials (data not shown).

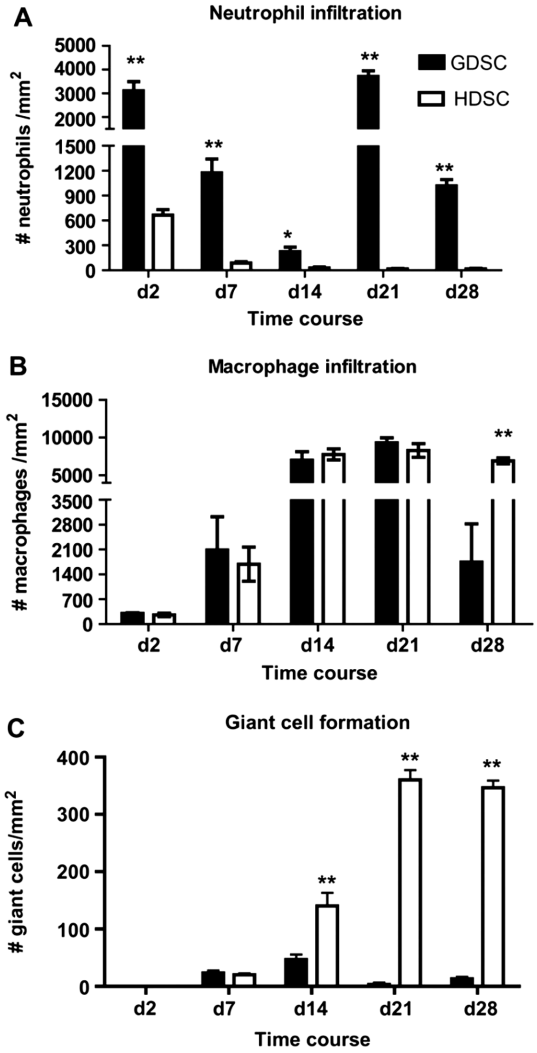

Figure 3.2. Comparison of cellular infiltration between HDSC and GDSC scaffolds in the foreign body reaction. (A) Higher numbers of neutrophils were present in GDSC than HDSC throughout time, and reached peaks at day 2 and day 21 in GDSC. (B) Comparable number of macrophages were present in both scaffolds at all time points except day 28, by which GDSC was almost completely degraded. (C) The giant cells were present from day 7 onwards and the numbers were increasing according to the time in HDSC, while in GDSC the giant cells were nearly absent. Values are depicted as mean S.D. (n : 6 for each group). * : $p < 0.05$; ** : $p < 0.01$.

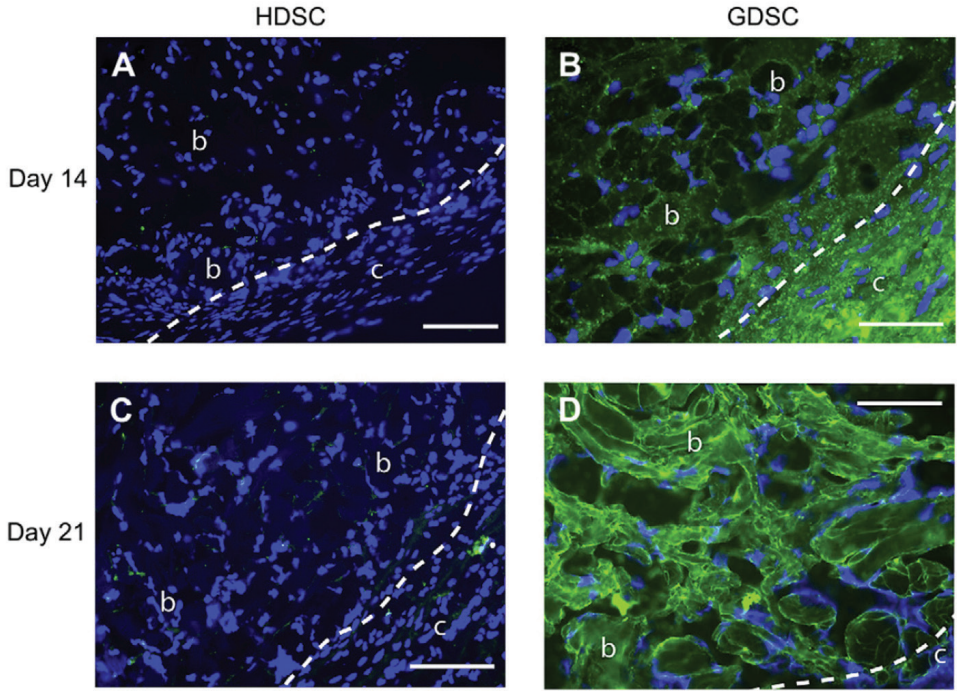

Figure. 3.3 Collagenolytic activity in HDSC and GDSC scaffolds at day 14 and day 21 after implantation. Nearly no collagenolytic activity in HDSC was seen at day 14 (A) and day 21 (C). Marked collagenolytic activity was observed in GDSC at day 14 and day 21, and the activity shifted from the fibro-capsule at day 14 (B) to the GDSC collagen bundles at day 21 (D). Symbols: b : collagen bundle, c : fibro-capsule; b : collagen bundle. Scale bar : 20 mm.

3.2. Scaffold degradation: cellular and molecular regulatory mechanisms

Both extracellular (enzymatic) and intracellular (phagocytic) degradation was observed for GDSC implants while HDSC implants were not degraded either way. *In situ* zymography showed a high collagenolytic activity in GDSC disks during the progression of FBR at day 14 and 21 (Fig. 3.3B, D). This enzyme activity was associated with the collagen bundles. In contrast, MMP activity was absent in HDSC disks

at all time points (Fig. 3.3A, C). Phagocytosis of implanted collagen by macrophages was observed in GDSC at day 2 and day 21 only (Fig. 3.4B, D); in HDSC, phagocytosis was never observed (Fig. 3.4A, C).

As shown by immunohistochemistry, protein staining of TIMP-1 in HDSC was markedly higher than that in GDSC at day 14. In HDSC, TIMP-1 was present both in the capsule and in the biomaterial, while in GDSC, the expression of TIMP-1 in the biomaterial was negligible (Fig. 3.5A, B). Notably, the presence of TIMP-1 coincided with an absence of the collagenolytic activity as revealed by *in situ* zymography (Fig. 3.5A, B). The quantification of TIMP-1 and MMP activity showed

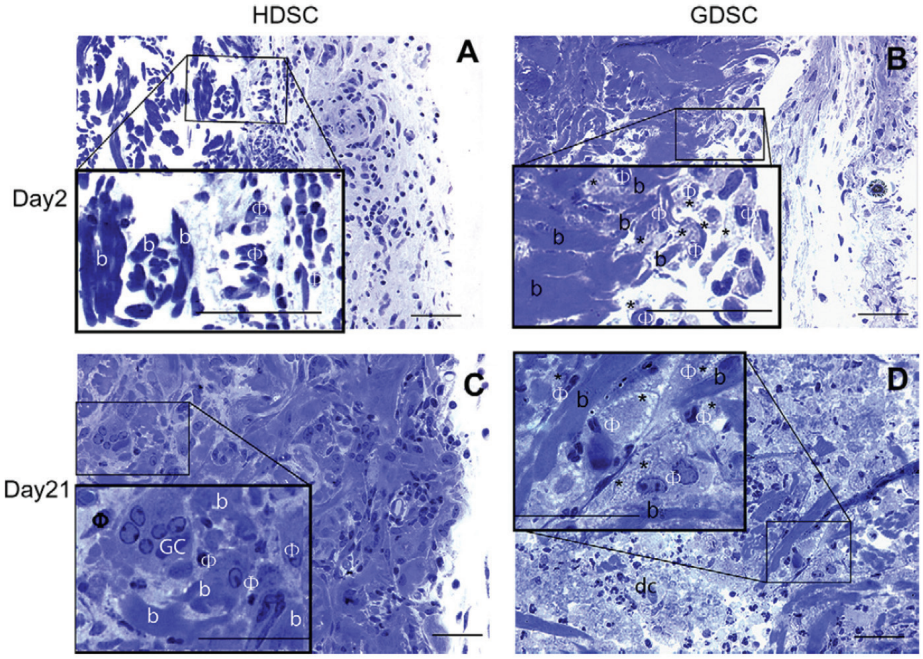

Figure 3.4. Phagocytosis in HDSC and GDSC scaffolds during the foreign body reaction. No phagocytosis was observed in HDSC throughout the time course (A, C). Marked phagocytosis by macrophages was observed in GDSC only at day 2 (B) and day 21 (D). Symbols: F : macrophage; b : collagen bundle; dc : dead cell. Scale bar : 20 mm; the tissue slices are stained with toluidine blue.

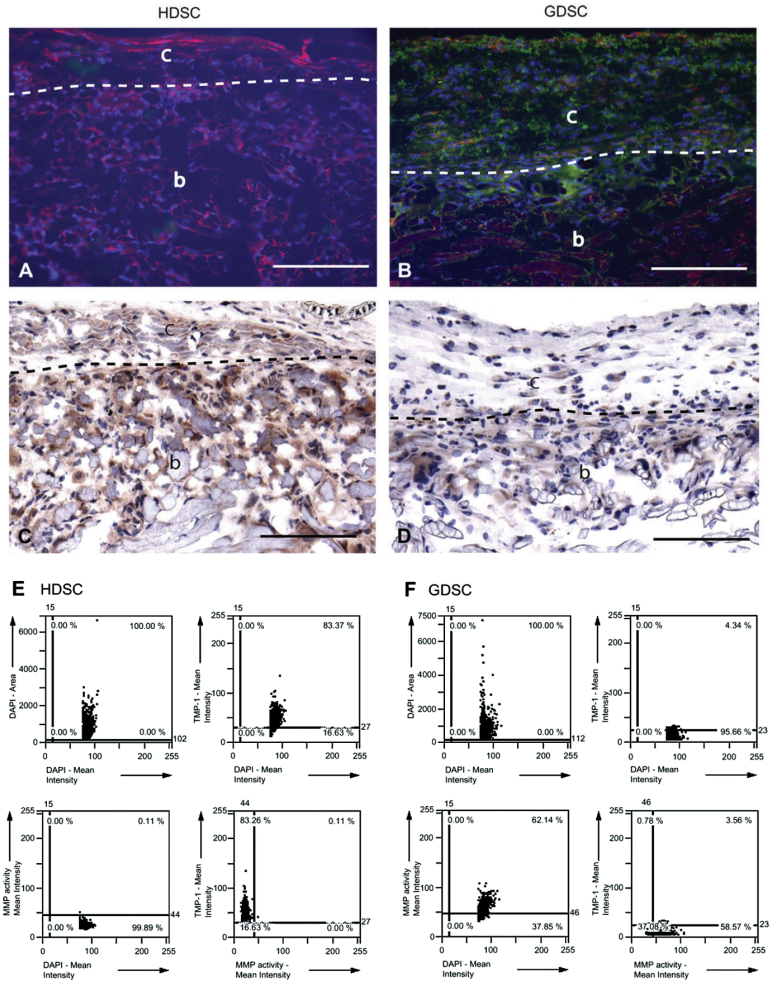

Figure 3.5. Collagenolytic activity and its relation with the expression of TIMP-1 and IL-10 in HDSC and GDSC scaffolds during the foreign body reaction. (A) The high level of TIMP-1 protein (red) resulted in the absence of collagenolytic activity (green) in HDSC. (B) In contrast, the near absence of TIMP-1 protein resulted in a marked collagenolytic activity in the capsule surrounding GDSC. (C,D) Immunohistochemistry shows the same distribution patterns of IL-10 (brown) as that of TIMP-1 in HDSC and GDSC, respectively. (E,F) Quantification of TIMP-1 expression and MMP activity in GDSC and HDSC using Tissue-Quest 2.2. Scattergrams show the percentages of cells that associated with TIMP-1 expression and MMP activity in HDSC (E) and GDSC (F), n : 3 for each scattergram. Symbols: c : fibro-capsule; b : collagen bundle. Scale bar : 20 mm.

that in HDSC more than 80% cells express TIMP-1 while less than 1% cells show MMP activity (Fig. 3.5E); In contrast, less than 5% cells express TIMP-1 and more than 60% cells show MMP activity in GDSC (Fig. 3.5F). Furthermore, we also investigated the presence of IL-10, which is a cytokine that upregulates transcription of the TIMP-1 gene. Immunohistochemistry showed higher IL-10 protein expression in HDSC than in GDSC (Fig. 3.5C, D). Indeed, the expression pattern of IL-10 largely coincided with the distribution pattern with TIMP-1 in the capsule. In contrast to TIMP-1, IL-10 was also expressed in the outer rim of the biomaterial in GDSC disks (Fig. 3.5C, D).

Because IL-10 apparently plays an important role in the initiation of TIMP-1 expression and thus in regulating the degradation rate of the scaffolds, we investigated the cellular origin of IL-10. As shown in the immunohistochemical staining, the presence of IL-10 in HDSC strongly correlated with IL-10 expressing giant cells but not that of macrophages (Fig. 3.6A, B). In fact, the majority of giant cells expressed IL-10. In contrast, in GDSC only few cells expressed IL-10, which may be related to the near absence of giant cells in this type of scaffold (Fig. 3.6A, C). More than 90% of giant cells in HDSC and 50% of giant cells in GDSC expressed IL-10 whereas less than 3% of macrophages expressed IL-10 in both biomaterials (data not shown). Therefore, the IL-10 seems to be primarily produced by giant cells at all time points, albeit at levels that is material-dependant.

3.3. Molecular mediators/regulators during the FBR

To further dissect the micro-environment of the FBR, we analyzed and compared the expression of known mediators of macrophage and giant function. For this the gene expression was determined of chemokines (MCP-1; MIP-1α) and cytokines (IL-4, IL-6, IL-10, IL-13, IFN-γ, TGF-β) in HDSC and GDSC. Our data showed that both MIP-1α and MCP-1 are always expressed, but that there seems to be a tendency that MCP-1 is less expressed at later time points in both materials (Fig. 3.7). The expression of monocyte/macrophage attractants MCP-1 and MIP-1α were comparable

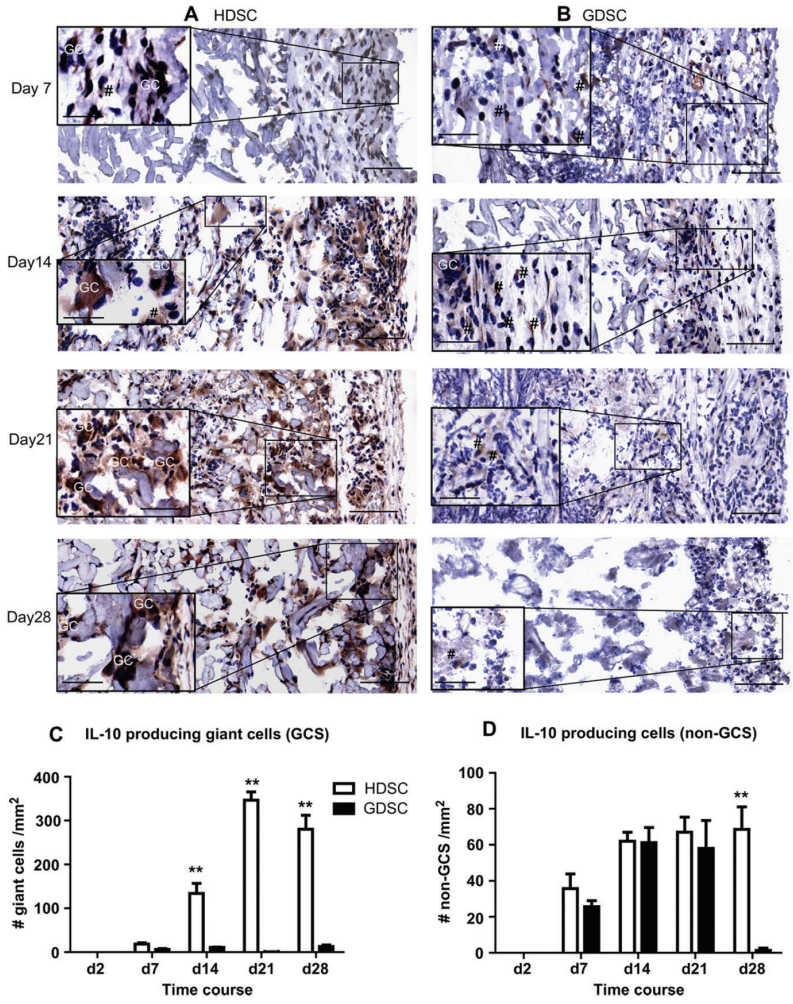

Figure 3.6. IL-10 expression is largely associated with the presence of giant cells. (A,B) Immunohistochemistry of IL-10 (brown) show that IL-10 is mainly produced in HDSC (A) and nearly absent in GDSC (B). Scale bar :10 mm for the inserts and 30 mm for the rest. (C,D) classification of IL-10 producing cells as giant cells and non-giant cells. The first IL-10 producing giant cells were seen at day 7 in HDSC, the number increased to 150/mm2 at day 14, and peaked in HDSC at day 14 and 21 (350/mm2 and 300/mm2, respectively). In contrast, less than 70/mm2 non-giant cells produced IL-10 throughout the time course (HDSC and GDSC). Hardly any giant cells were observed in GDSC. Values are depicted as mean S.D. (n : 4 for each group). Symbols: GC : giant cell; # : non-giant cell; ** : $p < 0.01$.

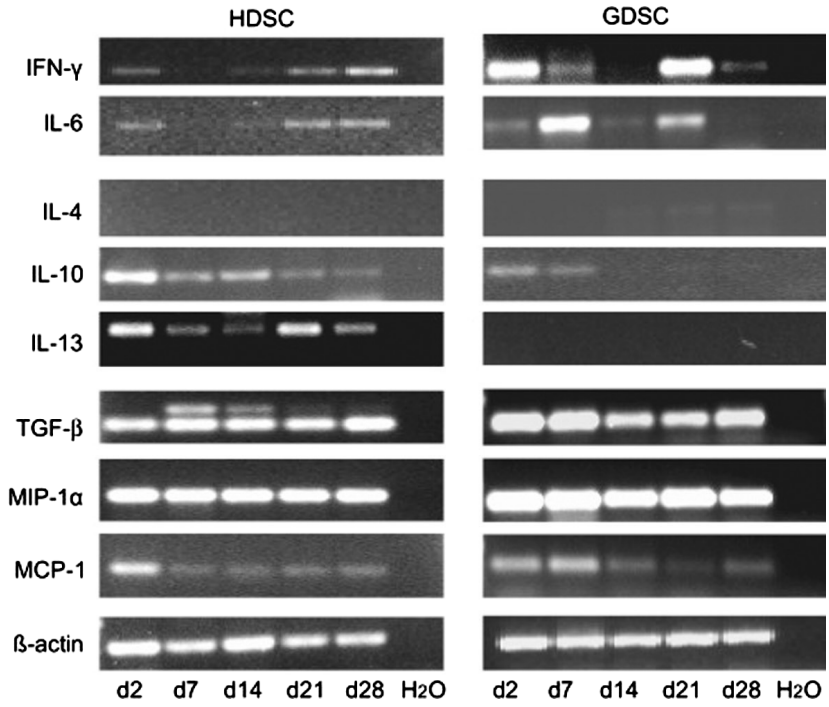

Figure 3.7. Dissection of the micro-environment in HDSC and GDSC scaffolds during the foreign body reaction. mRNA expression show that higher levels of the pro-inflammatory cytokines IL-6 and IFN-g were expressed in GDSC compared to that of HDSC. In contrast, higher levels of the anti-inflammatory cytokines IL-10 and IL-13 were expressed in HDSC compared to that of GDSC. IL-4 was absent in both scaffolds.

between the two biomaterials. As a result, we found comparable numbers of macrophages in both biomaterials (Fig. 3.3B). Expression of IL-4 was near absent in both biomaterials whereas the expression of TGF-β was high at all time points both in GDSC and HDSC (Fig. 3.7). Remarkably, distinct expression patterns of the pro-inflammatory cytokines (IL-6, IFN-γ) and anti-inflammatory cytokines (IL-10, IL-13) were observed between the two biomaterials. In GDSC, IL-13 is totally absent throughout the time course and IL-10 was expressed only during the first week. In contrast, both IL-10 and IL-13 were always expressed in HDSC during the FBR. Both IL-6 and IFN-γ showed a dynamic expression pattern, e.g.

both genes are expressed at early time points, then downregulated and upregulated again after 3 weeks. Notably, a higher expression levels of IL-6 and IFN-γ (day 2, day 21) are seen in GDSC compared to that of HDSC (Fig. 3.7). This dynamic micro-environment probably has consequences for the functioning of the macrophage and/or giant cells.

4. Discussion

The main finding of our study is, that the FBR against cross-linked dermal sheep collagen is driven by the implant micro-environment. We showed that by altering the type of cross-linking, the collagen could alter the subcutaneous micro-environment such that it was degraded. In the current study, we investigated molecular and cellular factors that were involved in the FBR of two differently cross-linked dermal sheep collagen type scaffolds (HDSC and GDSC) implanted subcutaneously in mice. It was found that HDSC was hardly degraded after 28 days, whereas GDSC was almost completely degraded. Large differences were found, amongst others, in the infiltration of neutrophils with respect to cell numbers and time course: in GDSC much higher numbers were found at all time points and infiltration took place in two waves instead of one.

Our previous studies revealed that the FBR towards hexamethylenediisocyanate cross-linked type I collagen showed large differences in mice, depending on the site of implant (subcutaneously versus epicardially). The degradation only took place epicardially and seemed correlated with the presence of neutrophils during the FBR [11] and [12]. Moreover, also Dacron, which is a non-degradable biomaterial, elicited a similar response on the heart, i.e. influx of neutrophils and associated MMP expression [12]. Clearly, in our current animal model, the subcutaneously implanted GDSC created at least part of the epicardial micro-environment via attraction of neutrophils. Neutrophils are known as one of the first groups of inflammatory cells that arrive at the implant site. Previous studies suggested that the crucial role of neutrophils in the FBR was to produce chemokines to attract other inflammatory cells, including monocytes [10]. The current study shows that, although the time course of the presence of neutrophils differed between HDSC and GDSC, the expression of monocyte attractant chemokines, MCP-1 and MIP-1α as well as the numbers of macrophages were comparable

between the two biomaterials. This indicates that – at least under the conditions of the current model– the neutrophils may not play an important role in continuously attracting inflammatory cells during the FBR process, although it might play a role in the early stage of the FBR. A more important role of neutrophils in the current model –as suggested by the obtained data– appears to be as a pro-inflammatory regulator. With the presence of neutrophils in GDSC scaffolds, pro-inflammatory factors (IL-6 and IFN-γ) were upregulated, while the anti-inflammatory factors (IL-10 and IL-13) were downregulated. It is well known that IFN-γ is secreted by lymphocytes, dendritic cells or NK cells [21] and [22]. However, our data show that none of the above cells were present in the FBR. Because of the strong correlation between the expression of IFN-γ and the presence of neutrophils (day 2 and day 21), we speculate that neutrophils contribute to the expression of IFN-γ during the FBR. Neutrophils are able to express IFN-γ [23] and [24].

The behavior of macrophages within the FBR depends on their micro-environment. Despite similar numbers of macrophages in both biomaterials, the role of macrophages in the FBR between HDSC and GDSC was fundamentally different. In GDSC, macrophages degraded the collagen bundles both by means of MMPs and by phagocytosis. Phagocytosis was only observed at day 2 and day 21. At these two time points, a high expression was found of IFN-γ a cytokine that is known to promote macrophage activation. The IFN-γ which was probably secreted by neutrophils as these cells coincided with the phagocytic behavior of the macrophages. In contrast, in HDSC the macrophages fused into the giant cells. These giant cells induced TIMP-1 expression via secretion of IL-10 protein, resulting in a net decrease of MMP activity. One of the prime factors that drives fusion of macrophages is IL-13, the difference in giant cell formation between GDSC (absent) and HDSC (present) appeared to be due to the expression of IL-13 (absent in GDSC, present in HDSC) [25],[26] and [27]. The absence of IFN-γ (and consequently the absence of phagocytic activity of macrophages) and the high levels of TIMP-1 (and consequent inhibition of collagenolytic activity) may explain the near absence of degradation of HDSC.

The current data clearly showed that not only the implant site of the scaffold in the body, but also the nature of the scaffold determines the outcome of the FBR. The scaffold itself can create its own molecular and cellular micro-environment. Notably, the GDSC created subcutaneous micro-environment differs somewhat from the epicardial micro-environment as described previously: in the current study phagocytosis occurred, which is absent in the epicardial setting. Perhaps, less IFN-γ is present epicardially. Therefore, we have in part mimicked the epicardial FBR micro-environment in subcutaneous implants by means of GDSC.

5. Conclusions

The current study shows that changes in scaffold composition, e.g. chemical cross-linkers, will result in a difference in the FBR, and that this difference is correlated with differences in inflammatory micro-environment and the presence of neutrophils. In GDSC, a strong pro-inflammatory milieu is observed. Inflammatory mediators such as IFN-γ, which seems to be secreted by neutrophils, influences the behavior of macrophages during the FBR, and leads to the degradation of the biomaterial. While in HDSC, an anti-inflammatory milieu is seen. In the presence of IL-13, macrophages fuse into foreign body giant cells and start to produce IL-10 which on its turn promoted TIMP-1 expression, finally resulting in a delay of the enzymatic degradation of collagen by MMPs. We therefore conclude that the function of macrophages in mice is largely influenced by differences in the local micro-environment induced by the implanted biomaterials and that the presence/absence of neutrophils play a major role in the shaping of this micro-environment. Our data deepen the understanding of the molecular and cellular mechanisms of the degradation of collagen scaffolds during the FBR.

Acknowledgements

This study was supported by RuG Jan Kornelis de Cock-Stiching for Q. Ye. The authors wish to acknowledge the excellent technical support of Mrs. Linda Brouwer and Mrs. Jose A. Plantinga.

References

1. R.A. Brown, J.B. Phillips. Cell responses to biomimetic protein scaffolds used in tissue repair and engineering. Int Rev Cytol, 262 (2007), pp. 75–150

2. E. Sachlos, J.T. Czernuszka. Making tissue engineering scaffolds work. Review on the application of solid freeform fabrication technology to the production of tissue engineering scaffolds. Eur Cell Mater, 5 (2003), pp. 29–39

3. H. Tai, M.L. Mather, D. Howard, W. Wang, L.J. White, J.A. Crowe *et al.* Control of pore size and structure of tissue engineering scaffolds produced by supercritical fluid processing. Eur Cell Mater, 14 (2007), pp. 64–77

4. Y.H. Choi, C. Stamm, P.E. Hammer, K.F. Kwaku, J.J. Marler, M. Jones *et al.* Cardiac conduction through engineered tissue. Am J Pathol, 169 (2006), pp. 72–85

5. D.A. Wahl, E. Sachlos, C. Liu, J.T. Czernuszka. Controlling the processing of collagen-hydroxyapatite scaffolds for bone tissue engineering. J Mater Sci Mater Med, 18 (2007), pp. 201–209

6. J.K. Leach. Multifunctional cell-instructive materials for tissue regeneration. Regen Med, 1 (2006), pp. 447–455

7. S. Munirah, S.H. Kim, B.H. Ruszymah, G. Khang. The use of fibrin and poly(lactic-co-glycolic acid) hybrid scaffold for articular cartilage tissue engineering: an in vivo analysis. Eur Cell Mater, 15 (2008), pp. 41–52

8. J.M. Anderson, J.A. Jones. Phenotypic dichotomies in the foreign body reaction. Biomaterials, 28 (2007), pp. 5114–5120

9. J.M. Anderson, A. Rodriguez, D.T. Chang. Foreign body reaction to biomaterials. Semin Immunol, 20 (2008), pp. 86–100

10. D.T. Luttikhuizen, M.C. Harmsen, M.J. van Luyn. Cellular and molecular dynamics in the foreign body reaction. Tissue Eng, 12 (2006), pp. 1955–1970

11. D.T. Luttikhuizen, M.J. van Amerongen, P.C. de Feijter, A.H. Petersen, M.C. Harmsen, M.J. van Luyn. The correlation between difference in foreign body reaction between implant locations and cytokine and MMP expression. Biomaterials, 27 (2006), pp. 5763–5770

12. M.J. van Amerongen, M.C. Harmsen, A.H. Petersen, G. Kors, M.J. van Luyn . The enzymatic degradation of scaffolds and their replacement by vascularized extracellular matrix in the murine myocardium. Biomaterials, 27 (2006), pp. 2247–2257

13. T.R. Kyriakides, M.J. Foster, G.E. Keeney, A. Tsai, C.M. Giachelli, I. Clark-Lewis *et al.* The CC chemokine ligand, CCL2/MCP1, participates in macrophage fusion and foreign body giant cell formation. Am J Pathol, 165 (2004), pp. 2157–2166I.M. Khouw, P.B. van Wachem, J.A. Plantinga, L.F. de Leij, M.J. van Luyn. Enzyme and cytokine effects on the impaired onset of the murine foreign-body reaction to dermal sheep collagen. J Biomed Mater Res, 54 (2001), pp. 234–240

14. 14. I.M. Khouw, P.B. van Wachem, J.A. Plantinga, L.F. de Leij, M.J. van Luyn. Enzyme and cytokine effects on the impaired onset of the murine foreign-body reaction to dermal sheep collagen. J Biomed Mater Res, 54 (2001), pp. 234–240

15. J.A. Jones, A.K. McNally, D.T. Chang, L.A. Qin, H. Meyerson, E. Colton *et al.* Matrix metalloproteinases and their inhibitors in the foreign body reaction on biomaterials. J Biomed Mater Res A, 84 (2008), pp. 158–166

16. D.T. Luttikhuizen, M.C. Harmsen, M.J. van Luyn. Cytokine and chemokine dynamics differ between rats and mice after collagen implantation. J Tissue

Eng Regen Med, 1 (2007), pp. 398–405

17. Q. Ye, M.J. van Amerongen, J.A. Sandham, R.A. Bank, M.J. van Luyn, M.C. Harmsen. Site-specific tissue inhibitor of metalloproteinase-1 governs the matrix metalloproteinases-dependent degradation of crosslinked collagen scaffolds and is correlated with interleukin-10. J Tissue Eng Regen Med (2010)

18. I.M. Khouw, P.B. van Wachem, G. Molema, J.A. Plantinga, L.F. de Leij, M.J. van Luyn . The foreign body reaction to a biodegradable biomaterial differs between rats and mice. J Biomed Mater Res, 52 (2000), pp. 439–446

19. P.B. van Wachem, M.J. van Luyn, L.H. Olde Damink, P.J. Dijkstra, J. Feijen, P. Nieuwenhuis . Biocompatibility and tissue regenerating capacity of cross-linked dermal sheep collagen. J Biomed Mater Res, 28 (1994), pp. 353–363

20. L.H. Olde Damink, P.J. Dijkstra, M.J. van Luyn, P.B. van Wachem, P. Nieuwenhuis, J. Feijen. Changes in the mechanical properties of dermal sheep collagen during in vitro degradation. J Biomed Mater Res, 29 (1995), pp. 139–147

21. K. Kubota. Innate IFN-gamma production by subsets of natural killer cells, natural killer T cells and gammadelta T cells in response to dying bacterial-infected macrophages. Scand J Immunol, 71 (2010), pp. 199–209

22. H. Shiomi, A. Masuda, S. Nishiumi, M. Nishida, T. Takagawa, Y. Shiomi *et al.* Gamma Interferon produced by antigen-specific CD4+ T cells regulates the mucosal immune responses to citrobacter rodentium infection. Infect Immun, 78 (2010), pp. 2653–2666

23. L. Li, L. Huang, S.S. Sung, P.I. Lobo, M.G. Brown, R.K. Gregg *et al.* NKT Cell Activation mediates neutrophil IFN-gamma production and renal ischemia-reperfusion injury. J Immunol, 178 (2007), pp. 5899–5911

24. M.F. Denny, S. Yalavarthi, W. Zhao, S.G. Thacker, M. Anderson, A.R. Sandy

et al. A distinct subset of proinflammatory neutrophils isolated from patients with systemic lupus erythematosus induces vascular damage and synthesizes type I IFNs. J Immunol, 184 (2010), pp. 3284–3297

25. T. Ikeda, K. Ikeda, K. Sasaki, K. Kawakami, K. Hatake, Y. Kaji *et al.* IL-13 as well as IL-4 induces monocytes/macrophages and a monoblastic cell line (UG3) to differentiate into multinucleated giant cells in the presence of M-CSF. Biochem Biophys Res Commun, 253 (1998), pp. 265–272

26. K.M. DeFife, C.R. Jenney, E. Colton, J.M. Anderson . Cytoskeletal and adhesive structural polarizations accompany IL-13-induced human macrophage fusion. J Histochem Cytochem, 47 (1999), pp. 65–74

27. K.M. DeFife, C.R. Jenney, A.K. McNally, E. Colton, J.M. Anderson . Interleukin-13 induces human monocyte/macrophage fusion and macrophage mannose receptor expression. J Immunol, 158 (1997), pp. 3385–3390

CHAPTER 4

ENDO180 AND MT1-MMP ARE INVOLVED IN THE PHAGOCYTOSIS OF COLLAGEN SCAFFOLDS BY MACROPHAGES AND IS REGULATED BY INTERFERON-GAMMA

Qingsong Ye [1,2,3]
Quang Xing [2]
Yijin Ren [2]
Martin C. Harmsen [1]
Ruud A. Bank [1]

[1] Stem Cell and Tissue Engineering Research Group, Department of Pathology and Medical Biology, University of Groningen, The Netherlands

[2] Department of Orthodontics, University Medical Centre Groningen, University of Groningen, The Netherlands

[3] School of Medicine and Dentistry, James Cook University, Cairns, Australia

EUROPEAN CELLS AND MATERIALS VOL.20 2010 (PAGES 197-209)

Abstract

Subcutaneously implanted disks of hexamethylenediisocyanate or glutaraldehyde cross-linked sheep collagen (referred to as HDSC and GDSC, respectively) in mice show large differences in degradation rate. Although comparable numbers of macrophages are seen in HDSC and GDSC, phagocytosis of collagen by macrophages occurred only in GDSC. The molecular mechanisms involved in the phagocytosis of collagen by macrophages are essentially unknown. Immunofluorescence and RT-PCR showed that Endo180 was expressed in GDSC only. TissueFaxs showed that Endo180 co-localized with MT1- MMP on F4/80 positive cells, which is likely responsible for the phagocytosis in GDSC. RT-PCR further showed that Endo180 expression correlated with high levels of IFN- γ mRNA. *In vitro*, IFN-γ induced the expression Endo180 and MT1-MMP in murine macrophages cultured on collagen type I (although too high levels of IFN-γ dampened the expression of Endo180 and MT1-MMP). Moreover, the expression of Endo180 and MT1-MMP induced by IFN- γ can be inhibited through IL-10. The differences in microenvironment between GDSC and HDSC (high IFN- γ and low IL-10 levels in GDSC, low IFN-γ and high IL- 10 levels in HDSC) provide an explanation why phagocytosis of collagen by macrophages is only seen in GDSC. In summary, we show for the first time that the IFN-γ dependent co-expression of Endo180 and MT1- MMP on macrophages coincides with collagen phagocytosis, thus providing evidence that the mechanism of collagen phagocytosis operating in the foreign body reaction by macrophages is comparable with the mechanism of intracellular collagen degradation by fibroblasts seen under physiological conditions.

Introduction

The interaction of tissues with biomaterials is a field of crucial importance to all kinds of medical technologies, including tissue engineering (Sachlos *et al.*, 2006; Tai *et al.*, 2007; Munirah *et al.*, 2008). The tissue response towards implanted biomaterials, also called the foreign body reaction, is influenced to a large degree by the morphology and composition of the biomaterial, and the location where the biomaterial is implanted (Luttikhuizen *et al.*, 2006a; Anderson and Jones, 2007; Yeghiazaryan *et al.*, 2007; Anderson *et al.*, 2008; Dinnes *et al.*, 2008). By changing certain biochemical or biophysical characteristics (Khouw *et al.*, 1998; Van Putten *et al.*, 2009), the tissue response will alter, for example by attracting more or specific cells to the scaffold. The microenvironment of the implant further changes due to the secretion of proteins by the attracted cells as they secrete cytokines and/or chemokines. The microenvironment by itself also has a major impact on the phenotypic properties of macrophages (Luttikhuizen *et al.*, 2006b; Luttikhuizen *et al.*, 2007), a cell type that plays a central role in the outcome of the foreign body reaction (Brown *et al.*, 2009; Valentin *et al.*, 2009). Macrophage activation gives rise to different populations of cells with distinct functions (Mosser and Edwards, 2008), and it has been shown that the phenotype of the macrophages participating in the foreign body reaction is a determinant of biological scaffold remodelling (Badylak *et al.*, 2008; Brown *et al.*, 2009).

Collagen scaffolds are often used in tissue engineering. We have recently observed that there are marked differences in the degradation rate of two differently crosslinked dermal sheep collagen scaffolds (hexamethylenediisocyanate and glutaraldehyde cross-linked, referred to as HDSC and GDSC, respectively) in mice implanted in one anatomical location, namely subcutaneously (Ye *et al.*, submitted). GDSC disks were almost completely degraded after four weeks, whereas HDSC disks did not degrade after four weeks. Phagocytosis was seen in GDSC

disks at certain time points (day 2 and day 21); furthermore, increased matrix metalloproteinase (MMP) activities were seen. In HDSC disks, no phagocytic activity was seen, and collagenolytic activity was effectively inhibited by increased levels of the tissue inhibitor of matrix metalloproteinase TIMP-1. Phagocytosis of GDSC coincided with high levels of interferon-gamma (IFN-γ) in the microenvironment; in HDSC disks less IFN-γ is seen in combination with increased levels of interleukin-10 (IL-10). The high levels of IFN-γ were attributed to the infiltration of neutrophils in GDSC, whereas the increased levels of IL-10 was attributed to the presence of giant cells in HDSC (Ye *et al.*, submitted).

Although phagocytosis of the collagen by macrophages has repeatedly been reported (Parakkal, 1969; Knapp *et al.*, 1974; Deporter, 1979; Svoboda and Deporter, 1980; Inouye *et al.*, 1983; Ciapetti *et al.*, 1996; Lucattelli *et al.*, 2003), and it is intuitive and logical that phagocytic cells such as macrophages are involved in phagocytosis of collagen bundles, essentially nothing is known about this phenomenon in the foreign body reaction and the mediators of this process. In fibroblasts, phagocytosis and intracellular digestion of collagen is intensively studied (Everts *et al.*, 1996). The membrane-bound matrix metalloproteinase MT1-MMP plays an essential role in collagen phagocytosis of fibroblasts (Beertsen *et al.*, 2002; Lee *et al.*, 2006; Lee *et al.*, 2007). It has recently been postulated that the urokinase plasminogen activator receptor-associated protein (also known as uPARAP or Endo180) is, in combination with the membrane-bound matrix metalloproteinase MT1-MMP, responsible for the phagocytic uptake of collagen by fibroblasts (Engelholm *et al.*, 2003b; Madsen *et al.*, 2007). Endo180 is a membrane-bound receptor that is able to bind collagen and is involved in the subsequent endocytic collagen uptake (East *et al.*, 2003; Behrent and Bugge (2003); Wienke *et al.*, 2003; Kjoller *et al.*, 2004; Curino *et al.*, 2005; Mousavi *et al.*, 2005; Thomas *et al.*, 2005). Although Endo180 has been reported to be present on macrophages (Sheikh *et al.*, 2000; Honardoust *et al.*, 2006), nothing is known about its role in collagen phagocytosis by macrophages. In this paper we have investigated whether there is a relationship between the expression of Endo180 and MT1-MMP and the presence/absence of collagen phagocytosis by macrophages in GDSC and HDSC, respectively.

Furthermore, we investigated whether IFN-γ and IL-10 are involved in the regulation of Endo180 and MT1-MMP expression.

Materials and Methods

Biomaterial processing

Non-crosslinked dermal sheep collagen (DSC), processed from sheep skin, was obtained from the Zuid-Nederlandse Zeemlederfabriek (Oosterhout, the Netherlands). DSC was crosslinked with either glutaraldehyde (henceforth referred to as GDSC) or hexamethylenediisocyanate (henceforth referred to as HDSC), according to the protocols described previously (Van Wachem *et al*., 1994; Olde Damink *et al*., 1995). Disks (6 mm in diameter, 0.75 mm in thickness) were punched from pieces of HDSC and GDSC from the same batch, and sterilized with ethylene oxide. Endotoxin content of surface-associated endotoxin levels of Col-I disks were below 0.25 EU/ml, as determined by the LALmethod (LAL kinetic-QCL®; Cambrex, East Rutherford, NJ, USA).

Animals and operating procedures

All procedures performed on animals were approved by the local committee for care and use of laboratory animals of the University of Groningen and were performed according to international and governmental guidelines on animal experimentation. Male C57BL/6 mice (10 weeks old, Harlan, Horst, The Netherlands) were housed individually in a conventional condition with food and water *ad libitum*. Mice were anaesthetized with 4% isoflurane and maintained by 2% isoflurane inhalation in combination with a mixture of equal volumes of N2O and O2. The back was shaved and disinfected with chlorhexidine, two incisions were made and subcutaneous pockets were created on both sides. The HDSC or GDSC scaffolds were implanted about one centimetre away from the incision site, thus minimising the effect of wound healing on the foreign body reaction itself. The incisions were closed with 6-0

non-absorbable Prolene sutures. Finally, mice received pure oxygen until awakening. The Col-I disks (HDSC or GDSC) were removed at the following time points after implantation (related to the different phases of the FBR in mice): 2 days (onset), 7 days (early progression), 14 and 21 days (intermediate progression), and 28 days (late progression), n=6 per time point. The disks were snap-frozen in liquid nitrogen immediately after explantation.

Cell culture and interventions

The murine monocytic macrophage cell line RAW 264.7 (American Type Culture Collection, ATCC, Manassas, VA, USA) was cultured in RPMI-1640 (BioWhittaker, Verviers, Belgium) with 10% foetal bovine serum (FBS), supplemented with 2 mM glutamine, 100 μg/ml streptomycin and 100 IU/ml penicillin.

The 6-well cell culture plates (BD Falcon™, Franklin Lakes, NJ, USA) and 6-well diagnostic slides (Menzel- Glaser, Braunschweig, Germany) were coated overnight at 37°C in a humidified 5% CO2 atmosphere using 300 μg/ml rat tail type I collagen (BD Bioscience) in 1 mM NaOH/PBS (1 ml/well for culture plates and 100 μl/well for diagnostic slides). RAW 264.7 cells (1.2 × 104 cells/ cm2) were seeded into 6-well cell culture plates and 6- well diagnostic slides with or without collagen coating. After a preincubation of 24 hours, the cells were treated with different concentrations of inflammatory mediators: recombinant human IFN-γ (PeproTech, London, UK) from 0 to 25 ng/ml, recombinant human IL-1β (PeproTech) from 0 to 25 ng/ml, recombinant murine TNF-α (BioVision, Mountain View, CA, USA) from 0 to 25 ng/ml, and recombinant murine IL-10 (R&D Systems Inc., Minneapolis, MN, USA) from 0 to 25 ng/ml together with 2.5 ng/ml human IFN-γ. All cells were subsequently incubated at 37°C in a humidified 5% CO2 atmosphere for 48 h. The cells in the culture plates were then harvested for gene expression analysis by Reverse Transcription Polymerase Chain Reaction (RT-PCR), and cells on the slides were used for *in situ* detection of Endo 180 and MT1-MMP proteins by immunofluorescence staining. N=5 for all *in vitro* experiments.

Gene expression analysis

One μg of total RNA (either extracted from snap frozen explants or RAW 267.4 cells) was used to generate the first strand cDNA synthesis using M-MuLV reverse transcriptase (MBI Fermentas, St. Leon-Rot, Germany) and random hexamer primers, according to the manufacturer's protocol. Ten ng of cDNA were used for each PCR reaction. PCR for Endo180, IFN-γ and the housekeeping gene β- actin was performed in a final reaction volume of 25 μl containing 1.5 mM MgCl2, 0.25 mM dNTP mix, 1 μM primer Mix and 1 U Taq DNA polymerase.

Primer sequences

Endo180
GGCATCACTGTAGATCACTTGG (forward)
ATCCGAGCACAGCGCTAGGG (reverse)
IFN-γ
TGGAGGAACTGGCAAAAGGATGGT (forward)
TTGGGACAATCTCTTCCCCAC (reverse)
β-**actin**
GTGAAAAGATGACCCAGATCAT (forward)
GCTTCTCTTTGATGTCACGCACGAT (reverse)

Amplification was performed on a MyCycler (Bio-Rad, Hercules, CA, USA) for 35 cycles at annealing temperature of 66°C, 56°C and 60°C for Endo180, IFN-γ and β-actin, respectively. The amplimers were separated in a 2% agarose gel.

Immunofluorescence microscopy

Expression of Endo180 and MT1-MMP *in vivo* and *in vitro* was verified by means of *in situ* immunofluorescent staining on explants of two materials at all time points and on cells cultured on the diagnostic slides. Tissue sections (5 μm) were mounted on silane-coated

slides. Both cryosections and cell cultured slides were fixed with 2% paraformaldehyde (PFA)/PBS at room temperature (RT) for 10 min, then washed in 0.1% Triton X-100 in PBS (5 min) for 3 times. After that, samples were incubated with 1:100 goat anti-mouse Endo180 antibody (Santa Cruz Biotechnology, Santa Cruz, CA, USA) and 1:200 rabbit anti-mouse MT1-MMP antibody (Epitomics Inc.,Burlingame, CA, USA) in PBS with 0.5% Triton X-100 and 2% normal goat serum for 2.5 h in the dark at RT. After incubation, samples were washed in 0.1% Triton X-100 in PBS (5 min) for 3 times. The secondary antibody for MT1-MMP, namely swine anti-rabbit FITC (1:100, Dako, Carpinteria, CA, USA) in PBS with 4',6-diamidino- 2-phenylindole (DAPI, 1:5000, Sigma-Aldrich, Zwijndrecht, The Netherlands), was incubated for 30 min. Samples were then washed in 0.1% Triton X-100 in PBS (5 min) for 4 times to wash off non-bound secondary antibodies (FITC). The secondary antibody for Endo180, namely rabbit anti-goat Cy3 (1:100, Zymed Laboratories Inc., San Francisco, CA, USA) in PBS with DAPI (1:5000) was incubated for 30 min. Next, samples were washed 4 times in 0.1% Triton X-100 in 1x PBS (5 min) to wash off the secondary antibodies (Cy3). Samples were mounted with Citifluor (London, UK) followed by examination under the immunofluorescence microscope.

To unravel the identity of the Endo180 expressing cells, a double staining was performed as described above using the previously mentioned Endo180 antibodies (in combination with rabbit anti-goat Cy3) together with a murine macrophage marker, rat anti-mouse F4/80 antibodies (1:100, Serotec Ltd. Oxford, UK). After incubation in combination with .with primary antibodies for 2.5 h, The secondary antibody for Endo180 (1:100, rabbit anti-goat Cy3) in PBS with DAPI (1:5000) was added and incubated for 30 min. Samples were then washed in 0.1% Triton X-100 in PBS (5 min) for 4 times to wash off non-bound secondary antibodies (Cy 3). The secondary antibody for F4/80, namely goat anti rat FITC (1:100; Southern Biotech, Birmingham, AL, USA) was incubated for 30 min. thereafter, samples were washed 4 times in 0.1% Triton X-100 in 1x PBS (5 min) to wash off the secondary antibodies (FITC). Finally, samples were mounted with Citifluor followed by examination under the immunofluorescence microscope.

For the negative controls, samples were stained as described above, except that the primary antibodies were replaced with the same dilution of serum from the same species as used for the specific first antibodies, namely, normal goat serum (1:100, Sanquin Pharmaceutical Services, Amsterdam, Netherlands), normal rabbit serum (1:200, Dako, Carpinteria, USA) and normal rat serum (1:100, Invitrogen, Carlsbad, CA, USA) for Endo180, MT1-MMP and F4/80, respectively.

Each section was viewed using a Leica DMRXA Immumofluorescence microscope (Leica Microsystems, Rijswijk, The Netherlands) with FITC and Cy3 filter, fitted with a Leica DC350 FX high resolution fluorescence digital camera and Leica Qwin Pro image analysis software. A compensation procedure was performed to prevent the influence of the overlap between FITC and Cy3.

Quantification of Endo180 and MT1-MMP immunostaining

To further quantify the number of cells with Endo180, MT1-MMP and F4/80 immunostaining, three representative images (magnification: 40×) of each tissue section were analyzed with TissueFaxs®, Zeiss AxioImager Z1 Microscope System (Tissue-Gnostics GmbH, Vienna, Austria). Single cells were identified by their nuclei (DAPI staining). This identification mask was then applied to determine gray values in the two corresponding channels FITC (MT1-MMP or F4/80) and Cy3 (Endo180) of each object in all images. The percentage of MT1-MMP or F4/ 80 and Endo180 positive cells was determined and depicted as scattergrams. Each scattergram represents average values calculated from analysis of all three images of one entire tissue section. Based on the degree of fluorescence intensity in the negative controls, appropriate threshold values for positive immunofluorescence staining were defined. Pictures were digitised, analysed, and protein expression was quantified. To quantify the fraction of MT1-MMP and Endo180 positive cells cultured on 6-well diagnostic slides, four representative fields (20×) were taken in each well. Percentages of MT1-MMP or Endo180 positive cells were determined through counting the total cell number and the

number of MT1-MMP or Endo180 positive cells in each micrograph. The experiments were repeated 4 times. Data from these experiments (n=5 ; *x4*) were presented as average percentage of positive cells.

Statistical analyses

All quantitative data are indicated as mean ± standard deviation (SD). The data were analyzed using statistical software (GraphPad Prism, GraphPad Software, La Jolla, CA, USA). Differences were analyzed by two-way ANOVA followed by *post hoc* Tukey's test. A difference of $p<0.05$ was considered statistically significant.

Results

Phagocytosis of collagen bundles is correlated with the co-expression of the membrane proteins MT1- MMP and Endo180

We have shown previously that phagocytosis of implanted collagen by macrophages was observed in GDSC at day 2 and day 21 (and not at day 7, 14 and 28). Mononuclear cells closely aligned to the biomaterial were considered phagocytic macrophages, especially when the cells show an accumulation of vacuoles or when the biomaterial has a more irregular shape opposite the cell (Fig. 4.2E). In HDSC, phagocytosis was never observed. Since nothing is known about the molecular mechanisms how macrophages phagocytose collagen, here we continue our previous study regarding GDSC and HDSC disks to further investigate the expression of Endo180 and MT1-MMP, membranebound proteins that are known to be involved in the phagocytosis of collagen in fibroblasts. In GDSC the Endo180 gene was expressed at days 2, 7 and day 21, but its expression was absent in HDSC at all time points (Fig. 4.1A). In GDSC, immunohistochemistry revealed that although MT1-

Figure 4.1 (on next page) Gene transcript and/or protein expression analysis of IFN-γ, MT1-MMP and Endo180 in HDSC and GDSC scaffolds during the foreign body reaction in mice. Gene transcript was performed for IFN-γ and Endo180 in both collagen scaffolds at all time points (A). Protein expression analysis of MT1-MMP and Endo180 in HDSC and GDSC scaffolds at day 14 (B1-B4, D1-D4) and day 21(C1-C4, E1-E4): MT1-MMP protein (FITC, green) was expressed in both biomaterials (B2, C2, D2, E2). In contrast, the expression of Endo180 (Cy3, red) was mainly observed in GDSC at day 21 (C3) and low at day 14 (B3). In HDSC, Endo180 expression was not observed D3, E3). Cell nuclei were stained with DAPI (blue). Scale bar = 20 μm. Quantification of MT1-MMP and Endo180 expression in GDSC and HDSC using TissueFaxs® 2.2 (F-I): Scattergrams (n=3) show the percentages of cells that co-expressed MT1-MMP and Endo180 proteins in GDSC (F,G) and HDSC (H,I) at day 14 and day 21, respectively.

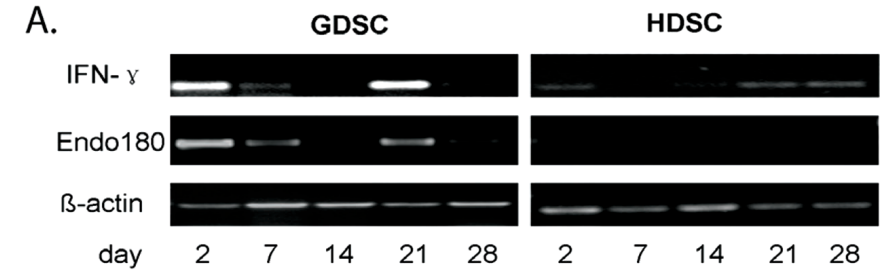
A.
GDSC
HDSC
IFN- γ
Endo180
ß-actin
day
2
7
14
21
28
2
7
14
21
28

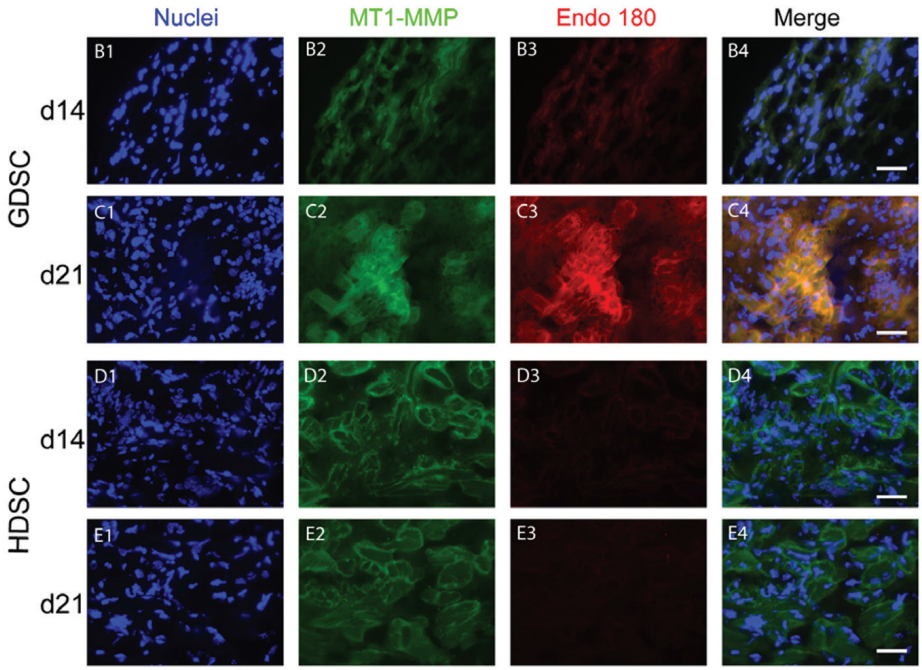
Nuclei
MT1-MMP
Endo 180
Merge
GDSC
HDSC
d14
d21
d14
d21
B1
B2
B3
B4
C1
C2
C3
C4
D1
D2
D3
D4
E1
E2
E3
E4

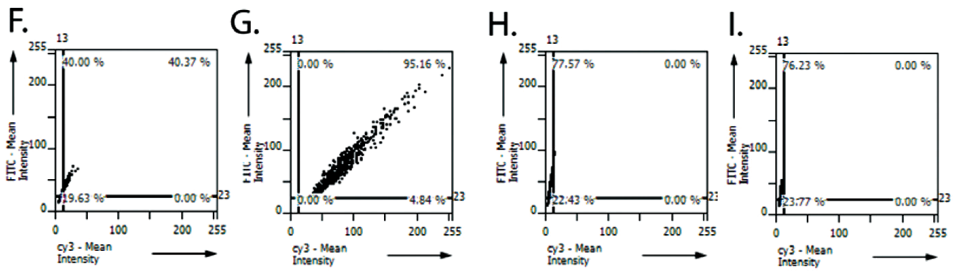
F.
G.
H.
I.
FITC - Mean Intensity
cy3 - Mean Intensity
40.00 %
40.37 %
19.63 %
0.00 %
0.00 %
95.16 %
0.00 %
4.84 %
77.57 %
0.00 %
22.43 %
0.00 %
76.23 %
0.00 %
23.77 %
0.00 %

MMP was expressed throughout the whole course of the FBR (Fig. 4.1, B2 and C2), but the expression of Endo180 was mainly observed at day 2 (data not shown) and day 21 (Fig. 4.1, C3). As phagocytosis of collagen by macrophages was observed only at day 2 and day 21, it seems likely that co-expression of Endo180 with MT1- MMP is needed to phagocytose collagen. Double immunofluorescence staining revealed that Endo180 and MT1-MMP co-localized on the cells (Fig. 4.1, B4 and C4); this was further substantiated by TissueFaxs (Fig. 4.1, F and G). In HDSC, MT1-MMP was expressed at all time points (Fig. 1, D3 and E3), yet Endo180 protein was never expressed throughout the whole course of the foreign body reaction (Fig. 4.1, D3, E3, H and I). As in HDSC no phagocytosis of collagen is seen, the HDSC data provide additional evidence that expression of Endo180 seems to be a prerequisite for the phagocytosis of collagen by macrophages.

Double immunofluorescence staining of GDSC at day 21 (Fig. 4.2, A1-D1) revealed that Endo180 was exclusively expressed on macrophages, as all Endo180 positive cells are positive for F4/80, a monoclonal antibody that specifically recognizes mouse macrophages (Austyn and Gordon, 1981). This shows that the phagocytic activity seen in GDSC should be attributed to the macrophages, and not to e.g. fibroblasts. Interestingly, over 90% of the detected macrophages present in the scaffold showed a co-staining with Endo180 (Fig. 4.2, A2 to D2). At day 2, also high numbers of $Endo180_{+}F4/80_{+}$ cells are seen, but at this time point also many macrophages are seen that do not show Endo180 expression (data not shown), indicating the presence of various macrophage populations.

Figure 4.2 (on next page) Endo180 (Cy3, red) is expressed (day 21) on cells that are positive for the macrophage marker F4/80 (FITC, green) (A1-D1). Quantification of Endo180 and F4/80 expression on day 21 using TissueFaxs® (A2-D2): the scattergrams show that the percentage of F4/80 positive cells that co-expressed Endo180 is >90%. Scale bar = 50 µm. In figure E macrophages are shown (marked with m) that phagocytose the biomaterial (marked with b). Scale bar = 15 µm. Representative micrographs of the negative controls for immunostaining of Endo180 (1:100 normal goat serum + rabbit anti-goat Cy3), MT1-MMP (1:200 normal rabbit serum + swine anti-rabbit FITC) and F4/ 80 (1:100 normal rat serum + goat anti-rat FITC) are shown in figures F, G, H, respectively. Scale bar = 50 µm.

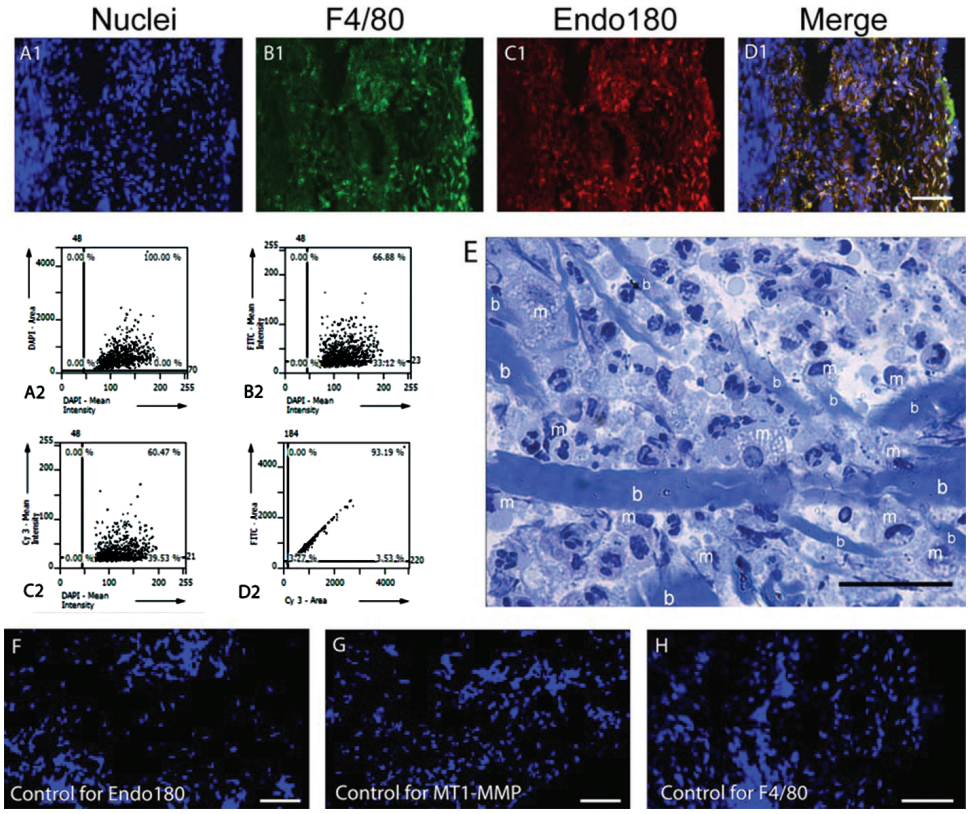
Nuclei
F4/80
Endo180
Merge
A1
B1
C1
D1
A2
B2
C2
D2
E
F
Control for Endo180
G
Control for MT1-MMP
H
Control for F4/80

IFN-γ induces the expression of Endo180 but not MT1-MMP in RAW 264.7 cells cultured without collagen coating

The microenvironment of GDSC and HDSC disks is governed by the cytokines that are present. At present, the regulation of Endo180 by cytokines has not been investigated. In GDSC disks a high expression of IFN-γ was seen at day 2 and 21 with lower levels at other time points, while in HDSC disks low levels of IFN-γ is seen during the FBR (Fig. 4.1A). As the high expression of IFN- γ at day 2 and 21 coincides with the expression as observed for Endo180 (Fig. 4.1A and C3), we surmised that IFN-γ induces the expression of Endo180. This was tested *in vitro* with the murine macrophage cell line RAW 264.7. Endo180 expression was tested in RAW 264.7 cells stimulated for 48 hours with a concentration series of IFN- γ. Expression of Endo180 was induced with 1 ng/ml IFN-γ, showed maximum levels at 2.5 and 5 ng/ml and, decreased at 10 ng/ml, and was near absent at 25 ng/ml (Fig. 4.2, B2-E2 and F). IFN-γ stimulation did not induce the expression of MT1-MMP in the absence of collagen coating (Fig. 4.3, B1-E1 and F). The expression of Endo180 after IFN-γ stimulation in macrophages was confirmed by RT-PCR (Fig. 4.3A).

Figure 4.3 (on next page) IFN-γ induces the expression of Endo180 but not MT1-MMP in RAW 264.7 macrophages cultured without collagen coating as determined by gene transcript and protein expression analyses. Cells were treated with 0-1-2.5- 5-10-25 ng/ml of IFN-γ for 48 h. After that, cells on 6-well cell culture plates and 6-well diagnostic slides were used for RT-PCR and immunofluorescent staining, respectively. mRNA levels of Endo180 was induced with 1 ng/ml IFN-γ, showed maximum levels at 2.5 and 5 ng/ml, and decreased dramatically at 10 ng/ml (A). In consistent with the gene expression, protein expression of Endo180 (red) also exhibited a bell-shape response to the different concentrations of IFN-γ (B2-E2 and F). Protein expression of MT1-MMP (green) was not observed (B1-E1 and F). Cell nuclei were stained with DAPI (blue). Values are depicted as mean ± S.D. (n=5). n.s.= P>0.05 (no significant difference); * = P<0.05 ; ** =P<0.01. Scale bar = 50 µm..

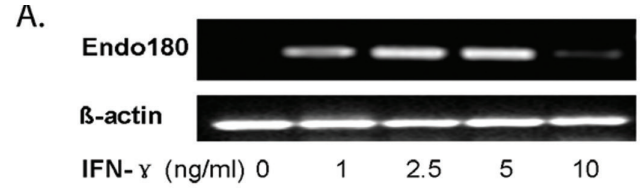
A.
Endo180
ß-actin
IFN-γ (ng/ml) 0 1 2.5 5 10

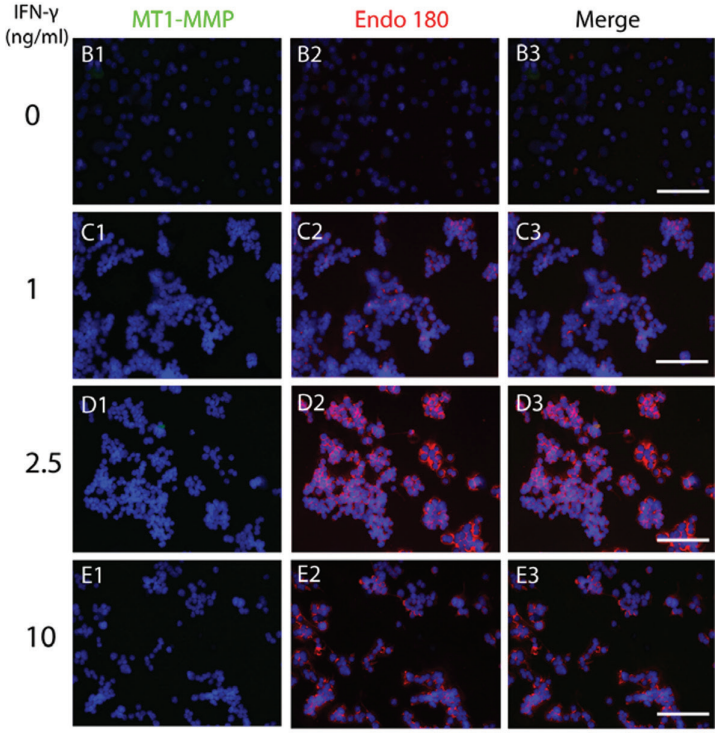
IFN-γ (ng/ml)
MT1-MMP
Endo 180
Merge
0
1
2.5
10
B1
B2
B3
C1
C2
C3
D1
D2
D3
E1
E2
E3

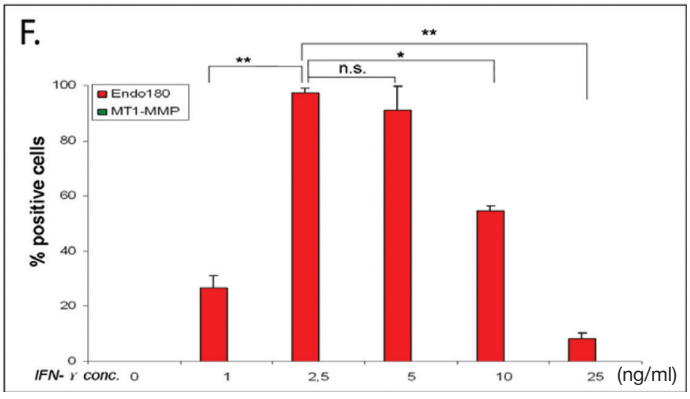
F.
**
*
n.s.
**
Endo180
MT1-MMP
% positive cells
100
80
60
40
20
0
IFN-γ conc. 0 1 2.5 5 10 25 (ng/ml)

IFN-γ induces the expression of Endo180 and MT1-MMP in RAW 264.7 cells cultured on collagen type I

The responses of cells depend on the extracellular matrix proteins that are contacted. Therefore, we repeated the experiments with RAW 264.7 cells cultured on collagen, because collagen is the substrate that macrophages encounter when they invade the collagen disks *in vivo*. Expression of Endo180 was high with 1 and 2.5 ng/ml, but the expression of Endo180 decreased at higher levels of IFN-γ (5, 10 and 25 ng/ml) (Fig. 4.4, B2-E2 and F). Thus as with the non-coated substrate, Endo180 is firstly upregulated and then down-regulated, although the sensitivity differed. However, a remarkable difference was seen with regard to the expression of MT1-MMP: on collagen, the expression pattern of MT1-MMP was comparable to the expression of Endo180 (Fig. 4.4, B1-E1 and F). Double immunofluorescence staining showed that the Endo180- expressing cells co-expressed MT1-MMP (Fig. 4.4, C3-E3). The expression of Endo180 under IFN-γ stimulation in macrophages with collagen coating was confirmed by RTPCR (Fig. 4.4A).

Figure 4.4 (on next page) IFN-γ induces the expression of Endo180 and MT1-MMP in RAW 264.7 cultured with collagen coating as determined by gene transcript and protein expression analyses. Cells were treated with 0-1-2.5-5-10-25 ng/ml of IFN-γ for 48 h, with the presence of collagen. Thereafter, cells on 6-well cell culture plates and 6-well diagnostic slides were used for RT-PCR and immunofluorescent staining, respectively. mRNA levels of Endo180 was induced with 1 ng/ml IFN-γ, showed maximum levels at 2.5, and decreased dramatically at 5 ng/ml or above (A). In consistent with the gene expression, the protein expression of Endo180 (red) also exhibited a bell-shape response to the different concentrations of IFN-γ (B2-E2 and F). Interestingly, the expression pattern of MT1-MMP (green) was comparable to the expression of Endo180 (B1-E1 and F). The Endo180 and MT1-MMP were co-localized (C3, D3). Cell nuclei were stained with DAPI (blue). Values are depicted as mean ± S.D. (n=5). * = $P<0.05$; ** = $P<0.01$ (comparison within group); # = $P<0.05$ (Endo180 versus MT1-MMP). Scale bar = 50 μm.

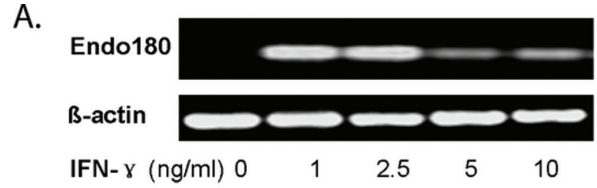
A.
Endo180
ß-actin
IFN-γ (ng/ml) 0 1 2.5 5 10

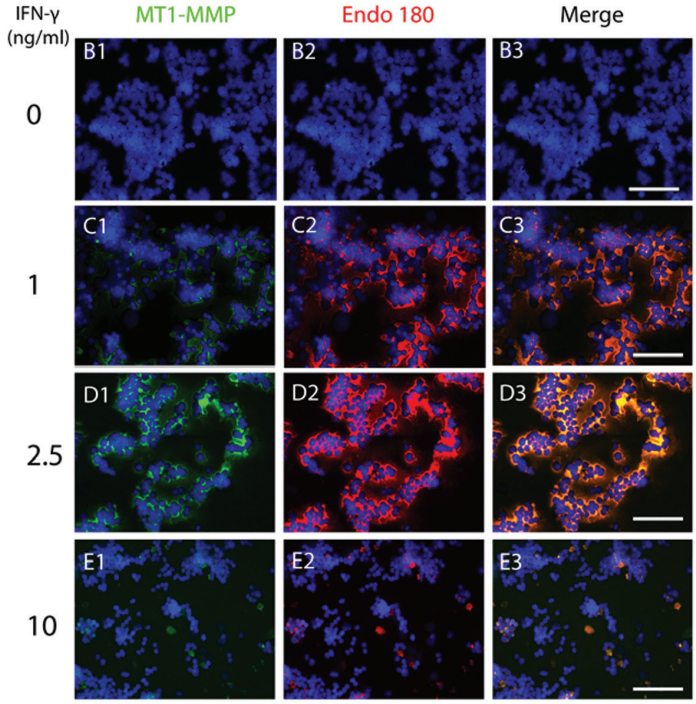
IFN-γ (ng/ml)
MT1-MMP
Endo 180
Merge
0
1
2.5
10
B1
B2
B3
C1
C2
C3
D1
D2
D3
E1
E2
E3

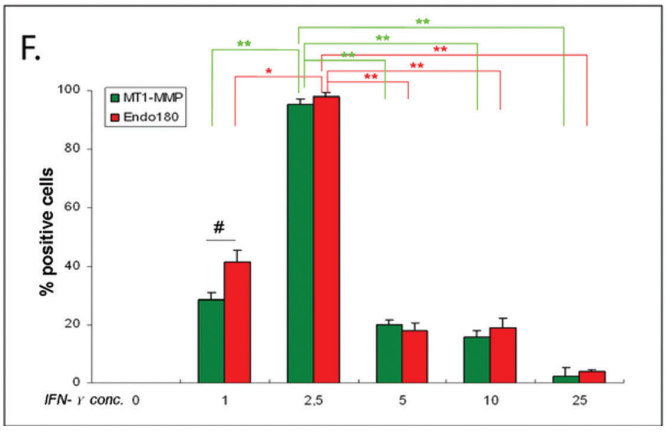
F.
MT1-MMP
Endo180
% positive cells
100
80
60
40
20
0
#
IFN-γ conc. 0
1
2,5
5
10
25

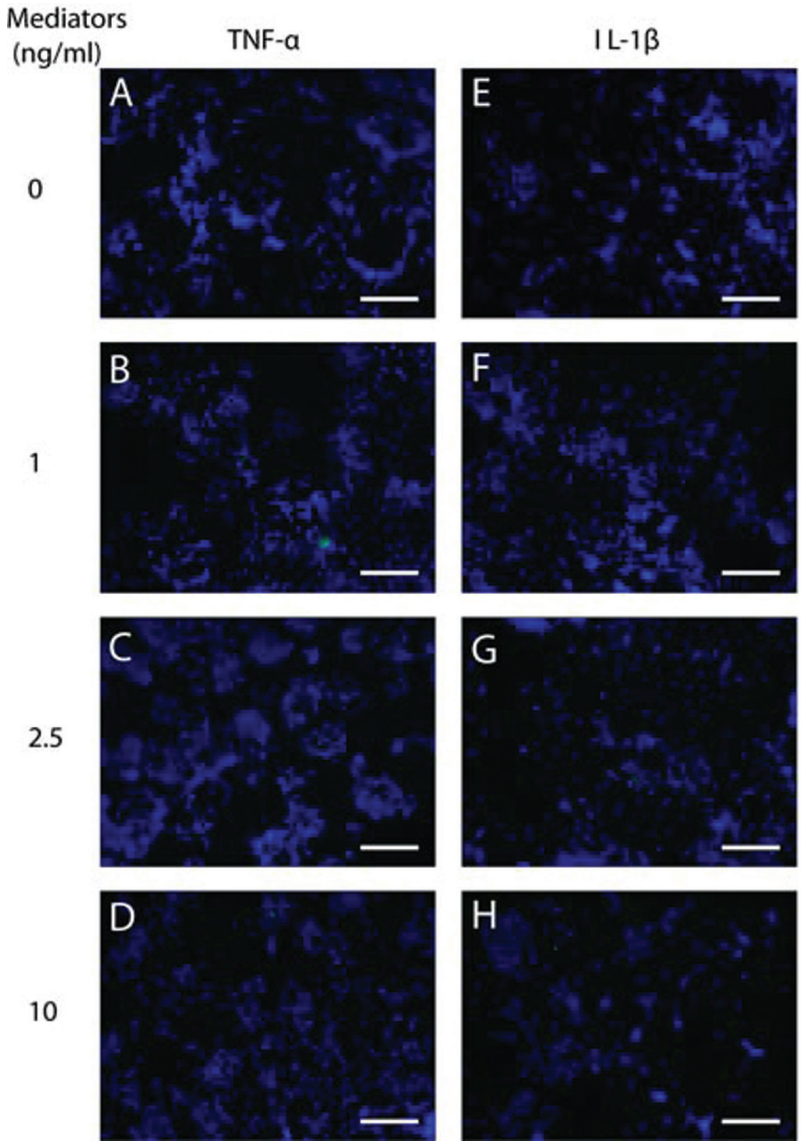

Figure 4.5. TNF-α and IL-1β do not induce the expression of Endo180 and MT1-MMP in RAW 264.7 cultured with collagen coating as determined by protein expression analyses with immunofluorescent staining. Neither Endo180 (red) or MT1-MMP (green) was detected on protein level, as shown in the merged picture of double staining of Endo180 and MT1-MMP (A-H). Cell nuclei were stained with DAPI (blue). Scale bar = 50μm

IFN-γ induces the expression of Endo180 and MT1-MMP in RAW 264.7 cells cultured on collagen type I

The responses of cells depend on the extracellular matrix proteins that are contacted. Therefore, we repeated the experiments with RAW 264.7 cells cultured on collagen, because collagen is the substrate that macrophages encounter when they invade the collagen disks *in vivo*. Expression of Endo180 was high with 1 and 2.5 ng/ml, but the expression of Endo180 decreased at higher levels of IFN-γ (5, 10 and 25 ng/ml) (Fig. 4.4, B2-E2 and F). Thus as with the non-coated substrate, Endo180 is firstly upregulated and then down-regulated, although the sensitivity differed. However, a remarkable difference was seen with regard to the expression of MT1-MMP: on collagen, the expression pattern of MT1-MMP was comparable to the expression of Endo180 (Fig. 4.4, B1-E1 and F). Double immunofluorescence staining showed that the Endo180- expressing cells co-expressed MT1-MMP (Fig. 4.4, C3-E3). The expression of Endo180 under IFN-γ stimulation in macrophages with collagen coating was confirmed by RTPCR (Fig. 4.4A).

The expression of Endo180 and/or MT1-MMP induced by IFN-γ is blocked by IL-10

To determine whether the expression of Endo180 induced by IFN-γ can be affected by the anti-inflammatory cytokine IL-10, we stimulated RAW 264.7 cells with a concentration series of IL-10, in the presence of 2.5 ng/ml IFN-γ. Our data showed that, regardless with collagen coating or not, the expression of IFN-γ induced Endo180 was 50% blocked by the exposure of the cells to 1 ng/ml IL-10, and was totally blocked at concentrations of 25 ng/ml IL-10 and above (Fig. 4.6, B-I, J and K). The expression of MT1- MMP was also blocked by IL-10 in accordance with Endo180 in RAW 264.7 cultured on collagen type I (Fig. 4.6, F-I and K). The inhibition of IFN-γ induced Endo180 expression by IL-10 was further confirmed at mRNA levels by RT-PCR (Fig. 4.6A).

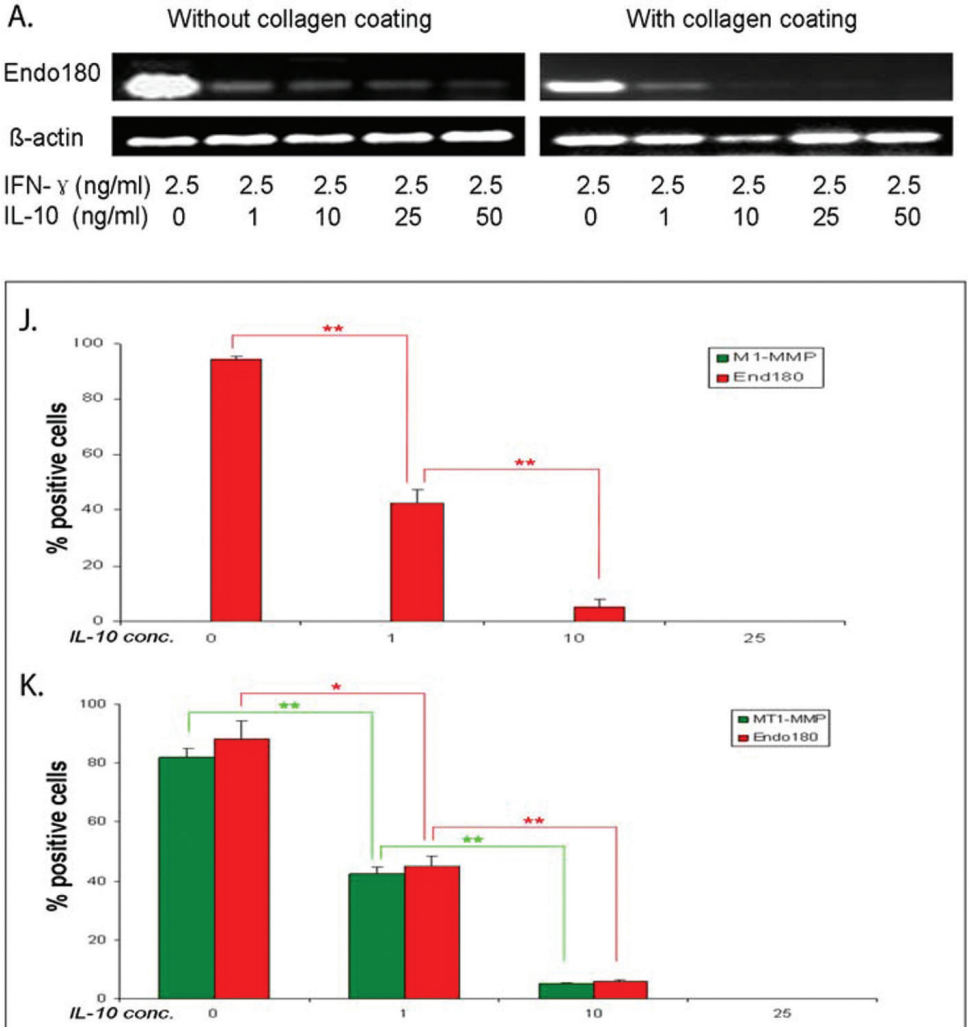

Figure 4.6 (above and next page) IL-10 inhibits the expression of Endo180 and/or MT1-MMP induced by IFN-γ in RAW 264.7 cultured with/without collagen coating as determined by gene transcript and protein expression analyses. Cells were treated with 0-1- 10-25-50 ng/ml of IL-10, with the presence of 2.5 ng/ml IFN-γ, for 48 h. Next, cells on 6-well cell culture plates and 6-well diagnostic slides were used for RTPCR and immunofluorescent staining, respectively. Regardless with collagen coating or not, the mRNA levels of Endo180 induced IFN-γ was decreased rapidly at 1 ng/ml IL-10 and almost absent at 10 ng/ml or above (A). The protein expression was consistent with the gene expression: expression of IFN-γ

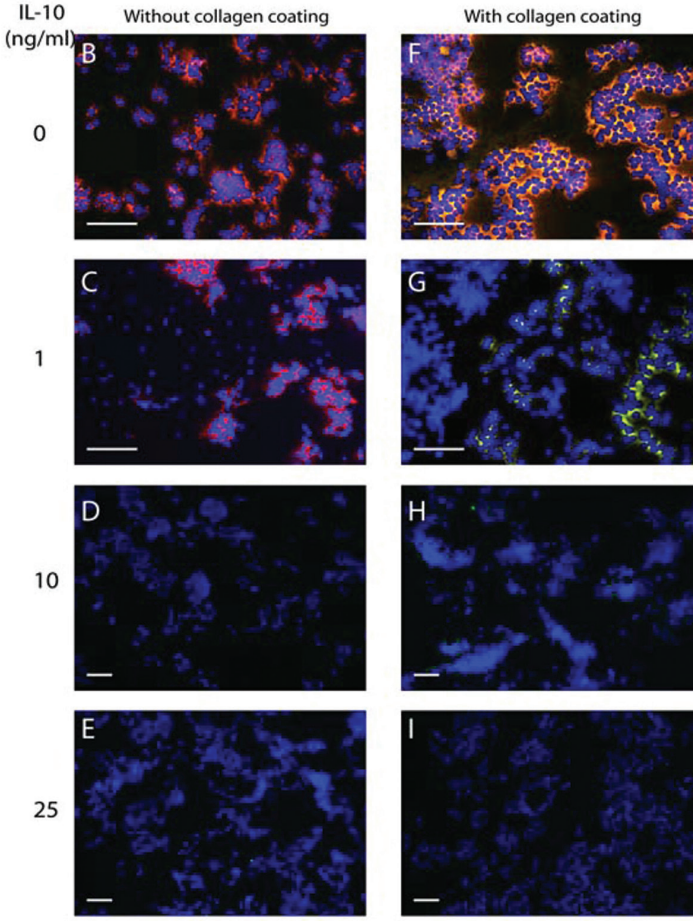

induced Endo180 was 50% blocked by the exposure of the cells to 1 ng/ml IL-10, and was totally blocked at concentrations of 25 ng/ml IL-10, as shown in the merged picture of double staining of Endo180 and MT1-MMP (B-I) and quantification of the positive cells without collagen coating (J) or with collagen coating (K). Cell nuclei were stained with DAPI (blue). Values are depicted as mean ± S.D. (n=5). * = $P<0.05$; ** =$P<0.01$. Scale bar = 50µm.

Discussion

In the current study, we investigate the molecular mechanisms of collagen phagocytosis by macrophages in the foreign body reaction. We show for the first time that the interplay between Endo180 and MT1-MMP correlated with collagen phagocytosis by macrophages, thus providing evidence that the mechanism of collagen phagocytosis operating in the FBR by macrophages is comparable with the mechanism of intracellular collagen degradation by fibroblasts seen under physiological conditions. Furthermore, our data showed that the expression of Endo180 and MT1-MMP is regulated by IFN-γ with the presence of collagen scaffolds.

We have previously shown that subcutaneously implanted glutaraldehyde or hexamethylenediisocyanate cross-linked dermal sheep collagen disks (GDSC and HDSC) in mice show a high and low degradation rate, respectively (Ye *et al.*, submitted). GDSC provoked the attraction of PMNs at day 2 and 21 after implantation. At both time points, increased levels of IFN-γ were seen, as well as phagocytic activity against the GDSC disks (Ye *et al.*, submitted). Although phagocytosis of collagen by macrophages has been repeatedly mentioned, no such reports are available for the foreign body reaction, and surprisingly little is known about the molecular mechanism that is involved in this phagocytosis. A main finding of our current study is that the endocytic transmembrane glycoprotein Endo180, a receptor that is able to bind to collagen and that is essential for cellular uptake of collagen, is highly expressed at day 2 and 21 in GDSC. In addition, we here show that MT1-MMP, a membrane-bound matrix metalloproteinase that is able to cleave collagen fibrils, is also highly expressed at day 2 and 21. Furthermore, we also show that the Endo180 receptor is localized on cells that stain positive for F4/80, i.e. the cells in question are macrophages.

Fibroblasts that lack Endo180 fail to internalize collagen; the same is observed with fibroblasts that have normal Endo180 levels but lack MT1-

MMP (Engelholm *et al.*, 2003a; Madsen *et al.*, 2007). This shows that the intracellular uptake of collagen by Endo180 depends on the liberation of collagen from the ECM by limited extracellular proteolysis, *i.e.* the cleavage of collagen fibrils located near the cell membrane by MT1-MMP. It is likely that this mechanism is also involved in the phagocytic degradation of GDSC disks by macrophages. In this respect it is of interest that macrophages in the HDSC disks only show expression of MT1-MMP but not of Endo180, the latter being the reason why phagocytosis is not observed in HDSC.

A limitation of our study is, that we have not provided direct evidence that the Endo180+MT1-MMP+F4/80+ cells indeed phagocytosed collagen, as we have not shown ingested collagen in the cells themselves by means of electron microscopy, or carried out any functional or knock-down studies. In addition, we cannot exclude the possibility that in addition to Endo180 other receptors are involved in the uptake of collagen, such as macrophage scavenger receptors (Greaves and Gordon, 2009). However, giant foreign body cells (that are formed as a result of macrophage fusion) do show pieces of collagen biomaterials intracellularly (Khouw *et al.*, 2000), and collagen has so far not been reported as a ligand for scavenger receptors. It is therefore likely, that the reported correlations in this study are indicative of a mechanistic relationship between macrophage activation by IFN-γ and collagen degradation and that involved mechanisms are comparable to those of fibroblast-mediated collagen degradation under physiological conditions.

Mechanisms on how the expression of Endo180 is regulated are not known. Another main finding of this study is that the pro-inflammatory cytokine IFN-γ stimulates the expression of Endo180 in murine macrophages (RAW 264.7 cells), providing an explanation why phagocytosis is seen only at day 2 and 21: only at these time points a high expression of IFN-γ is seen in GDSC disks. Interestingly, IFN-γ also induced the expression of MT1- MMP in RAW 264.7 cells, but only when the cells were plated on a collagen coating. This shows the importance of choosing the correct substrate when studying the response of macrophages towards cytokines.

Interestingly, we have found in the current study that the anti-

inflammatory cytokine IL-10 is able to counteract the expression of Endo180 as induced by IFN-γ. The microenvironment between the GDSC and HDSC disks differs with respect to IL-10 levels: a higher level of IL-10 is seen in HDSC disks compared to GDSC disks (Ye *et al.*, submitted). The presence of lower levels of IFN-γ in HDSC disks in combination with higher levels of IL-10 provides an explanation why phagocytosis of collagen by macrophages did not occur within HDSC disks.

In summary, we conclude that MT1-MMP and Endo180 seem to be involved in the phagocytic processing of collagenous biomaterials by macrophages through the ability of macrophages to cleave collagen fibrils near the cell membrane by MT1-MMP followed by the lysosomal delivery of cleaved collagen aggregates via binding to Endo180. In addition, the expression of Endo180 and MT1-MMP is induced by IFN-γ in the presence of collagen. Based on these results, regulation of phagocytosis of collagen by macrophage may be feasible through modulation of the expression level of IFN-γ, or through the addition of anti-inflammatory factors that counteract with IFN-γ, e.g. IL-10.

Acknowledgements

This study was supported by RuG Jan Kornelis de Cock- Stiching (Q. Ye). The authors wish to acknowledge the excellent technical support of Mr. Jasper Koerts, Ms. Saskia de Rond and Mrs. Linda Brouwer.

References

1. Anderson JM, Jones JA (2007) Phenotypic dichotomies in the foreign body reaction. Biomaterials **28**: 5114-5120.

2. Anderson JM, Rodriguez A, Chang DT (2008) Foreign body reaction to biomaterials. Semin Immunol **20**: 86-100.

3. Austyn JM, Gordon S (1981) F4/80, a monoclonal antibody directed specifically against the mouse macrophage. Eur J Immunol **11**: 805-815.

4. Badylak SF, Valentin JE, Ravindra AK, McCabe GP, Stewart-Akers AM (2008) Macrophage phenotype as a determinant of biologic scaffold remodeling. Tissue Eng A **14**: 1835-1842.

5. Beertsen W, Holmbeck K, Niehof A, Bianco P, Chrysovergis K, Birkedal-Hansen H, Everts V (2002) On the role of MT-1-MMP, a matrix metalloproteinase essential to collagen remodeling, in murine molar eruption and root growth. Eur J Oral Sci **110**: 445-451.

6. Behrendt N, Bugge TH (2003) uPARAP/Endo180 is essential for cellular uptake of collagen and promotes fibroblast collagen adhesion. J Cell Biol **160**: 1009-1015.

7. Brown BN, Valentin JE, Stewart-Akers AM, McCabe GP, Badylak SF (2009) Macrophage phenotype and remodeling outcomes in response to biologic scaffolds with and without a cellular component. Biomaterials **30**: 1482-1491.

8. Ciapetti G, Verri E, Granchi D, Cenni E, Gamberini S, Benetti D, Mian M, Pizzoferrato A (1996) *In vitro* assessment of phagocytosis of collagen by human monocytes/macrophages using a spectrophotometric

method. Biomaterials **17**: 1703-1707.

9. Curino AC, Engelholm LH, Yamada SS, Holmbeck K, Lund LR, Molinolo AA, Behrendt N, Nielsen BS, Bugge TH (2005) Intracellular collagen degradation mediated by uPARAP/Endo180 is a major pathway of extracellular matrix turnover during malignancy. J Cell Biol **169**: 977-985.

10. Deporter DA (1979) Collagen phagocytosis by stimulated mouse peritoneal macrophages *in vitro*. J Periodontal Res **14**: 323-331.

11. Dinnes DL, Santerre JP, Labow RS (2008) Influence of biodegradable and non-biodegradable material surfaces on the differentiation of human monocyte-derived macrophages. Differentiation **76**: 232-244.

12. East L, McCarthy A, Wienke D, Sturge J, Ashworth A, Isacke CM (2003) A targeted deletion in the endocytic receptor gene Endo180 results in a defect in collagen uptake. EMBO Rep **4**: 710-716.

13. Engelholm LH, List K, Netzel-Arnett S, Cukierman E, Mitola DJ, Aaronson H, Kjoller L, Larsen JK, Yamada KM, Strickland DK, Holmbeck K, Dano K, Birkedal- Hansen H, Behrendt N, Bugge TH (2003a) uPARAP/ Endo180 is essential for cellular uptake of collagen and promotes fibroblast collagen adhesion. J Cell Biol **160**: 1009-1015.

14. Everts V, van der Zee E, Creemers L, Beertsen W (1996) Phagocytosis and intracellular digestion of collagen, its role in turnover and remodeling. Histochem J **28**: 229-245.

15. Greaves DR, Gordon S (2009) The macrophage scavenger receptor at 30 years of age: current knowledge and future challenges. J Lipid Res **50**: S282-S286.

16. Honardoust HA, Jiang G, Koivisto L, Wienke D, Isacke CM, Larjava H, Hakkinen L (2006) Expression of Endo180 is spatially and temporally regulated during wound healing. Histopathology **49**: 634-648.

17. Inouye S, Iyama K, Usuku G (1983) A freeze-fracture study of two types of collagen-phagocytosing cell in the post-partum rat endometrium. Virchows Arch B Cell Pathol Incl Mol Pathol **42**: 243-249.

18. Khouw IMSL, van Wachem PB, de Leij LFMH, van Luyn MJA (1998) Inhibition of the tissue reaction to a biodegradable biomaterial by monoclonal antibodies to IFN-gamma. J Biomed Mater Res **41**: 202-210.

19. Khouw IMSL, van Wachem PB, Molema G, Plantinga JA, de Leij LFMH, van Luyn MJA (2000): The foreign body reaction to a biodegradable biomaterial differs between rats and mice. J Biomed Mater Res **52**: 439-446.

20. Kjoller L, Engelholm LH, Hoyer-Hansen M, Dano K, Bugge TH, Behrendt N (2004) uPARAP/endo180 directs lysosomal delivery and degradation of collagen IV. Exp Cell Res **293**: 106-116.

21. Knapp W, Menzel J, Brunner H, Steffen C (1974) Phagocytosis of soluble collagen-anticollagen complexes and of particulate collagen by peritoneal macrophages. Z Immunitatsforsch Exp Klin Immunol **146**: 283-291.

22. Lee H, Sodek KL, Hwang Q, Brown TJ, Ringuette M, Sodek J (2007) Phagocytosis of collagen by fibroblasts and invasive cancer cells is mediated by MT1-MMP. Biochem Soc Trans **35**: 704-706.

23. Lee H, Overall CM, McCulloch CA, Sodek J (2006) A critical role for the membrane-type 1 matrix metalloproteinase in collagen phagocytosis. Mol Biol Cell **17**: 4812-4826.

24. Lucattelli M, Cavarra E, de Santi MM, Tetley TD, Martorana PA, Lungarella G (2003) Collagen phogocytosis by lung alveolar macrophages in animal models of emphysema. Eur Respir J **22**: 728-734.

25. Luttikhuizen DT, Harmsen MC, van Luyn MJA (2006a) Cellular and molecular dynamics in the foreign body reaction. Tissue Eng **12**: 1955-1970.

26. Luttikhuizen DT, van Amerongen MJ, de Feijter PC, Petersen AH, Harmsen MC, van Luyn MJA (2006b) The correlation between difference in foreign body reaction between implant locations and cytokine and MMP expression. Biomaterials **27**: 5763-5770.

27. Luttikhuizen DT, Dankers PY, Harmsen MC, van Luyn MJA (2007) Material dependent differences in inflammatory gene expression by giant cells during the foreign body reaction. J Biomed Mater Res A **83A**: 879- 886.

28. Madsen DH, Engelholm LH, Ingvarsen S, Hillig T, Wagenaar-Miller RA, Kjoller L, Gardsvoll H, Hoyer- Hansen G, Holmbeck K, Bugge TH, Behrendt N (2007) Extracellular collagenases and the endocytic receptor, urokinase plasminogen activator receptor-associated protein/Endo180, cooperate in fibroblast-mediated collagen degradation. J Biol Chem **282**: 27037-27045.

29. Mosser DM, Edwards JP (2008) Exploring the full spectrum of macrophage activation. Nature Rev Immunol **8**: 958-969.

30. Mousavi SA, Sato M, Sporstol M, Smedsrod B, Berg T, Kojima N, Senoo H (2005) Uptake of denatured collagen into hepatic stellate cells: evidence for the involvement of urokinase plasminogen activator receptor-associated protein/Endo180. Biochem J **387**: 39-46.

31. Munirah S, Kim SH, Ruszymah BH, Khang G (2008) The use of fibrin and poly(lactic-co-glycolic acid) hybrid scaffold for articular cartilage tissue engineering: an *in vivo* analysis. Eur Cell Mater **15**: 41-52.

32. Olde Damink LH, Dijkstra PJ, van Luyn MJA, van Wachem PB, Nieuwenhuis P, Feijen J (1995) Changes in the mechanical properties of dermal sheep collagen during in vitro degradation. J Biomed Mater Res **29**: 139-147.

33. Parakkal PF (1969) Involvement of macrophages incollagen resorption. J Cell Biol **41**: 345-354.

34. Sachlos E, Gotora D, Czernuszka JT (2006) Collagen scaffolds reinforced with biomimetic composite nano-sized carbonate-substituted hydroxyapatite crystals and shaped by rapid prototyping to contain internal microchannels. Tissue Eng **12**: 2479-2487.

35. Sheikh H, Yarwood H, Ashworth A, Isacke CM (2000) Endo180, an endocytic recycling glycoprotein related to the macrophage mannose receptor is expressed on fibroblasts, endothelial cells and macrophages and functions as a lectin receptor. J Cell Sci **113**: 1021-1032.

36. Svoboda ELA, Deporter DA (1980) Phagocytosis of exogenous collagen by cultured murine fibroblasts and macrophages: A quantitative electron microscopic comparison. J Ultrastruct Res **72**: 169-173.

37. Tai H, Mather ML, Howard D, Wang W, White LJ, Crowe JA, Morgan SP, Chandra A, Williams DJ, Howdle SM, Shakesheff KM (2007) Control of pore size and structure of tissue engineering scaffolds produced by supercritical fluid processing. Eur Cell Mater **14**: 64-77.

38. Thomas EK, Nakamura M, Wienke D, Isacke CM, Pozzi A, Liang P (2005) Endo180 binds to the C-terminal region of type I collagen. J Biol Chem **280**: 22596-22605.

39. Valentin JE, Stewart-Akers AM, Gilbert TW, Badylak SF (2009) Macrophage participation in the degradation and remodeling of extracellular matrix scaffolds. Tissue Eng Part A **15**: 1687-1694.

40. Van Putten SM, Wubben M, Hennink WE, van Luyn MJA, Harmsen MC (2009) The downmodulation of the foreign body reaction by cytomegalovirus encoded interleukin-10. Biomaterials **30**: 730-735.

41. Van Wachem PB, van Luyn MJA, Olde Damink LH, Dijkstra PJ, Feijen J, Nieuwenhuis P (1994) Biocompatibility and tissue regenerating capacity of crosslinked dermal sheep collagen. J Biomed Mater Res **28**: 353-363.

42. Wienke D, MacFadyen JR, Isacke CM (2003) Identification and characterization of the endocytic transmembrane glycoprotein Endo180 as a novel collagen receptor. Mol Biol Cell **14**: 3592-3604.

43. Yeghiazaryan K, Skowasch D, Bauriedel G, Schild H, Golubnitschaja O (2007) Could activated tissue remodeling be considered as early marker for progressive valve degeneration? Comparative analysis of checkpoint and ECM remodeling gene expression in native degenerating aortic valves and after bioprosthetic replacement. Amino Acids **32**: 109-114.

CHAPTER 5

The role of collagen receptors Endo180 and DDR-2 in the foreign body reaction against non-crosslinked collagen and gelatin

Qingsong Ye [1,2,3,4]
Martin C. Harmsen [1]
Marja J.A. van Luyn [1]
Ruud A. Bank [1]

[1] Stem Cell and Tissue Engineering Research Group, Department of Pathology and Medical Biology, University of Groningen, The Netherlands

[2] West China College of Stomatology, the State Key Laboratory of Oral Diseases, Sichuan University, Chengdu, China

[3] Department of Orthodontics, University Medical Centre Groningen, University of Groningen, The Netherlands

[4] School of Medicine and Dentistry, James Cook University, Cairns, Australia

Biomaterials 32 (2011) 1339-1350

Abstract

Despite the use of collagen-derived scaffolds in regenerative medicine, little is known about the degradation mechanisms of these scaffolds *in vivo*. Non-crosslinked dermal sheep (NDSC) and gelatin disks were implanted subcutaneously in mice. NDSC disks showed a very low degradation rate, despite the presence of high numbers of macrophages and the influx of neutrophils. This was attributed to the presence of the matrix metalloproteinase inhibitor TIMP-1. The limited degradation occurred mainly in the later stages of the foreign body reaction, and could be attributed to (1) phagocytosis by macrophages due to a co-expression of Endo180 and MT1-MMP on these cells (intracellular degradation) and (2) the presence of MMP-13 due to an upregulation of the expression of the DDR-2 receptor (extracellular degradation). In contrast, gelatin disks degraded quickly, due to the efficient formation of large giant cells as well as the presence of MMP-13; the inhibitor TIMP-1 was absent. The DDR-2 receptor was not expressed in the gelatin disks. Endo180 and MT1-MMP were expressed, but at most times no co-expression was seen. We conclude that the physical state of collagen (native or denatured) had a dramatic outcome on the degradation rate and provoked a completely different foreign body reaction.

1. Introduction

Collagen is the most abundant protein in the mammalian body [1]. Especially connective tissues, like skin, bone, cartilage, tendons, and ligaments, are rich in collagen and other extracellular matrix molecules. Proper tissue homeostasis requires dynamic reciprocal interactions between cells and their environment, which often is the extracellular matrix in connective tissues. Connective tissues such as cartilage or bone have been the target for many regenerative therapies due to their relatively low complexity, low cellularity, and potential for regeneration or repair. In regenerative therapies including tissue engineering, biomaterial scaffolds are used, e.g. seeded with cells to augment tissue repair and functional restoration [2]. The performance of the seeded cells depends, among others, on the bio-inductive signals of the scaffold. Biomaterial scaffolds can be of a synthetic nature, or derived from natural biopolymers, such as collagen. The supposition of collagen scaffolds is, that seeded cells will function properly, due the close resemblance between scaffold and the natural cellular environment. [3] [4].

Like any other biomaterial, implanted collagen scaffolds induce series of damage-inflicted processes that include wound healing, inflammation and more specifically the biomaterial-directed by a foreign body reaction (FBR) [5] and [6]. Together these processes, which show a strong spatiotemporal overlap, comprise the tissue response towards implanted biomaterials. Macrophages play a pivotal role in the tissue response. These macrophages interrogate the biomaterial surface, and release proteolytic enzymes and may phagocytose the biomaterial too. Under certain circumstances, the macrophages may fuse, to form multinucleated foreign body giant cells [7], [8] and [9]. Collagen-based biomaterials can be cross-linked to enhance the stiffness and to dampen the rate of biological degradation. Alternatively, both non-crosslinked (native) collagen as well as denatured collagen, i.e. gelatin have been studied as such [10]. It is the

specific application that determines the choice of the biomaterial. Any treatment modality must take the tissue response towards biomaterials into account. In particular the degradation mechanism of implanted collagen scaffolds is important to understand, e.g. to provide cues to tune scaffolds to their intended application [11].

In previous studies we have shown that collagen disks treated with different crosslinking agents show marked differences in degradation rate and that the degradation rate depends on the implantation site as well as on the animal species [11], [12], [13], [14], [15] and [16]. Although several matrix metalloproteinases participate in the degradation of collagen scaffolds [11], the role of specific collagen receptors in this process has hardly been studied. With respect to the FBR, the collagen-binding integrins α1β1, α2β1, α10β1 and α11β1, have been well-studied. Yet, on other important collagen receptors members, like the discoidin domain receptors DDR-1 and DDR-2, and the mannose receptor family including Endo180 little knowledge exist for the FBR [17]. Two other collagen receptors, lipoprotein VI and LAIR-1, are involved in platelet adhesion/activation and immune cell regulation, respectively [17], and are therefore outside the scope of this paper.

We have recently shown, that implanted glutaraldehyde cross-linked collagen attracts neutrophils. These neutrophils express IFN-γ, which induces the expression of both Endo180 and MT1-MMP on macrophages that are present in the implanted collagen too [15]. The co-expression of Endo180 and MT1-MMP is responsible for the phagocytosis of collagen by fibroblasts [18] and [19]. Similarly, in our previous study, we have provided evidence that on FBR macrophages the co-expression of Endo180 and MT1-MMP coincides with the phagocytosis and degradation of implanted cross-linked collagen scaffolds [15]. As it appears from our previous findings the molecular nature of collagen scaffolds, i.e. chemical crosslinking, determines the type of degradation. Among the collagens, MMP-13, proved important in the FBR [11]. Interestingly, the collagen receptor DDR-2 is known to induce the expression of MMP-13 [20], [21], [22] and [23]. Thus we surmise that, together with the Endo180 – MT1-MMP axis, DDR-2 is important in the FBR too.

The aim of this study is to investigate the role of the collagen receptors

Endo180 and DDR-2 in the degradation of non-crosslinked types of collagen, namely native as well as denatured collagen (i.e. gelatin).

2. Materials and methods

2.1. Biomaterials

Non-crosslinked dermal sheep collagen (NDSC) sheet, processed from sheep skin [28], was obtained from the Zooid Nederland's Zeemlederfabriek (Oosterhout, The Netherlands). Commercially available non-crosslinked gelatin sponges Willospon (Will-Pharma, Benelux) were kindly provided by the Department of Oral Surgery of the University Medical Center Groningen. Disks (6 mm in diameter, 0.75 mm in thickness) were punched from pieces of NDSC and gelatin from the same batch, and sterilized with ethylene oxide. Surface-associated endotoxin levels were below 0.25 EU/ml, as determined by the LAL-method (Cambrex, LAL kinetic-QCL®).

2.2. Animals and operating procedures

All procedures performed on animals were approved by the local committee for care and use of laboratory animals of the University of Groningen and were performed according to international and governmental guidelines on animal experimentation. The operation procedures were carried out on male C57BL/6 mice (10 weeks old, Harlan, Horst, the Netherlands) according to the protocol as described before [11], [13], [14], [15] and [16]. The disks were removed at the following time points after implantation (related to the different phases of the FBR in mice): 2 days (onset), 7 days (early progression), 14 and 21 days (intermediate progression), and 28 days (late progression), n = 6 per time point. The disks were snap-frozen in liquid nitrogen immediately after explantation.

2.3. Histological techniques

Tissue sections (2 μm in thickness) of T 7100 (Heraeus Kulzer, Wehrheim, Germany) embedded explants were stained with toluidine blue (Fluka Chemie, Buchs, Switzerland) and mounted in Permount (Fisher, New Jersey, USA). The degradation of the scaffold was determined by image analysis as the percentage of the size of remained disk as compared with the original size (before implantation). The cellular ingrowths inside the disk was evaluated by image analysis as percentage of the entire cross-sectional area. The number of giant cells per square millimeter inside implant was counted as described in our previous study [13].

2.4. Gene expression analysis

Total RNA was extracted from snap-frozen explants as described previously [14]. One microgram of total RNA was used to generate the first strand cDNA synthesis using M-MuLV reverse transcriptase (MBI Fermentas, St. Leon-Rot, Germany) and random hexamer primers, following the instruction of the manufacturer's protocol. Ten nanogram of a cDNA mixture from 4 to 5 mice was pooled per time point for each reaction. The PCR reaction of 35 cycles was performed using primers specific collagenases (MMP-8, MMP-13), gelatinases (MMP-2, MMP-

Mediators	Forward	Reverse	Anneal
TIMP-1	CTGTGCCCCACCCCACCCAC	AAGGCTTCAGGTCATCGGGC	56 ° c
MMP-2	GGCCATGGCATGGGGCTGGA	CCAGTCTGATTTGATGCTTC	60 ° c
MMP-8	CAAGCAATCAATTCCGGTCT	ATTCCATTGGGTCCATCAAA	60 ° c
MMP-9	TGACGAGGTTGGGAAATGGT	CCGCCCCCTGATAGAGTCTT	60 ° c
MMP-13	AGGCCTTCAGAAAAGCCTTC	GAAATGGCTTTTGCCAGTGT	56 ° c
β-actin	GTGAAAAGATGACCCAGATCAT	GCTTCTCTTTGATGTCACGCACGAT	60 ° c

Table 5.1 PCR primers of MMPs,TIMP-1 and the control gene.

9), the tissue inhibitor of MMP (TIMP-1), as well as the reference gene β-actin (Table 5.1). Amplimers were separated in 2% agarose gels.

2.5. Immunohistochemistry

To determine the inflammatory cell infiltration during the time course, tissue expression was verified by means of *in situ* staining using immunohistochemistry (IHC) on explants of two materials at all time points. Tissue sections (5 μm) were mounted on silane-coated slides. Cryosections were fixed with 2% paraformaldehyde in PBS at room temperature (RT) for 30 min, followed by rehydration (1x PBS, 10 min), and subsequent incubation with 0.5% Triton X-100 in PBS (10 min). Sections were stained for neutrophils (monoclonal rat anti-mouse neutrophils, Serotec Ltd. Oxford, UK), macrophages (rat anti-mouse F4/80, Serotec Ltd. Oxford, UK) and lymphocytes (polyclonal hamster anti-mouse CD3ε, BD Pharmingen, USA), as described previously by our lab [12].

2.6. In situ zymography

To determine the collagenolytic activity during the foreign body reaction against NDSC and gelatin, an *in situ* zymographic technique was employed as described previously [16]. Briefly, cryosections (5 μm, n = 3 per time point) on glass slides were covered with DQ™ collagen type I from bovine skin conjugated to fluorescein (Invitrogen, Breda, The Netherlands) as a substrate. The substrate had a final concentration of 100 μg/ml in 50 mM Tris–HCl (pH 7.4), containing 16 mm CaCl2, 0.05% Brij 35 and 5 mm PMSF. After incubation (2 h in a dark, humidified chamber at 37 °C), unbound substrate was removed by washing in distilled water, followed by incubation with 1% Triton X-100 for 10 min. Next, the slides were incubated with 4′,6-diamidino-2-phenylindole (DAPI) to stain cell nuclei, and mounted in Citifluor. As a negative control the substrate was omitted to determine the autofluorescence of the sections. Other control slides were pre-incubated with the general MMP inhibitor 10-phenanthroline monohydrate at a concentration of 20 μg/ml in 50 mm Tris–HCl (pH 7.4).

2.7. Immunofluorescence microscopy

Expression of Endo180 and MT1-MMP was verified by means of *in situ* immunofluorescent double staining on explants of two materials at all time points. Goat anti-mouse Endo180 antibody (1:100, Santa Cruz Biotechnology, Santa Cruz, USA) in combination with rabbit anti-goat Cy3 (1:100, Zymed Laboratories Inc., San Francisco, USA), and rabbit anti-mouse MT1-MMP antibody (1:200, Epiomics Inc., CA, USA) in combination with swine anti-rabbit FITC (1:100, Dako, Carpinteria, USA) are applied for the double staining, as we described previously [15].

A similar double staining procedure was performed to unravel the expression patterns of the DDR-2 and MMP-13 in the FBR. Tissue sections (5 μm) were mounted on silane-coated slides. Cryosections (5 μm) were mounted on silane-coated slides, fixed with 2% paraformaldehyde in PBS at room temperature (RT) for 10 min, then washed in 0.1% Triton X-100 in PBS (5 min) for 3 times. The sections were incubated with a rabbit anti-mouse DDR-2 antibody (1:150, Santa Cruz Biotechnology, Santa Cruz, USA) and a sheep anti-mouse MMP-13 antibody (1:50, Abcam, Cambridge, UK) for 2.5 h. Next, the secondary antibodies for DDR-2 and MMP-13, respectively swine anti-rabbit TRITC (1:100, Dako, Carpinteria, USA) and donkey anti-sheep FITC (1:200, Molecular Probes Inc., CA, USA) in PBS with DAPI (1:5000) were added and incubated for 30 min. Sections were washed in 0.1% Triton X-100 in PBS (5 min) for 4 times to remove nonbound secondary antibodies (FITC and TRITC). Finally, samples were mounted with Citifluor followed by examination under the immunofluorescence microscope.

For the negative controls, samples were stained as described above, except that the primary antibodies were replaced with the same dilution of serum from the same species as used for the specific first antibodies, namely, normal goat serum (1:100, Sanquin Pharmaceutical Services, Amsterdam, Netherlands), normal rabbit serum (1:200, Dako, Carpinteria, USA), normal rabbit serum (1:150, Dako, Carpinteria, USA) and normal sheep serum (1:50, Jackson ImmunoResearch Laboratories, Inc, PA, USA) for Endo180, MT1-MMP, DDR-2 and MMP-13, respectively.

2.8. Quantification of Endo180, MT1-MMP, DDR-2 and MMP-13 immunostaining

To further quantify the number of cells with Endo180, MT1-MMP, DDR-2 and MMP-13 immunostaining, three representative images (magnification: 40×) of each tissue section were analyzed with TissueFaxs®, Zeiss AxioImager Z1 Microscope System (Tissue-Gnostics GmbH, Vienna, Austria). Single cells were identified by their nuclei (DAPI staining). This identification mask was then applied to determine gray values in the two corresponding channels FITC (MT1-MMP or MMP-13) and Cy3/TRITC (Endo180 or DDR-2, referred as Cy3 in the scattergrams) of each object in all images. The percentage of MT1-MMP, Endo180, DDR-2 and MMP-13 positive cells was determined and depicted as scattergrams. Each scattergram represents average values calculated from analysis of all three images of one entire tissue section. It should be noted that the limitation of this technique is, that FBR giant cells are not recognized as such. Instead giant cells are interpreted as single cells in a number that corresponds to the number of their nuclei. Yet, this has little effect on the mean fluorescence intensity per cell, because the surface area of giant cells seems to correspond to the sum of the surface areas to the number of fused macrophages that constitute the giant cell.

2.9. Statistical analyses

All quantitative data are presented as mean ± SD. The data were analyzed using statistical software (GraphPad Prism, GraphPad Software Inc.). Differences were analyzed by two-way ANOVA followed by Tukey's post hoc test or Student's t-test, as appropriate. A difference of $p < 0.05$ was considered statistically significant.

3. Results

3.1. Influx of macrophages and neutrophils and the presence of giant cells

In NDSC, a small number of macrophages was found at day 7, whereas the number of macrophages was about 7-fold higher at day 14, 21 and 28 compared to day 7 (Fig. 5.1A). No giant cells were seen at day 2, whereas small numbers of giant cells were seen at day 7, a number that increased at day 14 and 21, and showed a slight decrease at day 28 (Fig. 5.1B). In gelatin, which had totally disappeared by day 28, a small influx of macrophages was seen at day 2, with increasing numbers at day 7 and 14, and decreased at day 21 (Fig. 5.1A). In gelatin, giant cells appeared at day 2, increased at day 7, showed a steep increase at day 14, and decreased at day 21 (Fig. 5.1B), which coincided with the virtual disappearance of the implant. Remarkably, in gelatin the ratio of macrophages to giant cells at day 14 and 21 was around 10:1, whereas in NDSC the ratio was 45:1 and 20:1, respectively (Fig. 5.1A,B). Thus, in gelatin the fusion of macrophages to giant cells had occurred more frequently or was more efficient compared to NDSC. Moreover, the giant cells in gelatin showed more nuclei than the giant cells in NDSC, in other words, had a by far greater surface area (Fig. 5.3E,F).

High numbers of neutrophils were observed in NDSC at day 2, low numbers on day 7 and 14, emerged again at day 21 and remained at similarly high levels at 28 days. In gelatin, neutrophil infiltration was essentially absent (Fig. 5.1C).

3.2. Scaffold degradation

The NDSC disks showed little degradation during the 28 day time course; the majority (80%) of the scaffold had remained (Fig. 5.2A,C). Phagocytosis of NDSC was mainly observed at days 21 and 28 predominantly by

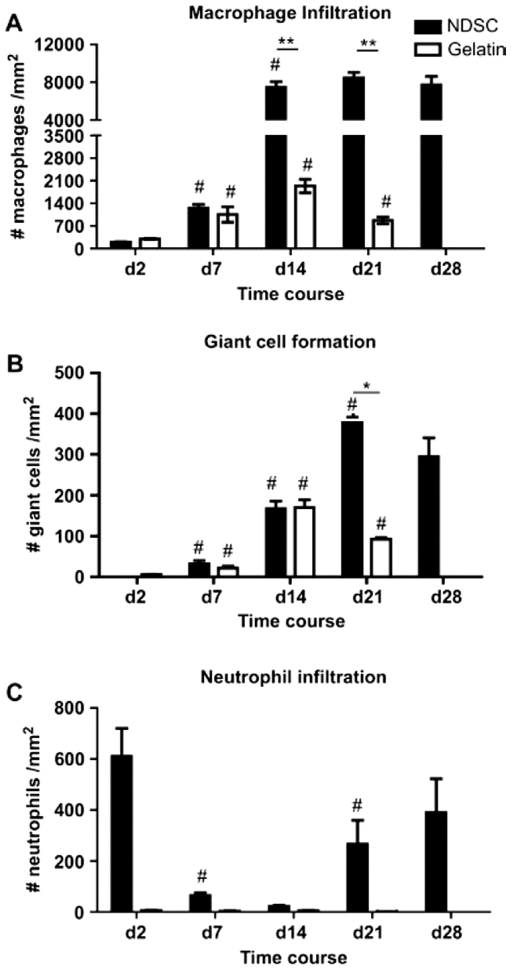

Figure 5.1 Comparison of cellular infiltration between NDSC and gelatin scaffolds in the foreign body reaction. (A) Number of macrophages were present in both scaffolds at all time points except day 28, by which gelatin was almost completely degraded. Higher numbers of macrophages were present in NDSC than Gelatin at days 14 and 28. (B) The giant cells were present from day 7 onwards and the numbers were increasing according to the time in NDSC, while in gelatin the first giant cells were formed at day 2, then the number is increased at day 7 and 14, and decreased at day 21. (C) In NDSC, neutrophils were observed at day 2 then rapidly disappeared at days 7 and 14, and emerged again from day 21 and day 28, while in gelatin the neutrophils were virtually absent throughout the time course. Values are depicted as mean SD (n : 6 for each group). # : $p < 0.05$ (compare with the previous time point within the same biomaterial);* : $p < 0.05$ or ** : $p < 0.01$ (NDSC vs. gelatin).

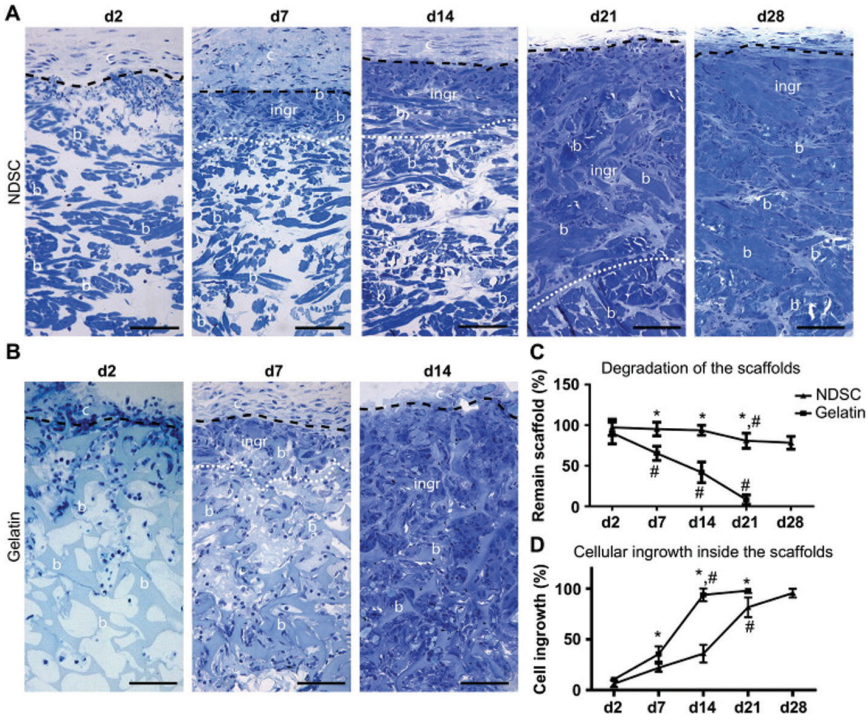

Figure 5.2. Comparison of degradation and cellular ingrowths between NDSC and gelatin disks in the foreign body reaction. The upper panel shows the fate of NDSC at all time points (A) and the left lower panel gelatin (B) at day 1, day 7 and day 14 (staining by means of toluidine blue) Symbols: b : collagen bundle, c : fibro-capsule; b : collagen bundle; Scale bar : 50 mm. The lower right panel shows the quantification of degradation (C) and cellular ingrowths (D) in NDSC and gelatin during the foreign body reaction. Values are depicted as mean SD (n : 5 for NDSC and n : 3 for gelatin). # : $p < 0.05$ (compare with the previous time point within the same biomaterial); * : $p < 0.05$ or ** : $p < 0.01$ (NDSC vs. gelatin).

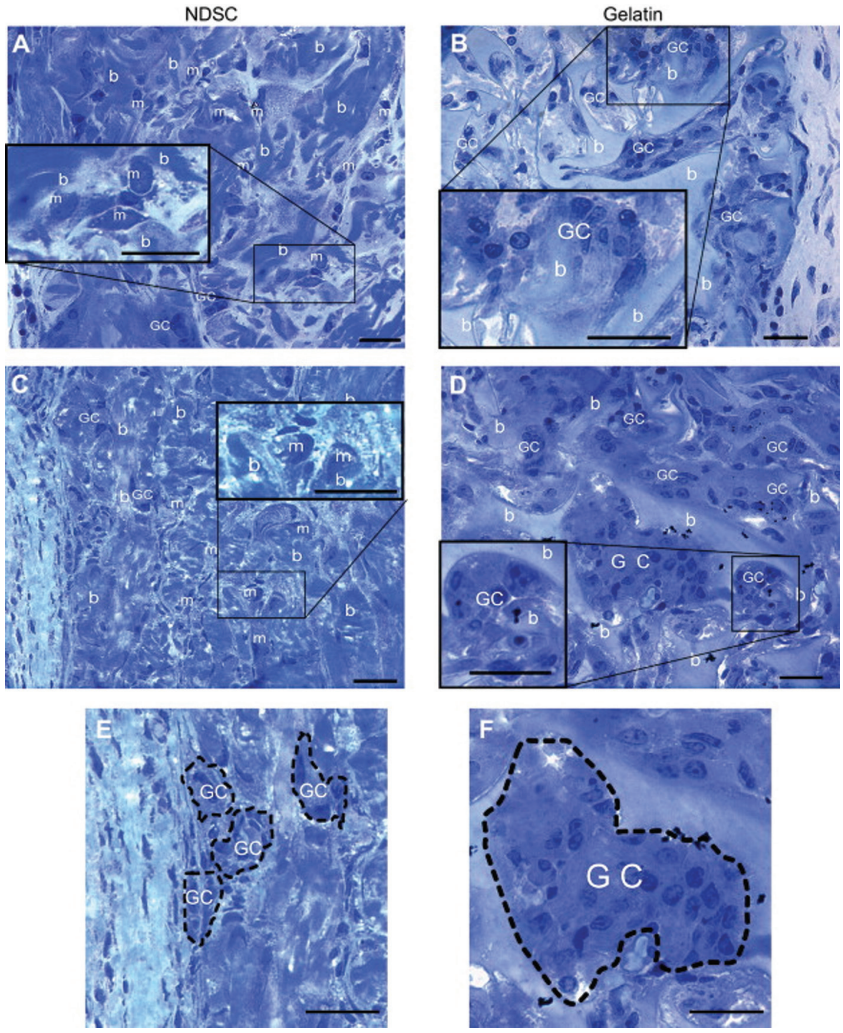

Figure 5.3. Phagocytosis in NDSC and gelatin scaffolds during the foreign body reaction. Marked phagocytosis was observed in NDSC only at late stage: day 21 (A) and day 28 (C) mainly by macrophages and also by giant cells. Phagocytosis was observed in gelatin by giant cells at day 7 (B) and day 14 (D). The giant cells in gelatine (F) showed more nuclei and greater surface area than the giant cells in NDSC (E). Symbols: m : macrophage; b : collagen bundle; GC : giant cell. Scale bar : 20 mm; the tissue slices are stained with toluidine blue.

macrophages as well as giant cells (Fig. 5.3A,C). Rapid degradation of the gelatin disks took place; after 21 days only a tiny fraction of the disk was present whereas no material could be traced at day 28 (Fig. 5.2B,C). Phagocytosis was observed at days 2, 7 and 14; mainly by multinucleated giant cells (Fig. 5.3B,D). In NDSC and gelatin, cellular ingrowths increased during the time course. Full (100%) ingrowths of the disk was observed at day 14 and 28 for gelatin and NDSC, respectively (Fig. 5.2D).

3.3. Gene expression of MMPs and TIMP-1

Significant differences were observed in the gene expression of the various MMPs and TIMP-1 in the tissue response towards NDSC and gelatin over time. TIMP-1 expression was observed at all time points in NDSC,

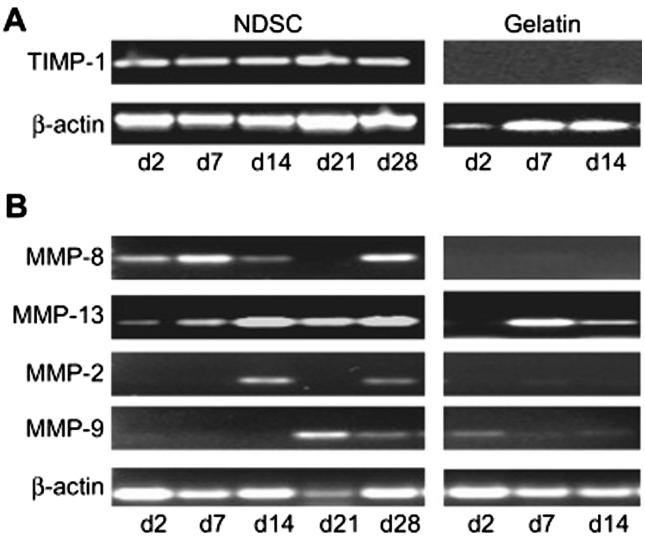

Figure 5.4. Dissection gene expression of TIMP-1 and MMPs in NDSC and gelatin. (A) In NDSC, TIMP-1 was expressed at all time points in NDSC, while no TIMP-1 was observed in gelatine. (B) mRNA expression show distinct patterns of collagenases (MMP-8,-13) and gelatinases (MMP-2,-9) between NDSC and gelatin during the FBR.

whereas TIMP-1 was never expressed in gelatine (Fig. 5.4A). In NDSC both collagenases, MMP-8 and MMP-13, appeared to be constitutively expressed throughout the 28 day time period. It should be noted that on day 21 their expression appeared absent, yet is explained by the low expression of the beta-actin reference gene. MMP-13 showed the highest expression on days 14, 21 and 28. The gelatinases MMP-2 and MMP-9, were expressed from later time points on, respectively day 14 and day 21 (Fig. 5.4B). Remarkably, in gelatin of the collagenases only MMP-13 was expressed (at days 7 and 14), while of the gelatinases only MMP-9 was expressed and only early after implantation (day 2) (Fig. 5.4B).

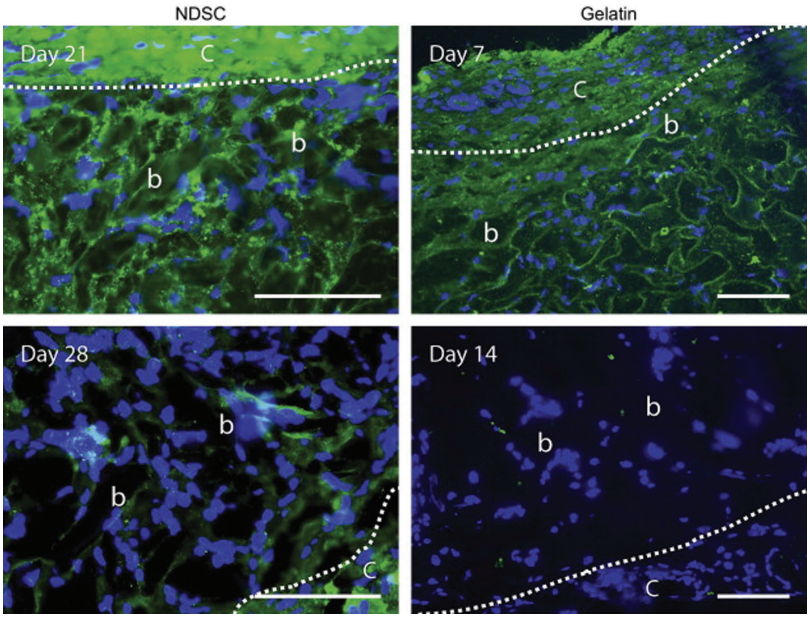

Figure 5.5 Collagenolytic activity in NDSC and gelatin scaffolds. Intensive collagenolytic activity was seen at day 21 in NDSC; much less activity was seen at day 28. In gelatin, high collagenolytic activity was seen at day 7, whereas this was essentially absent at day 14. Symbols: b : collagen bundle, c : fibro-capsule; b : collagen bundle. Scale bar : 20 mm.

3.4. In situ zymography

Intensive collagenolytic activity was seen at day 21 in NDSC; much less activity was seen at day 28 (Fig. 5.5) and day 14, it was absent at day 2 and 7 (data not shown). In gelatin, high collagenolytic activity was seen at day 7, whereas this was essentially absent at day 2 and 14 (Fig. 5.5).

3.5. Immunofluorescence: presence of Endo180, DDR-2, MT1-MMP and MMP-13

In NDSC, about 50% of the infiltrated cells expressed Endo180 albeit just above the detection limit, at day 2 (Fig. 5.6B1), whereas Endo180 expression was lost at day 7 and 14 (Fig. 5.6E1). At days 21 and 28 the majority of cells expressed Endo180, while at day 28 the expression had increased to its maximum (Fig. 5.6H1,K1). In NDSC, MT1-MMP was expressed at all time points on the majority of cells, yet only at day 28 did the expression reach significant levels (Fig. 5.6A1, D1, G1, J1)as was observed for Endo180. There was a strong co-localization of Endo180 with MT1-MMP at days 21 and 28 (Fig. 5.6I1, L1, I2, L2). In NDSC, DDR-2 was not expressed at days 2 and 7 (Fig. 5.7B1). By day 14 DDR-2 was expressed by the majority of infiltrated cells (Fig. 5.7E1), at days 21 and 28, the DDR-2 expression gradually reaches its maximum level(Fig. 5.7H1,K1). A similar expression pattern was observed for MMP-13 (Fig. 5.7A1, D1, G1, J1). The co-expression of MMP-13 and DDR-2 was observed at days 14, 21 and 28 (Fig. 5.7F1, I1, L1, F2, I2, L2).

In gelatin, about 73% of the cells expressed Endo180 at day 2 (Fig. 5.8B1), albeit at low levels. At day 7 all cells expressed Endo180 with a small decline at day 14 (Fig. 5.8E1, H1). The expression levels of Endo180 at day 7 and 14 were comparable and had increased compared to day 2. MT1-MMP followed the similar trend (Fig. 5.5.8A1, D1, G1). At day 2, Endo180 and MT1-MMP were not co-expressed (Fig. 5.8C1), whereas at day 7 Endo180 and MT1-MMP were co-expressed (Fig. 5.8F1, F2). This pattern changed at day 14: although Endo180 and MT1-MMP were still co-localized in many cells (Fig. 5.8I2), their molecular distribution pattern differed (Fig. 5.8I1). It should be noted that, in particular in

Figure 5.6 (next page) Protein expression analysis of MT1-MMP and collagen receptor Endo180 in NDSC scaffolds at days 2, 14, 21 and 28 (B1-L1): MT1-MMP protein was stained with FITC (green, A1, D1, G1, J1) and Endo180 with Cy3 (red, B1, E1, H1, K1). The co-localization of Endo180 and MT1-MMP was shown in the merged micrographs (C1, F1, I1, L1). Cell nuclei were stained with DAPI (blue). Scale bar : 20 mm. Quantification of MT1-MMP and Endo180 expression in NDSC using TissueFaxs/ 2.2: Scattergrams (n : 3) show the percentage of cells that expressed MT1-MMP (A2, D2, G2, J2) or Endo180 (B2, E2, H2, K2), and the percentage of cells that co-expressed MT1-MMP and Endo180 (C2, F2, I2, L2) in NDSC at the indicated time points.

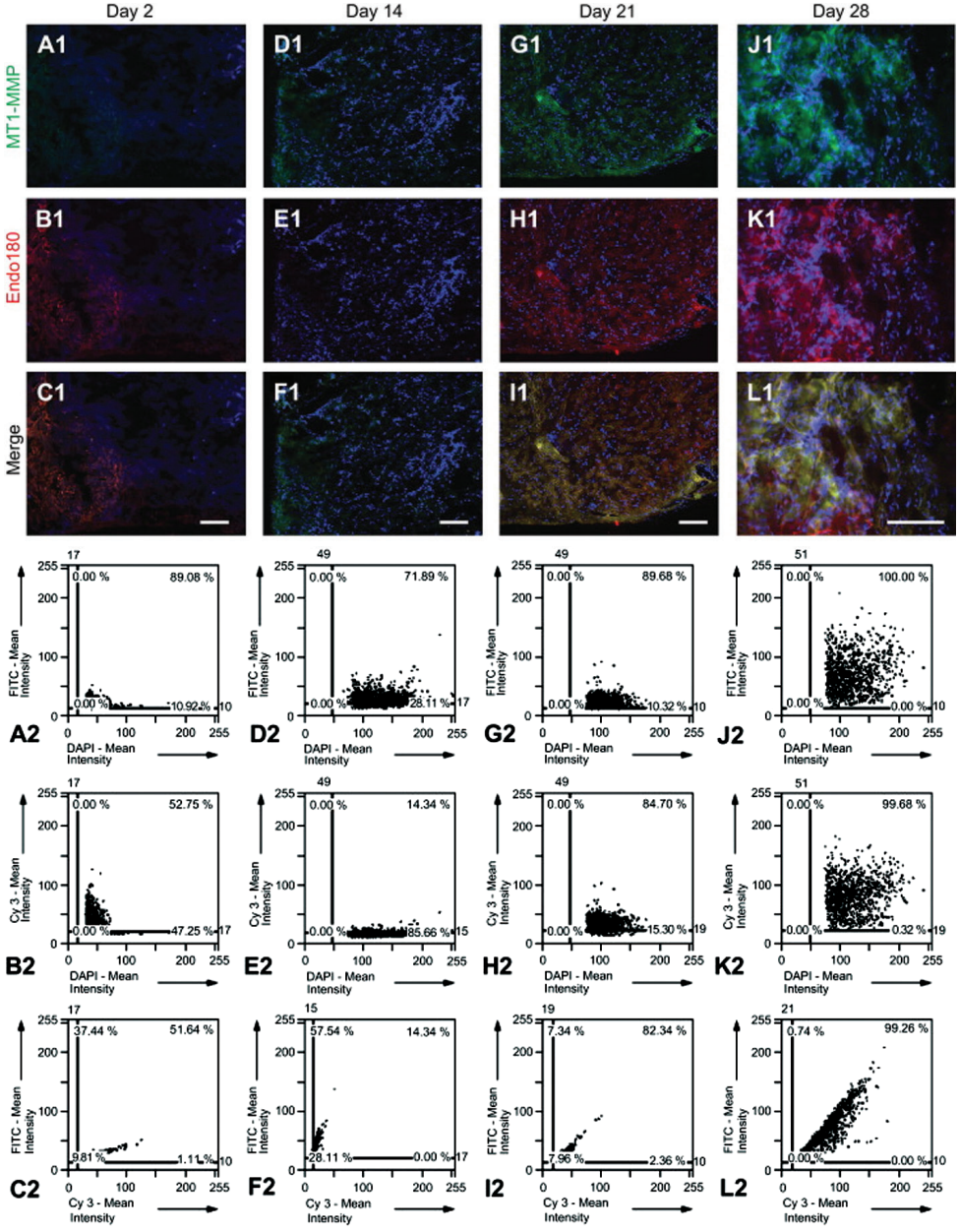
Day 2
Day 14
Day 21
Day 28
MT1-MMP
Endo180
Merge
A1
D1
G1
J1
B1
E1
H1
K1
C1
F1
I1
L1
A2
D2
G2
J2
B2
E2
H2
K2
C2
F2
I2
L2
FITC - Mean Intensity
Cy 3 - Mean Intensity
DAPI - Mean Intensity
0.00 %
89.08 %
10.92 %
71.89 %
28.11 %
89.68 %
10.32 %
100.00 %
0.00 %
52.75 %
47.25 %
14.34 %
85.66 %
84.70 %
15.30 %
99.68 %
0.32 %
37.44 %
51.64 %
9.81 %
1.11 %
57.54 %
14.34 %
28.11 %
7.34 %
82.34 %
7.96 %
2.36 %
0.74 %
99.26 %

Figure 5.7 (next page) Protein expression analysis of MMP-13 and collagen receptor DDR-2 in NDSC scaffolds at days 2, 14, 21 and 28 (B1-L1): MMP-13 protein was stained with FITC (green, A1, D1, G1, J1) and DDR-2 with TRITC (red, B1, E1, H1, K1). The co-localization of DDR-2 and MMP-13 was shown in the merged micrographs (C1, F1, I1, L1). Cell nuclei were stained with DAPI (blue). Scale bar : 20 mm. Quantification of MMP-13 and DDR-2 expression in NDSC using TissueFaxs/ 2.2: Scattergrams (n : 3) show the percentage of cells that expressed MMP-13 (FITC channel, A2, D2, G2, J2) or DDR-2 (Cy 3 channel, B2, E2, H2, K2), and the percentage of cells that co-expressed MMP-13 and DDR-2 (C2, F2, I2, L2) in NDSC at the indicated time points.

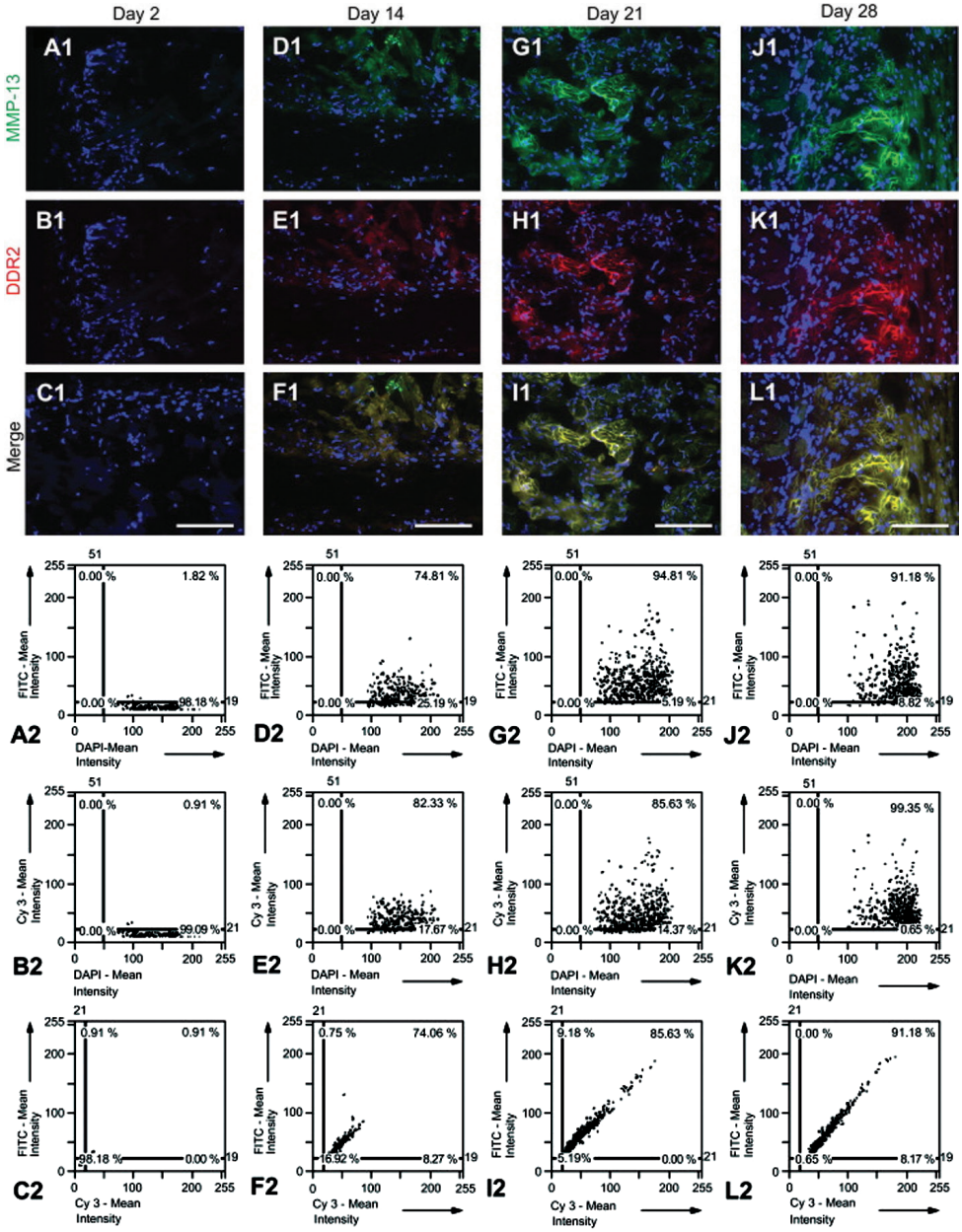
Day 2
Day 14
Day 21
Day 28
MMP-13
DDR2
Merge
A1
D1
G1
J1
B1
E1
H1
K1
C1
F1
I1
L1
A2
D2
G2
J2
B2
E2
H2
K2
C2
F2
I2
L2
FITC - Mean Intensity
Cy 3 - Mean Intensity
DAPI-Mean Intensity
DAPI - Mean Intensity
0.00 %
1.82 %
98.18 %
74.81 %
25.19 %
94.81 %
5.19 %
91.18 %
8.82 %
0.91 %
99.09 %
82.33 %
17.67 %
85.63 %
14.37 %
99.35 %
0.65 %
0.75 %
74.06 %
16.92 %
8.27 %
9.18 %
85.63 %
5.19%
8.17 %

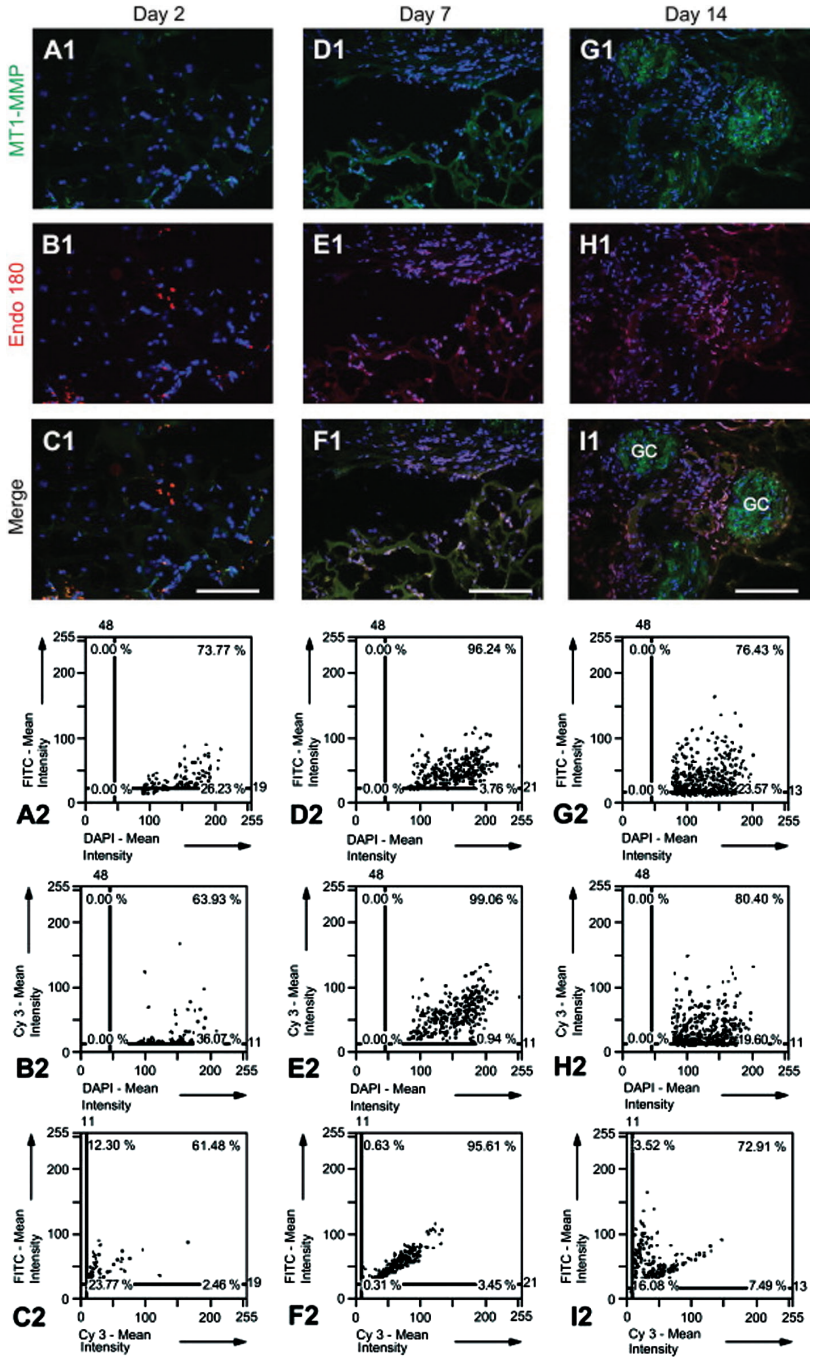
Day 2
Day 7
Day 14
MT1-MMP
Endo 180
Merge
A1
D1
G1
B1
E1
H1
C1
F1
I1
GC
GC
A2
D2
G2
B2
E2
H2
C2
F2
I2
FITC - Mean Intensity
DAPI - Mean Intensity
Cy 3 - Mean Intensity
0.00 %
73.77 %
26.23 %
96.24 %
3.76 %
76.43 %
23.57 %
63.93 %
36.07 %
99.06 %
0.94 %
80.40 %
19.60 %
12.30 %
61.48 %
23.77 %
2.46 %
0.63 %
95.61 %
0.31 %
3.45 %
3.52 %
72.91 %
16.08 %
7.49 %

Figure 5.8 (previous page) Protein expression analysis of MT1-MMP and collagen receptor Endo180 in gelatin scaffolds at days 2, 7 and 14 (B1-I1): MT1-MMP protein was stained with FITC (green, A1, D1, G1) and Endo180 with Cy3 (red, B1, E1, H1). The co-localization of Endo180 and MT1-MMP was shown in the merged micrographs (C1, F1, I1). Cell nuclei were stained with DAPI (blue). Scale bar : 20 mm. Quantification of MT1-MMP and Endo180 expression in gelatin using TissueFaxs/ 2.2: Scattergrams (n : 3) show the percentage of cells that expressed MT1-MMP (A2, D2, G2) or Endo180 (B2, E2, H2), and the percentage of cells that co-expressed MT1-MMP and Endo180 (C2, F2, I2) in gelatin scaffolds at the indicated time points. Symbols: GC : giant cell.

gelatin, the presence of giant cells was prominent (Fig. 5.8G1), as was their size which was larger than in NDSC. DDR-2 could not be observed (Fig. 5.9B1, E1, H1); MMP-13 was seen at day 7 and 14 (Fig. 5.9D1, G1) whereas it was absent at day 2 (Fig. 5.9A1).

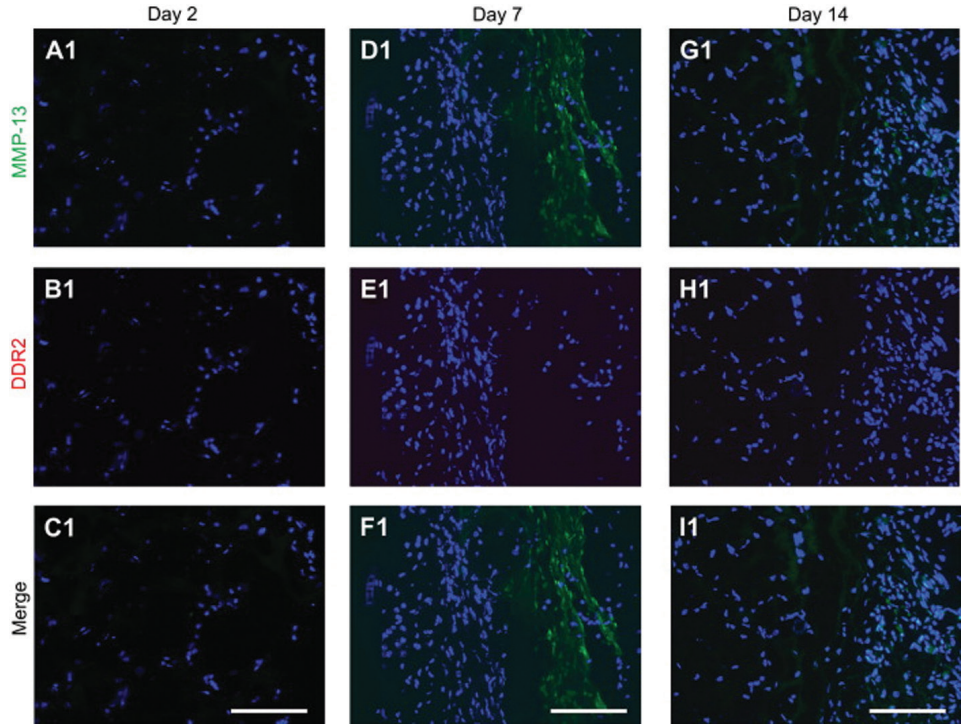

Figure 5.9. Protein expression analysis of MMP-13 and collagen receptor DDR-2 in gelatin scaffolds at days 2, 7 and 14 (B1-I1): MMP-13 proteinwas stained with FITC (green, A1, D1, G1) and DDR-2 with TRITC (red, B1, E1). The co-localization of DDR-2 and MMP-13 was shown in the merged micrographs (C1, F1, I1). MMP-13 was seen at day 7 and 14 whereas DDR-2 was absent throughout the time course. Cell nuclei were stained with DAPI (blue). Scale bar : 20 mm.

4. Discussion

The aim of our study was to investigate the putative role of collagen receptors in the degradation of native types of collagen during the foreign body reaction. We show that the degradation of denatured native collagen (gelatin) relates to the expression of Endo180 but not DDR-2, while MT1-MMP is involved too. In contrast, intact native collagen (NDSC) is degraded by macrophages and giant cells that express both collagen receptors and the accessory molecule MT1-MMP as well active collagenase MMP-13. The degradation rate of gelatin was far higher than NDSC, which correlated with the higher ratio of giant cells compared to macrophages in gelatin. Furthermore, the giant cells in gelatin were several times larger in gelatin than NDSC, and TIMP-1 expression was absent in gelatin whereas it was expressed at all time points in NDSC.

4.1. Gelatin and non-crosslinked native collagen (NDSC) disks show different degradation rates

The tissue response towards the gelatin disks and the non-crosslinked, native collagen disks differed markedly. with respect to the numbers of macrophages, the efficiency of giant cell formation, the size of the giant cells, the influx of neutrophils, and the micro-environment (presence of TIMP-1), the expression of MMPs, and the expression of the collagen receptors Endo180 and DDR-2. Thus, the physical state of the collagen itself (denatured or native) has a dramatic impact on the outcome of the foreign body reaction. Gelatin disks were almost completely degraded within three weeks after subcutaneous implantation in mice, whereas the largest part of the native collagen disks (around 80%) was still present after 28 days. We have previously seen major differences in the degradation rate of subcutaneously implanted disks consisting of native collagen that was cross-linked either by glutaraldehyde or hexamethylenediisocyanate. In the present study we have used non-crosslinked collagen; mainly the

physical state (native or denatured) differed. Clearly, the tissue response can be modulated by modifying the chemical and/or physical nature of collagen. This can be of help in the design of scaffolds that show a tuned regulation of degradation.

4.2. Degradation of NDSC disks

Despite the frequent use of collagen-based scaffolds in tissue engineering, remarkably little is known about the molecular mechanism that are involved in the breakdown of the scaffolds. We have here investigated the expression of the major collagenases MMP-8 and MMP-13, the major gelatinases MMP-2 and MMP-9, the membrane-bound MT1-MMP (also known as MMP-14) and the endogenous MMP inhibitor TIMP-1. Despite the presence of MMP-8 and MMP-13 expression at most time points, and at certain time points MMP-2, MMP-9 and MT1-MMP as well, only limited degradation of the NDSC disks is observed after 28 days. An explanation for this might be the expression of TIMP-1 at all time points. Indeed, *in situ* zymography (with DQ™ collagen type I form bovine skin conjugated to fluorescein as the substrate) was not able to detect collagenolytic activity at days 2 and 7, indicating that TIMP-1 was able to inhibit at these two days at least MMP-8 and MMP-13, the two enzymes that are able to degrade DQ™ collagen. On the other hand, *in situ* zymography detected (weak to strong) collagenolytic activity at day 14, 21 and 28. On these days, a marked increase is seen in the expression of MMP-13. In addition, MT1-MMP was present on these three time points. Since TIMP-1 is a very poor inhibitor of MT1-MMP [24] and [25], the collagenolytic activity as detected by *in situ* zymography seems to be due to MT1-MMP and/or the raised levels of MMP-13. The limited degradation of NDSC disks thus seems to be due to the presence TIMP-1, and the relatively late appearance of net collagenolytic activity as detected by DQ™ collagen. This collagenolytic activity seems to be derived from MMP-13 and/or MT1-MMP.

4.3. Degradation of gelatin disks

The gelatin disks were quickly degraded: almost the entire disk was degraded after 21 days. At first sight this seems surprising, as expression of MMP-9 was only detected at day 2 and not on the other days. However, there is a high expression of MMP-13 at day 7; this high expression coincides with the high collagenolytic activity seen at day 7 with DQ™ collagen. MMP-13 is, apart from being a collagenase, also an efficient gelatinase [26]. The absence of TIMP-1 expression also provides a good micro-environment for enzymes that are able to degrade gelatin to carry out their job. Another reason why the gelatin disks have a high degradation rate is the presence of large multinucleated foreign body giant cells that were actively phagocytosing. These giant cells were of an order of magnitude bigger in gelatin and thus better equipped to degrade/phagocytose the gelatin.

4.4. Possible role of Endo180 and DDR-2 in the degradation of the NDSC and gelatin disks

We have recently provided evidence that macrophages are able to express under certain circumstances both Endo180 and MT1-MMP, and that these cells are involved in the phagocytosis of collagen [15]. In the present study we showed a co-expression of Endo180 and MT1-MMP at day 21 and 28 in NDSC; histological examination showed at these time points many phagocytosing mononuclear cells. It is likely that the degradation of NDSC, that starts rather late after implantation, is partly due to phagocytosis of the collagen by macrophages by means of Endo180/MT1-MMP in a comparable way as it has been observed for fibroblasts: cleavage of the fibrils by MT1-MMP, binding to the Endo180 collagen receptor and subsequent internalization [18] and [19].
Another collagen receptor that showed interesting expression dynamics in NDSC disks is DDR-2, a receptor that recognizes collagen in its native (i.e. triple helical) state [20] and [27]. In chondrocytes and fibroblasts it was found that activation of the DDR-2 by native collagen induces the expression of MMP-13 [20], [21], [22] and [23]. In NDSC, infiltrating

cells started to highly express DDR-2 only late after implantation, Yet, DDR-2 expression coincided with gene expression of MMP-13. The semi-quantitative gene expression data would even suggest that an increased expression of MMP-13 coincides with DDR-2 upregulation. Our immunofluorescent staining data further strengthen this finding: in the NDSC disks in the areas rich in macrophages MMP-13 and DDR-2 always co-expressed. It is therefore tempting to speculate, that the MMP-13 expression is due to the activation of the DDR-2 receptor by the NDSC disks. Thus, beside phagocytosis by means of Endo180/MT1-MMP, the NDSC disks might also be subjected to extracellular degradation, through MMP-13 via the activation of DDR-2.

In the gelatin disks a different situation is seen with respect to Endo180 and DDR-2. Endo180 expression was already observed from the beginning (day 2), with increased levels at day 7 and 14. The same was seen for MT1-MMP. However, MT1-MMP showed a different cellular distribution than Endo180 at day 2 and 14, whereas they were co-expressed at day 7. More research needs to be carried out to understand the meaning of this. In addition, DDR-2 expressing cells were not observed in the gelatin disks. The expression of MMP-13 at day 7 and 14 in the gelatin disks cannot therefore have been induced by the activation of DDR. This absence of DDR-2 expression was expected, since (1) DDR-2 only recognizes collagen only in its native form [20] and [27], and (2) native collagen induces the expression of DDR-2, not denatured collagen [20]. The gelatin disks consist of denatured collagen only.

5. Conclusion

Degradation of gelatin disks and disks made of non-crosslinked native collagen (NDSC) showed major differences. Gelatin was almost completely degraded at day 21, whereas only about 20% of NDSC disk was degraded at day 28. The degradation of NDSC occurred only late during the tissue response. Essentially nothing is known about the role of the collagen receptors Endo180 and DDR-2 in the foreign body reaction (FBR). Here we report that the degradation of NDSC coincided with the co-expression of Endo180 and MT1-MMP on macrophages that most likely led to the phagocytic behaviour of these cells towards NDSC. Furthermore, we report the presence of DDR-2 on macrophages in the FBR. Cells expressing DDR-2 also co-expressed MMP-13 (as a consequence of DDR-2 activation), and it is likely that this enzyme was involved in the extracellular degradation of NDSC. No DDR-2 expression was observed in the gelatin disks. Although many Endo180-positive cells are seen in gelatin, they did not co-express MT1-MMP at most time points; the meaning of this needs to be investigated. Gelatin seemed to be mainly degraded by MMP-13 and by means of phagocytosis by giant cells.

Acknowledgements

This study was supported by RuG Jan Kornelis de Cock-Stichting (Q. Ye, De Cock 10-70). The authors wish to thank Professor Marja van Luyn for her kind assistance at the beginning of this study, and to acknowledge the excellent technical support of Mr. Jasper Koerts and Mrs. Linda Brouwer.

References

1. D.J. Prockop . What holds us together? Why do some of us fall apart? What can we do about it?. Matrix Biol, 16 (1998), pp. 519–528

2. R. Langer, J.P. Vacanti. Tissue engineering. Science, 260 (1993), pp. 920–926

3. S.F. Badylak, D.O. Freytes, T.W. Gilbert. Extracellular matrix as a biological scaffold material: structure and function. Acta Biomater, 5 (2009), pp. 1–13

4. J. Glowacki, S. Mizuno. Collagen scaffolds for tissue engineering. Biopolymers, 89 (2008), pp. 338–344

5. H.C. Liang, Y. Chang, C.K. Hsu, M.U. Lee, H.W. Sung. Effects of crosslinking degree of an acellular biological tissue on its tissue generation pattern. Biomaterials, 25 (2004), pp. 3541–3552

6. P.J. Geutjens, W.F. Daamen, P. Buma, W.F. Feitz, K.A. Faraj, T.H. van Kuppevelt. From molecules to matrix: construction and evaluation of molecularly defined bioscaffolds. Adv Exp Med Biol, 585 (2006), pp. 279–295

7. W.G. Brodbeck, J.M. Anderson. Giant cell formation and function. Curr Opin Hematol, 16 (2009), pp. 53–57

8. A. Vignery. Macrophage fusion: the making of osteoclasts and giant cells. J Exp Med, 202 (2005), pp. 337–404

9. L. Helming, S. Gordon. Molecular mediators of macrophage fusion. Trends Cell Biol, 19 (2009), pp. 514–522

10. V. Glattauer, J.F. White, W.B. Tsai, C.C. Tsai, T.A. Tebb, S.J. Danon et al.

Preparation of resorbable collagen-based beads for direct use in tissue engineering and cell therapy applications. J Biomed Mater Res A, 92 (2010), pp. 1301–1309

11. Ye Q, van Amerongen MJ, Sandham JA, Bank RA, van Luyn MJA, Harmsen MC. Site-specific tissue inhibitor of metalloproteinase-1 governs the matrix metalloproteinases-dependent degradation of crosslinked collagen scaffolds and is correlated with interleukin-10. J Tissue Eng Regen Med, in press.

12. M.J. van Amerongen, M.C. Harmsen, A.H. Petersen, G. Kors, M.J.A. van Luyn . The enzymatic degradation of scaffolds and their replacement by vascularized extracellular matrix in the murine myocardium. Biomaterials, 27 (2006), pp. 2247–2257

13. D.T. Luttikhuizen, M.C. Harmsen, M.J.A. van Luyn . Cytokine and chemokine dynamics differ between rats and mice after collagen implantation. J Tissue Eng Regen Med, 1 (2007), pp. 398–405

14. D.T. Luttikhuizen, M.J. van Amerongen, P.C. de Feijter, A.H. Petersen, M.C. Harmsen, M.J.A. van Luyn. The correlation between difference in foreign body reaction between implant locations and cytokine and MMP expression. Biomaterials, 27 (2006), pp. 5763–5770

15. Q. Ye, Q. Xing, Y. Ren, M.C. Harmsen, R.A. Bank. Endo180 and MT1-MMP are involved in the phagocytosis of collagen scaffolds by macrophages and is regulated by interferon-gamma. Eur Cell Mater, 20 (2010), pp. 197–209

16. Q. Ye, M.C. Harmsen, M.J.A. van Luyn, R.A. Bank . The relationship between collagen scaffold cross-linking agents and neutrophils in the foreign body reaction. Biomaterials, 31 (2010), pp. 9192–9201

17. B. Leitinger . Mammalian collagen receptors. Matrix Biol, 26 (2007), pp. 146–155

18. L.H. Engelholm, K. List, S. Netzel-Arnett, E. Cukierman, D.J. Mitola, H. Aar-

onson et al.. uPARAP/Endo180 is essential for cellular uptake of collagen and promotes fibroblast collagen adhesion. J Cell Biol, 160 (2003), pp. 1009–1015

19. D.H. Madsen, L.H. Engelholm, S. Ingvarsen, T. Hillig, R.A. Wagenaar-Miller, L. Kjøller et al. Extracellular collagenases and the endocytic receptor, urokinase plasminogen activator receptor-associated protein/Endo180, cooperate in fibroblast-mediated collagen degradation. J Biol Chem, 282 (2007), pp. 27037–27045

20. L. Xu, H. Peng, D. Wu, K. Hu, M.B. Goldring, B.R. Olsen et al. Activation of the discoidin domain receptor 2 induces expression of matrix metalloproteinase 13 associated with osteoarthritis in mice. J Biol Chem, 280 (2005), pp. 548–555

21. I.G. Sunk, K. Bobacz, J.G. Hofstaetter, L. Amoyo, A. Soleiman, J. Smolen et al. Increased expression of discoidin domain receptor 2 is linked to the degree of cartilage damage in human knee joints. Arthritis Rheum, 56 (2007), pp. 3685–3692

22. L. Xu, H. Peng, S. Glasson, P.L. Lee, K. Hu, K. Ijiri et al. Increased expression of the collagen receptor discoidin domain receptor 2 in articular cartilage as a key event in the pathogenesis of osteoarthritis. Arthritis Rheum, 56 (2007), pp. 2663–2673

23. J. Su, J. Yu, T. Ren, W. Zhang, Y. Zhang, X. Liu et al. Discoidin doamin receptor 2 is associated with the increased expression of matrix metalloproteinase-13 in synovial fibroblasts of rheumatoid arthritis. Mol Cell Biochem, 330 (2009), pp. 141–152

24. M.H. Lee, M. Rapti, V. Knäuper, G. Murphy . Threonine 98, the pivotal residue of tissue inhibitor of metalloproteinases (TIMP-1) in metalloproteinase recognition. J Biol Chem, 279 (2004), pp. 17562–17569

25. H. Nagase, R. Visse, G. Murphy . Structure and function of matrix metalloproteinases and TIMPs. Cardiovasc Res, 69 (2006), pp. 562–573

26. V. Knäuper, C. López-Otin, B. Smith, G. Knight, G. Murphy. Biochemical characterization of human collagenase-3. J Biol Chem, 271 (1996), pp. 1544–1550

27. B. Leitinger. Molecular analysis of collagen binding by the human discoidin domain receptors, DDR1 and DDR-2. J Biol Chem, 278 (2003), pp. 16761–16769

28. I.M. Khouw, P.B. van Wachem, J.A. Plantinga, L.F. de Leij, M.J. van Luyn . Enzyme and cytokine effects on the impaired onset of the murine foreign-body reaction to dermal sheep collagen. J Biomed Mater Res, 54 (2001), pp. 234–240

CHAPTER 6

The presence of cathepsin K in the foreign body reaction: evidence for different subsets of giant cells

Qingsong Ye [1,2]
Ruud A. Bank [1]

[1] Stem Cell and Tissue Engineering Research Group,
Department of Pathology and Medical Biology, University of Groningen, The Netherlands

[2] School of Medicine and Dentistry,
James Cook University, Cairns, Australia

Manuscript in Preparation

Abstract

In tissue engineering, both synthetic and natural biomaterials are used as a guidance for cells to produce *de novo* tissues. All these biomaterials provoke a foreign body reaction (FBR) when implanted *in vivo*. In order to accommodate new tissue formation, scaffolds needs to be degraded. With regard to the degradation of collagen scaffolds, all studies focussed on the role of matrix metalloproteinases. Yet nothing is known on cathepsin K, a strong collagenolytic enzyme, in the involvement of the FBR. This study reports for the first time that cathepsin K and TRAP, two enzymes that are highly expressed in osteoclasts (cells that are invowlved in bone degradation), are present in the FBR towards non-crosslinked collagen (NDSC), glutaraldehyde cross-linked collagen (GDSC) and hexamethylenediisocyanate cross-linked collagen (HDSC), but not in the FBR against gelatin implants. Cathepsin K is not involved in the fast degradation of gelatin due to its absence. In GDSC, cathepsin K-positive cells are seen at day 14 and 21, which may contribute partially to the rapid degradation of glutaraldehyde cross-linked collagen (GDSC) scaffolds. Despite the presence of cathepsin K at various time points in both non-crosslinked collagen (NDSC) and hexamethylenediisocyanate crosslinked collagen (HDSC), the NDSC scaffolds are only marginally degraded and HDSC scaffolds essentially remain intact during the time period studied (4 weeks). In the FBR towards NDSC the main cells showing cathepsin K positivity are the multinucleated cells, whereas in the FBR towards GDSC the main cells showing cathepsin K positivity are the mononucleated cells. The giant cells in the FBR towards gelatin and NDSC show different phenotypic properties, as they are cathepsin K negative and cathepsin K positive, respectively. So far, hardly any attention has been paid to the role of giant cell heterogeneity and cathepsin K in the tissue response towards biomaterials. More investigations are needed to gain further insight into the role of cathesin K and giant cell heterogeneity in the foreign body reaction.

Introduction

Cathepsin K, first described in 1994/1995 [1-5], is an enzyme that shows a high degrading potential towards collagen and elastin [6]. For example, it is able to cleave native (triple helical) collagen at multiple sites [7-9]. Its high presence in osteoclasts suggests a major role of cathepsin K in the proteolytic degradation of bone collagen, which was confirmed by knock-out studies [10-11] and by the phenotypic properties of pycnodysostosis, a hereditary disease caused by mutations in the cathepsin K gene [12, 13].

Osteoclasts are bone-degrading multinucleated cells derived from cells of the myeloid lineage [14]. In chronic inflammatory conditions, especially in the granulomatous response to tissue injury caused by micro-organisms or other foreign particles, multinucleated cells (also known as giant cells) are often seen as well. The same is seen in the foreign body reaction towards implanted biomaterials. These multinucleated cells are, like osteoclasts, derived from cells from the myeloid lineage, in particular macrophages. The fusion process of mononuclear myeloid cells into osteoclasts or giant cells shows many similarities [15, 16]. It seems therefore likely that cathepsin K, abundantly expressed in osteoclasts, is also present in giant cells. Indeed, cathespin K has been reported in giant cells from various soft tissue lesions (granulomas) of diverse aetiology [17-23], atherosclerotic plaques [24], synovium [25-27], and giant cell tumours and carcinomas [19, 28-30].

So far, hardly any attention has been given towards cathepsin K in the foreign body reaction directed against implanted materials. To our knowledge, only three papers mention the presence of cathepsin K-positive giant cells in the foreign body reaction, namely towards wear debris derived from the gliding surfaces of prostheses used in joint replacements [17, 21, 22]. Tissue engineering exploits the use of biomaterials as an alternative to artificial tissue substitutes such as prostheses. Numerous biomaterials have been developed, based on synthetic polymers and/

or natural polymers. All of these biomaterials provoke a foreign body reaction after implantation.

Collagenous biomaterials have been introduced for various tissue engineering applications. The degradation rate of these biomaterials is determined to a large extent by the course of the foreign body reaction. Although quite some data are available with respect to the presence of matrix metalloproteinases in collagenous scaffolds [45-48], nothing is known regarding the presence of cathepsin K. We here investigate the relationship between the presence of giant cells and cathepsin K in disks based on gelatin or (non)cross-linked collagen as well as two cross-linked collagen (HDSC, GDSC) that are implanted in mice. In addition, we studied the presence of tartrate-resistant acid phosphatase (TRAP), an enzyme that has long been used as a histochemical marker for the osteoclast.

Material & Methods

2.1 Animals and biomaterials

Male C57BL/6 mice (10 weeks old, Harlan, Horst, the Netherlands) were housed individually under conventional conditions with food and water *ad libitum*.

Non-crosslinked dermal sheep collagen (NDSC), processed from sheep skin, was obtained from the Zuid Nederlandse Zeemlederfabriek (Oosterhout, the Netherlands). DSC was cross-linked with either glutaraldehyde (henceforth referred to as GDSC) or hexamethylenediisocyanate (henceforth referred to as HDSC), according to protocols described previously [47]. Commercially available non-crosslinked gelatin sponges Willospon (Will-Pharma, Benelux) were kindly provided by the Department of Oral Surgery of the University Medical Center Groningen. Disks (6 mm in diameter, 0.75 mm in thickness) were punched from pieces of HDSC and GDSC from the same batch, and sterilized with ethylene oxide. Surface-associated endotoxin levels were below 0.25 EU/ml, as determined by the LAL-method (Cambrex, LAL kinetic-QCL®).

2.2 Operating procedures

All procedures performed on animals were approved by the local committee for care and use of laboratory animals of the University of Groningen and were performed according to international and governmental guidelines on animal experimentation.

Implantation: mice were anesthetized with 4% isoflurane and maintained by 2% isoflurane inhalation in combination with a mixture of equal volumes of N_2O and O_2. The back was shaved and desinfected with chlorhexidine, two incisions were made and subcutaneous pockets were created on both sides. The HDSC or GDSC disks were implanted

about one centimeter away from the incision site, thus minimizing the effect of wound healing on the inflammatory reaction. The incisions were closed with 6-0 non-absorbable Prolene sutures. Finally, mice received pure oxygen until awakening.

Explantation: the Col-I disks were removed at the following time points after implantation (related to the different phases of the FBR in mice): 2 days (onset), 7 days (early progression), 14 and 21 days (intermediate progression), and 28 days (late progression), n=6 per time point. The disks were snap-frozen in liquid nitrogen immediately after explantation.

2.3 Histological techniques

Tissue sections (2 μm in thickness) of T 7100 (Heraeus Kulzer, Wehrheim, Germany) embedded explants were stained with toluidine blue (Fluka Chemie, Buchs, Switzerland) and mounted in Permount (Fisher, New Jersey, USA). Sections were analyzed by light microscopy. The number of giant cells per square millimeter inside implant on blinded samples was counted independently by two investigators. The degradation of the scaffold was determined by image analysis as the percentage of the size of remained disk as compared with the original size (before implantation). The cellular ingrowth inside the disk was evaluated by image analysis as percentage of the entire cross-sectional area, as described in our previous study [45].

2.4 Immunohistochemistry

To determine the infiltration of macrophages during the time course, sections were stained for macrophages (rat anti-mouse F4/80, Serotec Ltd. Oxford, UK), as described previously by our lab [46].

2.5 Cathepsin K activity

Cathepsin K activity was measured according to the protocol described previously [49]. In brief, cryo-sections (5 μm) from the snap-frozen explanted scaffold, cut in the middle of the explant transversally, were

immersed in sodium acetate buffer (0.1 M, pH 6, 0.2% Triton), extracted overnight in the same buffer at 4 °C, and thereafter centrifuged at 15,000 rpm for 5 minutes. The supernatant from different samples was retained and equalized with respect to protein concentration, incubated with Z-Gly-Pro-Arg-4-MNA (1 mg/ml cathepsin K substrate) in 100 mM phosphate buffer (pH 6.0; in the presence of dithiothreitol, EDTA, and cysteine) for 1 hour, and analyzed using a multilabel counter (Wallac 1420 Victor2; Perkin Elmer Life Sciences, Turku, Finland). A proteinase inhibitor (E-64) was added to the extract in the control groups. For the histochemistry, cryo-sections (7 μm, n = 4 per time point) on glass slides, prepared according to the standard procedure as previously described [49]. Briefly, the sections were incubated for up to 3h at 37°C in an aqueous solution of Z-Gly-Pro-Arg-4-MNA (1 mg/ml cathepsin K substrate) in 100 mM phosphate buffer (pH 6.0; in the presence of dithiothreitol, EDTA, and cysteine) [50]. After that, the sections were immediately washed with 10 mM N-ethylmaleimide in 0.1 M phosphate buffer (pH 8) to cease the reaction. The insoluble fluorescent (NSA) was added to the incubation medium to visualize liberated MNA. Control sections were incubated in the presence of substrate and E-64 (inhibitor). The insoluble fluorescent (NSA) was observed under a Leica microscope with or without epifluorescence and micrographs were made with Kodak 400 ASA film. Control sections were negative.

Consecutive sections were prepared for the activity of tartrate-resistant acid phosphatase (TRAP).

2.6 TRAP activity

Cryo-sections (5 μm) from the snap-frozen explanted scaffold, cut in the middle of the explant transversally, were immersed in TRAP test buffer (50 mM NaAc, pH 4, 0.1% Triton), extracted overnight in the same buffer at 4 °C, and thereafter centrifuged at 15,000 rpm for 5 minutes. Extracted tissue samples were equalized with respect to protein content, and TRAP enzyme activity was assayed in 96-well plates using pNPP as the substrate in an incubation medium containing 10 mM pNPP, 0.1 M Na-acetate (pH 5.8), 0.15 M KCl, 0.1% (v/v) Triton X-100, 10 mM Na-tartrate, 1

mM ascorbic acid, and 0.1 mM FeCl3. The p-nitrophenol liberated after 1 hour of incubation at 37°C was converted into p-nitrophenylate by the addition of 100 µL of 0.3 M NaOH, and the absorbance was read at 405 nm using a multilabel counter (Wallac 1420 Victor2; Perkin Elmer Life Sciences, Turku, Finland). One unit of TRAP activity hydrolyzes 1 µM of pNPP per minute at 37°C. This assay proved to be linear both within the range of enzyme dilutions used and for the time of incubation (up to 1 hour).

For the histochemistry, cryo-sections (7 µm, n = 4 per time point) on glass slides, were prepared according to the standard procedure as described previously [50].In brief, sample sections were incubated for 1h at 37°C in ATP substrate (12.6 mg ATP, 20 ml 0.2 M TRIS-maleate, 1.5 ml 2% lead nitrate and 2.5 ml 0.1 M magnesium nitrate, pH 6) and 50mM disordium tartrate. Immediately after the incubation, sections were washed in 0.05 M acetate buffer (pH 6) with 0.2M sucrose for 2 times, followed by 0.1% ammonium sulfide to visualize the reaction product of TRAP activity. The same procedures were applied for the control samples except for the incubation medium which either contained no substrate or added with inhibitor (10mM soldium-ortho-vanadate). Control sections were negative.

2.7 Statistical analyses

All quantitative data are presented as mean ± SEM. The data were analyzed using statistical software (GraphPad Prism, GraphPad Software Inc.). Differences within groups were analyzed by two-way ANOVA followed by Tukey's *post hoc* test. Differences between groups were analyzed by one-way ANOVA and Student's t-test. A difference of $p<0.05$ was considered statistically significant.

Results

Influx of macrophages and presence of giant cells

In gelatin, a small number of macrophages was seen at day 2, with increasing numbers at day 7 and 14, decreasing at day 21 (Figure 6.1A). Giant cells appeared at day 2, increased at day 7, showed a steep increase at day 14, and decreased at day 21. In NDSC, a small number of macrophages was found at day 7, whereas the number of macrophages

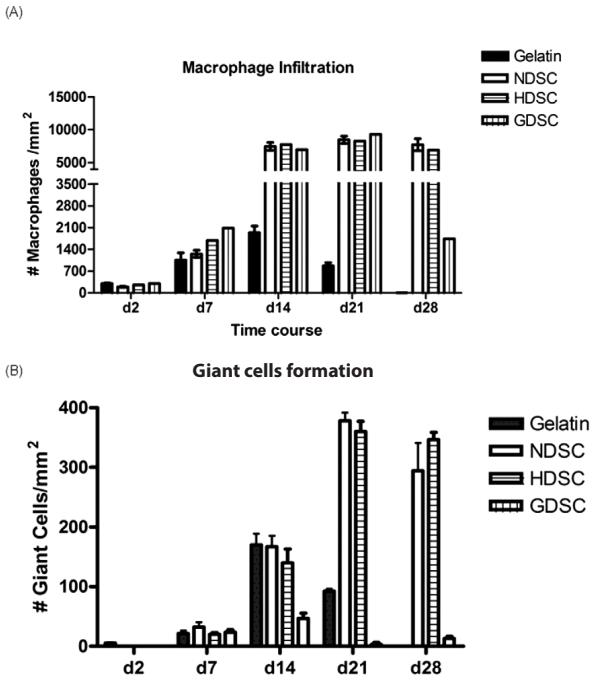

Figure 6.1. Comparison of the infiltration of macrophages (A) and the formation of giant cells (B) in gelatine, NDSC, HDSC and GDSC disks (Data presented as Mean ± SEM).

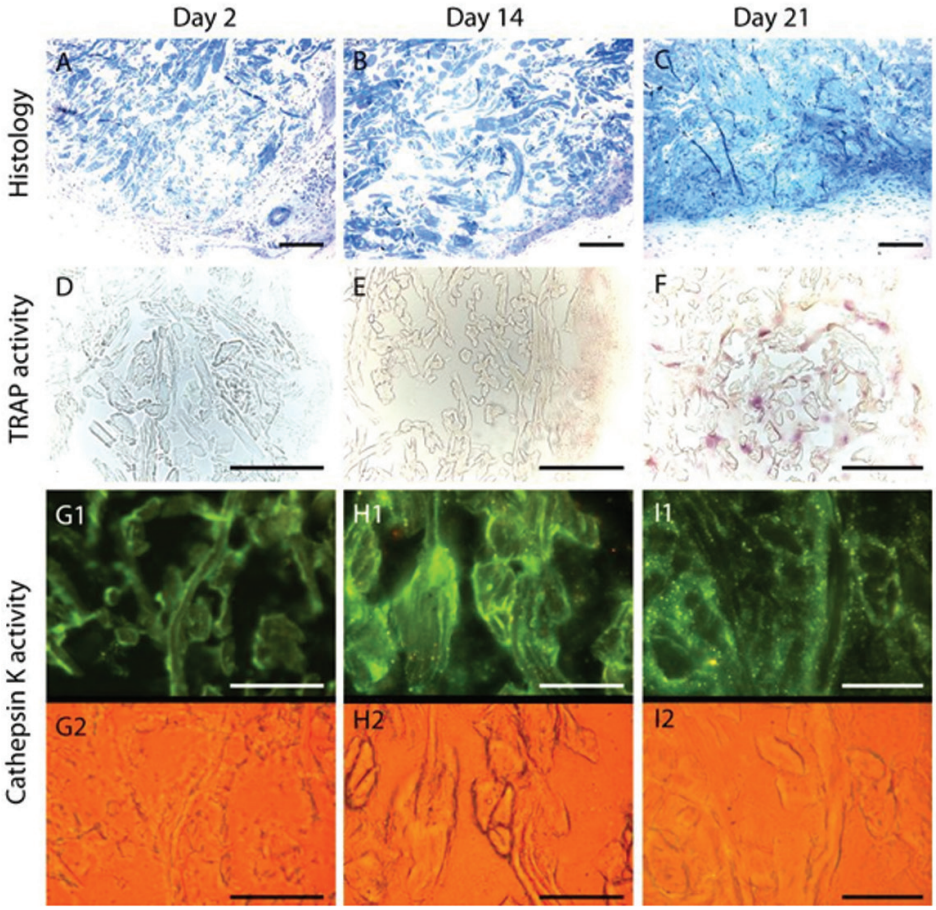

Figure 6.2. General histology, as well as histochemistry of TRAP and cathepsin K activity in NDSC at day 2, day 14 and day 21. A-B: marginal degradation, > 80% of the scaffold was still present; D-E: elevated levels of TRAP was observed at days 2, 14 and 21; G1-I1: no active cathepsin K was observed at day 2, whereas at day 14 cells were seen containing active cathepsin K. The number of cathepsin K-positive cells was considerably increased at day 21. The cathepsin K positive cells were mostly multinucleated cells, based on the size of the coloured spots (G2-I2). Scale bar = 20 µm.

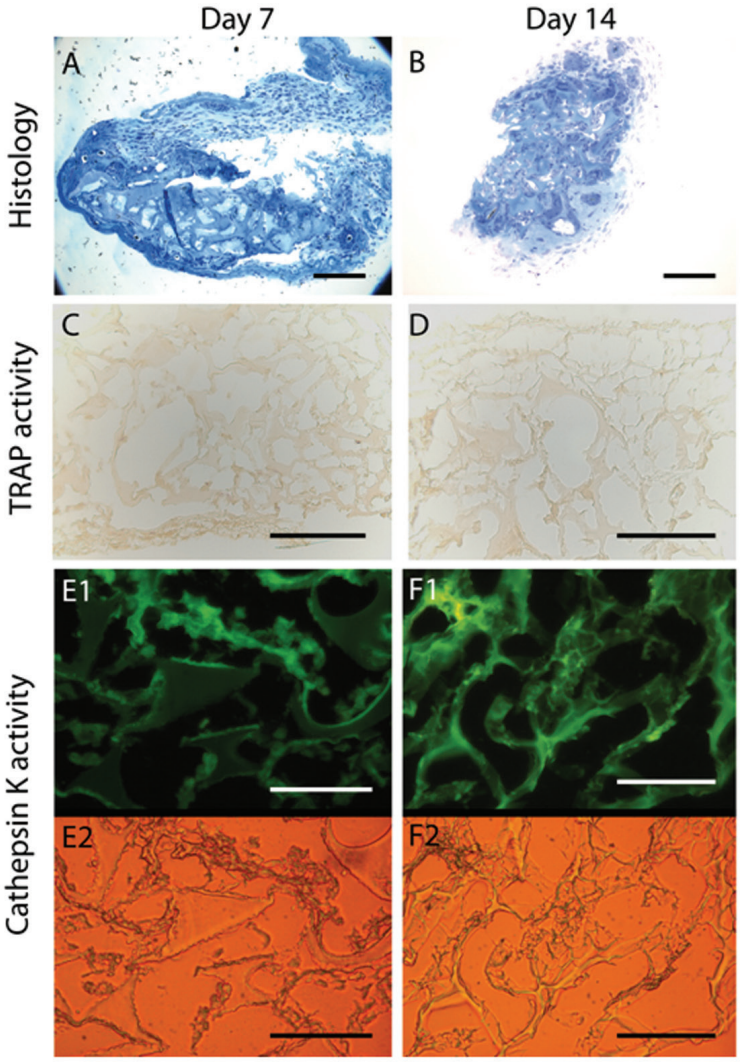

Figure 6.3. General histology, as well as histochemistry of TRAP and cathepsin K activity in gelatin at day 7 and day 14. A-B: gelatin disks were rapidly degraded during the time course; C-D: no TRAP activity was observed; E1-F1: no cathepsin K activity was observed at the related site (E2-F2). Scale bar = 20 µm

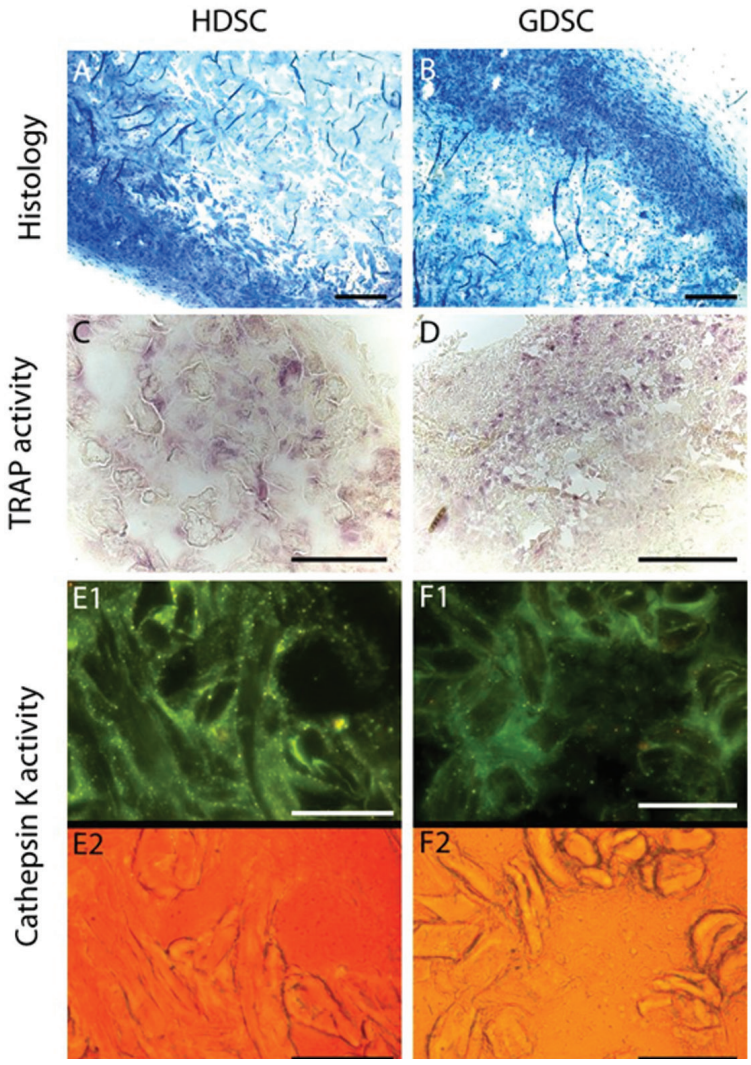

Figure 6.4. General histology, as well as histochemistry of TRAP and cathepsin K activity in HDSC and GDSC at day 21. A: HDSC collagen bundles remained intact at day 21; B: 70% of GDSC collagen bundles was degraded at day 21; C-D: TRAP activity was observed in both HDSC and GDSC at day 21; E1-F1: cathepsin K activities was observed in both HDSC and GDSC (E1-E2) at day 21. Scale bar = 20 µm.

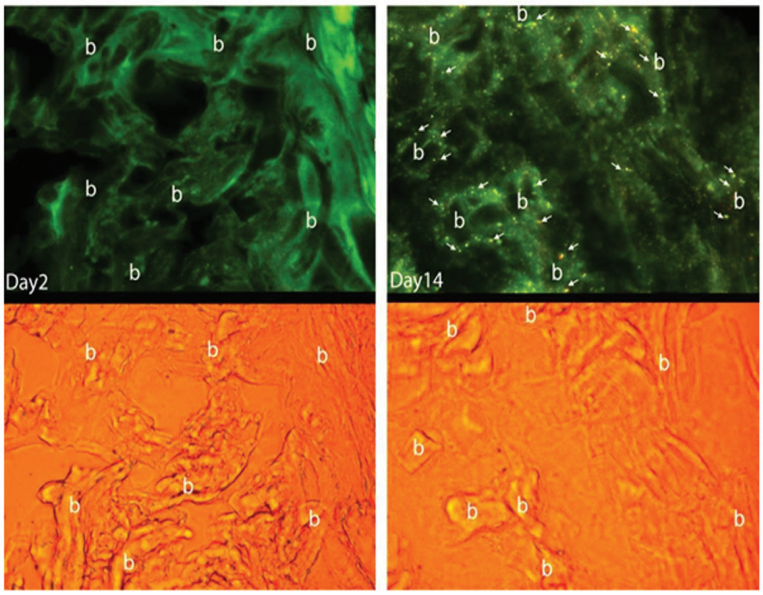

Figure 6.5. Enlarged picture of cathepsin K activity staining in NDSC at day 2 day 14. No cathepsin K activity was observed at day 2; the activity of cathepsin K at day 14 exhibited a dot-like pattern alongside the collagen bundles. Symbols: b = collagen bundles; arrows: cathepsin K activity.

was about 7-fold higher at day 14, 21 and 28 compared to day 7 (Figure 6.1A). No giant cells were seen at day 2, whereas small numbers of giant cells were seen at day 7, a number that increased at day 14 and 21, and showed a slight decrease at day 28.
In HDSC, the number of macrophages was gradually increased during the FBR course; whereas in GDSC, the number of macrophages was increased steadily and reached its peak at day 21, and then rapidly reduced at day 28 (Figure 6.1A). The presence in time and the abundance of giant cells did not differ between HDSC and NDSC. Virtually no giant cells were observed in GDSC.

The ratio of macrophages to giant cells at day 14 and 21 in NDSC and HDSC was around 40:1 and 20:1, respectively, whereas in gelatin this ratio was around 10:1 for both time points. Thus, the formation of giant cells out of macrophages was most effective in gelatin, less effective in NDSC and HDSC, and incapable in GDSC disks.

Scaffold degradation

Rapid degradation of the gelatin disks took place (Figure 6.3A-B); after 21 days only a tiny fraction of the disk was present whereas no residual material could be traced at day 28. Phagocytosis was observed at days 2,7 and 14 by multinucleated giant cells [45]. The NDSC disks were still present at day 21 (Figure 6.2C); although degradation had been taken place, the majority of the scaffold (> 80%) was still present. Phagocytosis was observed at days 21 and 28 mainly by mononucleated macrophages [45].

In HDSC, no phagocytosis was observed and the disks remained intact throughout the time course (Figure 6.4A). Phagocytosis of collagen by macrophages was observed at days 2 and 21 in GDSC [47], and more than 70% of the GDSC disk was degraded at day 21 (Figure 6.4B).

Presence of active cathepsin K

The activity of cathepsin K exhibited a dot-like pattern alongside the collagen bundles as showed in Figure 6.5. In gelatin, no cathepsin

K-positive cells were seen at day 7 and 14 by means of histochemistry (Figure 6.3); this was confirmed by the cathepsin K enzyme activity assay (Figure 6.6A). In NDSC, no active cathepsin K was observed at day 2 by means of histochemistry, whereas at day 14 cells were seen containing active cathepsin K (Figure 6.2 G1,H1). The number of cathepsin K-positive cells was even higher at day 21 (Figure 6.2 I1). The data fit with that of the cathepsin K enzyme activity assay: background levels at day 7, an increased level at day 14, a maximum level at day 21, and decreasing again at day 28 (Figure 6.6A). The cathepsin K positive cells were mostly -if not all- multinucleated cells, based on the size of the coloured spots (Figure 6.2 H1,H2,I1,I2).

In HDSC, low activity levels were seen at day 14, followed by a steep increase at day 21, and a subsequent decrease at day 28 (Figure 6.4 E1, Figure 6.6A). In GDSC, comparable activity levels were observed at day 14 and 21; essentially no activity was seen at day 2, 7 and 28 (Figure 6.4 F1, Figure 6.6A).

Presence of TRAP acitivity

In gelatin, TRAP activity remained at all days at background levels, a situation that was also found for cathepsin K (Figure 6.3 C,D, Figure 6.6B). In NDSC, elevated levels of TRAP was observed at days 2, 7, 14 and 21 (Figure 6.2 D,E,F, Figure 6.6B); the highest levels were seen at days 7 and 21 whereas it was absent at day 28 (Figure 6.6B). This is in contrast with the situation seen for cathepsin K: the highest level was seen at day 21, lower levels at day 14 and 28, background levels at day 7.

In HDSC, high TRAP activity levels were observed at day 14 and 21 (with a maximum at day 21), low levels at day 7 and 28, and a background activity at day 2. This is in contrast with the situation seen for cathepsin K: the highest level was seen at day 21, much lower levels at day 14 and 28, and background levels at day 2 and 7 (Figure 6.4C, Figure 6.6B). In GDSC, high TRAP activity levels were found at days 14 and 21 (with a maximum at day 21); no activity was observed at days 2, 7 and 28. A comparable situation was found for cathepsin K (Figure 6.4D, Figure 6.6B).

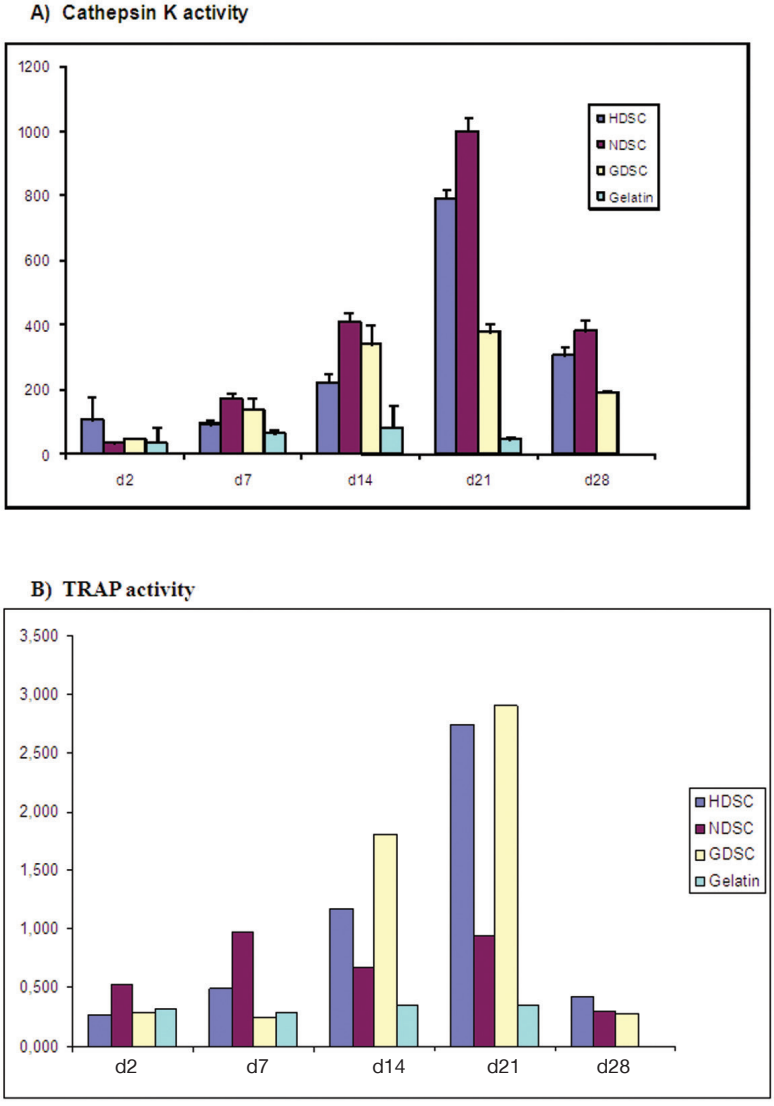

Figure 6.6: Quantitification of cathepsin K activity and TRAP acitivity. A: Cathepsin K activity in the four biomaterials during the time course (n = 3 for each group); B: TRAP activity in the four biomaterials during the time course (n = 1 for each group). Values are depicted as mean ± SEM

Discussion

So far, only matrix metalloproteinases were taken into consideration in the degradation of collagen scaffolds, as well as phagocytosis. This is the first report showing the presence of cathepsin K, a strong collagenolytic enzyme, in the foreign body reaction towards collagen/gelatin implants. However, it is not known if cathepsin K is indeed involved in the degradation of these biomaterials. No cathepsin K could be detected in the gelatin scaffolds, indicating that the enzyme was not involved in the fast degradation of these scaffolds, although cathepsin K is known to exhibit gelatinolytic activity [6]. In GDSC, cathepsin K-positive cells are seen at day 14 and 21; GDSC scaffolds are quickly degraded and it is possible that cathepsin K takes part in this degradation process. On the other hand, the NDSC scaffolds are only marginally degraded after 4 weeks, despite the presence of cathepsin K at various time points. Furthermore, also HDSC scaffolds are hardly degraded after 4 weeks, although numerous cathepsin K-positive cells are seen at day 14 and 21.

Although we cannot conclude from our data that cathepsin K is in certain circumstances indeed involved in the degradation of the collagenous scaffolds, our study obtained some interesting observations.

Firstly, despite comparable numbers of giant cells in the gelatin and NDSC scaffolds at day 14, only the giant cells in the NDSC showed cathepsin K activity. It thus seems that the giant cells in the NDSC scaffolds show a different phenotype than the giant cells in the gelatin scaffold. This is of interest, as this contrasts with the situation seen in the various granulomas: in these soft tissue lesions, almost 100% of the giant cells are cathepsin K positive [17, 20-22]. It is tempting to speculate that the substrate difference (gelatin versus triple helical collagen) provoked the formation of subsets of giant cells with differential phenotypic and functional properties. A comparable situation has been observed in the synovial membrane-like interface tissue seen between the implant and

adjacent bone: the giant cells associated with the polyethylene particles showed a considerable lower cathepsin K expression compared to the giant cells on the bone surface [21]. In one of our studies, we found major differences in the expression of e.g. the chemokines CXCL1 and CXCL2 between giant cells harvested from HDSC or Dacron [31]. Although it is likely that in all these cases the substrate determined the differential phenotype of the giant cells, it cannot be excluded that the differences in the overall micro-environment, or differences in the nature of the precursor cells involved in cell fusion, also have an impact on the final properties of giant cells. For example, different osteoclasts can be obtained *in vitro* by changing culture conditions [32]. In either case, one should take into consideration that giant cells do not form a uniform cell population: considerable differences can occur in functional properties. In this context it is of interest to mention, that osteoclasts from long bones and osteoclasts from the calvarium exhibit different phenotypic properties [33]; and that the biochemical make-up of long bones and the calvarium is substantially different [34].

Secondly, in GDSC, giant cells are only sporadically seen; the many cathepsin K-positive cells in GDSC are thus mononuclear of origin. In granulomas, containing both giant cells and macrophages, the macrophages are normally cathepsin K negative [17-20]. However, cathepsin K-positive mononuclear cells have been reported, namely epithelioid cells (which are highly activated CD68+ cells) [17, 18, 20], dendritic cells [35], macrophages in osteolytic lesions, synovium, carcinomas, giant cell tumors, and atherosclerotic plaques [21, 23, 25, 29, 30, 36, 37], and fibroblast-like cells [22, 25, 38]. Since the macrophages in GDSC are highly involved in the degradation of the collagenous disks, it is possible that part of these cells are in fact epithelioid cells, but this remains to be determined.

In NDSC and HDSC the amount of TRAP activity and cathepsin K activity did not always match. It remains to be investigated if this mismatch is also reflected in protein or gene expression levels. On the other hand, TRAP seems to have a much wider tissue distribution, as it has been reported in a variety of tissues [39-40]. TRAP has also been

found in activated macrophages in soft tissues [41], and seems to be involved in e.g. cytokine production by macrophages [42-44]. A partial uncoupling of cathepsin K and TRAP expression in macrophages or giant cells seems therefore likely.

In summary, we have shown for the first time that cathepsin K and TRAP, two enzymes that are highly expressed in osteoclasts, can also be observed in the foreign body reaction towards cross-linked and non-crosslinked collagen, but not in the foreign body reaction towards gelatin. In the FBR towards non-crosslinked collagen (NDSC) the main cells showing cathepsin K positivity are the multinucleated cells, whereas in the FBR towards glutaraldehyde cross-linked collagen (GDSC) the main cells showing cathepsin K positivity are the mononucleated cells. The giant cells in the FBR towards gelatin or NDSC show different phenotypic properties, as they are cathepsin K negative and cathepsin K positive, respectively. So far, hardly any attention has been paid to the role of giant cell heterogeneity and cathepsin K in the tissue response towards biomaterials; clearly, this field needs to be explored in more detail in order to understand the ins and outs of the foreign body reaction.

References

1. Tezuka K, Tezuka Y, Maejima A, Sato T, Nemoto K, Kamioka H, Hakeda Y, Kumegawa M: Molecular cloning of a possible cysteine proteinase predominantly expressed in osteoclasts. J Biol Chem 1994; 269: 1106-1109.

2. Brömme D, Okamoto K: Human cathepsin O2, a novel cysteine protease highly expressed in osteoclastomas and ovary. Molecular cloning, sequencing and tissue distribution. Biol Chem Hoppe Seyler 1995; 376: 379-384.

3. Inaoka T, Bilbe G, Ishibashi O, Tezuka K, Kumegawa M, Kokubo T: Molecular cloning of human cDNA for capthepsin K: novel cysteine proteinase predominantly expressed in bone. Biochem Biophys Res Commun 1195; 206: 89-96.

4. Shi GP, Chapman HA, Bhairi SM, DeLeeuw C, Reddy VY, Weiss SJ: Molecular cloning of human cathepsin O, a novel endoproteinase and homologue of rabbit OC2. FEBS Lett 1995; 357: 129-134.

5. Li YP, Alexander M, Wucherpfennig AL, Yelick P, Chen W, Stashenko P: Cloning and complete coding sequence of a novel human cathepsin expressed in giant cells of osteoclastomas. J Bone Miner Res 1995; 10: 1197-1202.

6. Brömme D, Okamoto K, Wang BB, Biroc S: Human cathepsin O2, a matrix protein-degrading cysteine protease expressed in osteoclasts. Functional expression of human cathepsin O2 in Spodoptera frugiperda and characterization of the enzyme. J Biol Chem 1996; 271: 2126-2132.

7. Kafienah W, Brömme D, Buttle DJ, Croucher LJ, Hollander AP: Human cathepsin K cleaves native type I and II collagens at the NH2-terminal end of the triple helix. Biochem J 1998; 331: 727-732.

8. Li Z, Hou WS, Brömme D: Collagenolytic activity of cathepsin K is specifically modulated by cartilage-resident chondroitin sulfates. Biochemistry 2000; 39: 529-536.

9. Garnero P, Borel O, Byrjalsen I, Ferreras M, Drake FH, McQueney MS, Foged NT, Delmas PD, Delaissé JM: The collagenolytic activity of cathepsin K is unique among mammalian proteinases. J Biol Chem 1998; 273: 32347-32352.

10. Saftig P, Hunziker E, Wehmeyer O, Jones S, Boyde A, Rommerskirch W, Moritz JD, Schu P & Figura K von: Impaired osteoclastic bone resorption leads to osteopetrosis in cathepsin-K-deficient mice. Proc Natl Acac Sci USA 1998; 95: 13453-13458.

11. Gowen M, Lazner F, Dodds R, Kapadia R, Feild J, Tavaria M, Bertoncello I, Drake F, Zavarselk S, Tellis I, Hertzog P, Debouck C, Kola I: Cathepsin K knockout mice develop osteopetrosis due to a deficit in matrix degradation but not demineralization. J Bone Miner Res 1999; 14: 1654-1663.

12. Gelb BD, Shi GP, Chapman HA, Desnick RJ: Pycnodysostosis, a lysosomal disease caused by cathepsin K deficiency. Science 1996; 273: 1236-1238.

13. Motyckova G, Fischer DE: Pycnodysostosis: role and regulation of cathepsin K in osteoclast function and human disease. Curr Mol Med 2002; 2: 407-421.

14. de Vries TJ, Schoenmaker T, Hooibrink B, Leenen PJM, Everts V: Myeloid blasts are the mouse bone marrow cells prone to differentiate into osteoclasts. J. Leukoc Biol 2009; 85: 919-927.

15. Yagi M, Miyamoto T, Sawatani Y, Iwamoto K, Hosogane N, Fujita N, Morita K, Ninomiya K, Suzuki T, Miyamoto K et al.: DC-STAMP is essential for cell-cell fusion in osteoclasts and foreign body giant cells. J Exp Med 2005; 203: 345-351.

16. Helming L, Gordon S: The molecular basis of macrophage fusion. Immunobiol 2008; 212: 785-793.

17. Bühling F, Reisenauer A, Gerber A, Krüger S, Weber E, Brömme D, Roessner A, Ansorge S, Welte T, Röcken Ch: Cathepsin K – a marker of macrophage differentiation? J Pathol 2001; 195: 375-382.

18. Díaz A, Willis AC, Sim RB: Expression of the proteinase specialized in bone resorption, cathepsin K, in granulomatous inflammation. Molec Med 2000; 6: 648-659.

19. Friedrich RE, Eisenmann J, Röser K, Scheuer HA, Löning T: Expression of proteases in giant cell lesions of the jaws, tendon sheath and salivary glands. Anticancer Res 2010; 30: 1645-1652.

20. Samokhin AO, Bühling F, Theissig F, Brömme D: ApoE-deficient mice on cholate-containing high-fat diet reveal a pathology similar to lung sarcoidosis. Am J Pathol 2010; 176: 1148-1156.

21. Shen Z, Crotti TN, McHugh KP, Matsuzaki K, Gravallese EM, Bierbaum BE, Goldring SR: The role played by cell-substrate interactions in the pathogenesis of osteoclast-mediated peri-implant osteolysis. Arthr Res Ther 2006; 8: R70

22. Mandelin J, Li TF, Hukkanen M, Liljeström M, Salo J, Santavirta S, Konttinen YT: Interface tissue fibroblasts from loose total hip replacement prosthesis produce receptor activator of nuclear factor-κB ligand, osteoprotegerin, and cathepsin K. J Rheuamtol 2005; 32: 713-720

23. Liu B, Yu SF, Li TJ: Multinucleated giant cells in various forms of giant cell containing lesions of the jaws express features of osteoclasts. J Oral Pathol Med 2003; 32: 367-375.

24. Samokhin AO, Wilson S, Nho B, Gracia Lizame ML, Eliseo Musenden OE, Brömme D: Cholate-containing high-fat diet induces the formation of multinucleated giant cells in atherosclerotic plaques of apolipoprotein E-/- mice. Arterioscler Thromb Vasc Biol 2010; 30: 1166-1173.

25. Hou WS, Li W, Keyszer G, Weber E, Levy R, Klein MJ, Gravallese EM, Goldring SR, Brömme D: Comparison of cathepsins K and S expression within the rheumatoid and osteoarthritic synovium. Arthr Rheum 2002; 46: 663-674.

26. Dodds RA, Connor JR, Drake FH, Gowen M: Expression of cathepsin K messenger RNA in giant cells and their precursors in human osteoarthritic synovial tissues. Arthr Rheum 1999; 42: 1588-1593.

27. Gravallese EM, Manning C, Tsay A, Naito A, Pan C, Amento E, Goldring SR: Synovial tissue in rheumatoid arthritis is a source of osteoclast differentiation factor. Arthr Rheum 2000; 43: 250-258.

28. Lindeman JHN, Hanemaaijer R, Mulder A, Dijkstra PDS, Szuhai K, Brömme D, Verheijen JH, Hogendoorn PCW: Cathepsin K is the principal protease in giant cell tumor of bone. Am J Pathol 2004; 165: 593-600.

29. Gaumann A, Hansen T, Köhler HH, Kommoss F, Mann W, Maurer J, Kirkpatrick CJ, Kriegsmann J: The expression of cathepsins in osteoclast-like giant cells of an anaplastic thyroid carcinoma with tracheal perforation. Pathol Res Pract 2001; 197: 257-262.

30. Hansen T, Petrow PK, Gaumann A, Keyszer GM, Otto M, Kirkpatrick CJ, Kriegsmann J: Expression of cysteine proteinases cathepsins B and K and of cysteine proteinase inhibitor cystatin C in giant cell tumor of tendon sheath. Mod Pathol 14: 318-324.

31. Luttikhuizen DT, Dankers PYW, Harmsen MC, van Luyn MJA: Material dependent differences in inflammatory gene expression by giant cells during the foreign body reaction. J Biomed Mater Res 2007; 83: 879-886.

32. Yuasa K, Mori K, Ishikawa H, Sudo A, Uchida A, Ito Y: Characterization of two types of osteoclasts from human peripheral blood monocytes. Biochem Biophys Res Commun 2007; 356: 354-360.

33. Everts V, de Vries TJ, Helfrich MH: Osteoclast heterogeneity: lessons from

osteopetrosis and inflammatory conditions. Biochim Biophys Acta 2009; 1792: 757-765.

34. van den Bos T, Speijer D, Bank RA, Brömme D, Everts V: Differences in matrix composition between calvaria and long bone in mice suggest differences in biomechanical properties and resorption: special emphasis on collagen. Bone 2008; 43: 459-468.

35. Maitra R, Follenzi A, Yaghoobian A, Montagna C, Merlin S, Cannizzo ES, Hardin JA, Cobelli N, Stanley ER, Santambrogio L. Dendritic cell-mediated *in vivo* bone resorption. J Immun 2010; 185: 1485-1491.

36. Barascuk N, Skjøt-Arkil H, Register TC, Larsen L, Byrjalsen I, Christiansen C, Karsdal MA: Human macrophage foam cells degrade atherosclerotic plaques through cathepsin K mediated processes. BMC Cardiovasc Disorders 2010; 10: 19

37. Jaffer FA, Kim DE, Quinti L, Tung CH, Aikawa E, Pamde AN, Kohler RH, Shi GP, Libby P, Weissleder R: Optical visulaization of cathepsin K activity in atherosclerosis with a novel, protease-activatable fluorescence sensor. Circulation 2007; 115: 2292-2298.

38. Neidhardt M, Baraliakos X, Seemayer C, Zelder C, Gay RE, Michel BA, Boehm H, Gay S, Braun J: Expression of cathepsin K and matrix metalloproteinase 1 indicate persistent osteodestructive activity in long-standing ankylosing spondylitis. Ann Rheum Dis 2009; 68; 1334-1339.

39. Hayman AR, Bune AJ, Bradley JR, Rashbass J, Cox TM: Osteoclast tartrate-resistant acid phopshatse (Acp 5): its localization to dendritic cells and diverse murine tissues. J Histochem Cytochem 2000; 48: 219-228.

40. Hayman AR, Macary P, Lehner PJ & Cox TM: Tartrate-resistant acid phosphatase (Acp 5): Identification in diverse human tissues and dendritic cells. J Histochem Cytochem 2001; 49: 675-683.

41. Efstratiadis T, Moss DW: Tartrate-resistant acid phosphatase in human alveolar macrophages. Enzyme 1987; 34: 140-143.

42. Räisänen SR, Halleen J, Parikka V, Väänänen HK: Tartrate-resistant acid phosphatase facilitates hydroxyl radical formation and colocalizes with phagocytosed Staphylococcus aureus in alveolar macrophages. Biochem Biophys Res Commun 2001; 288: 142-150.

43. Räisänen SR, Alatalo SL, Ylipahkala H, Halleen JM, Cassady AI, Hume DA, Väänänen HK: Macrophages overexpressing tartrate-resitatnt acid phosphatase show altered profile of free radical production and enhanced capacity of bacterial killing. Biochem Biophys Res Commun 2005; 331: 120-126.

44. Bune AJ, Hayman AR, Evans MJ, Cox TM: Mice lacking tartrate-resistant acid phosphatase (Acp 5) have diordered macrophage inflammatory responses and reduced clearance of the pathogen, Staphylococcus aureus. Immunology 2001; 102: 103-113.

45. Ye, Q, Harmsen MC, Ren Y, Bank RA: The role of collagen receptors Endo180 and DDR-2 in the foreign body reaction against non-crosslinked collagen and gelatin. Biomaterials 2011; 32 : 1339-1350.

46. Ye Q, Xing Q, Ren Y, Harmsen MC, Bank RA: Endo180 and MT1-MMP are involved in the phagocytosis of collagen scaffolds by macrophages and is regulated by interferon-gamma. European Cells & Materials 2010; 20: 197-209.

47. Ye Q, Harmsen MC, van Luyn MJA, Bank RA: The relationship between collagen scaffold cross-linking agents and neutrophils in the foreign body reaction. Biomaterials 2010; 31: 9192-9201.

48. Ye Q, van Amerogen M, Sandham A, Bank RA, van Luyn MJA, Harmsen MC: Site-specific tissue inhibitor of metalloproteinase-1 governs the matrix metalloproteinases-dependent degradation of crosslinked collagen scaffolds and is correlated with interleukin-10.Journal of Tissue Engineering and Regenerative Medicine, 2011; 5:264-274.

49. Everts V, Korper W, Jansen DC, Steinfort J, Lammerse I, Heera S, Docherty AJP, Beertsen W: Functional heterogeneity of osteoclasts: matrix metalloproteinases participate in osteoclastic resorption of calvarial bone but not resorption of long bone. FASEB J. 1999; 13: 1219-1230.

50. van Noorden CJF, and Frederiks WM: *Enzyme Histochemistry. A Laboratory Manual of Current Methods*. Microscopy Handbooks 26, 1993; Oxford University Press Inc., New York

51. Andersson GN, Marks SC: Tartrate-resistant acid ATPase as a cytochemical marker for osteoclasts. J. Histochem. Cytochem. 1989; 37: 115-117.

CHAPTER 7

Summary and general discussion

The biopolymer collagen is often used as a scaffolding biomaterial in tissue engineering. Like any other biomaterial, the implantation of collagen scaffolds induces a local inflammatory reaction known as a foreign body reaction (FBR). As introduced in **Chapter 1**, the interaction between the scaffold and the local tissue is generally species-, biomaterial-, and implant site-specific. The FBR to collagen scaffolds involves a complex cascade of spatiotemporally regulated and interconnected processes that include cellular infiltration, activation of inflammatory cells, phagocytosis and proteolysis, which ultimately result in the resolution and degradation of the implanted scaffold. Degradation of the collagen scaffold is an important part of the FBR. Ideally, the degradation rate should match the speed of tissue regeneration. There are two major pathways for collagen degradation: (a) phagocytosis of collagen bundles by surrounding inflammatory cells, i.e., macrophages and giant cells (fused macrophages) and (b) enzymatic degradation by secreted enzymes such as matrix metalloproteinases (MMPs). Although several cellular and molecular factors have been shown to be involved in the degradation of collagen, the exact mechanisms are largely unknown. Therefore, a series of experiments was performed to investigate this subject.

In **Chapter 2,** we studied the nature and regulation of MMP-based proteolytic degradation of cross-linked collagen scaffolds in subcutaneous and epicardial implantation sites. Collagen disks were quickly degraded epicardially, whereas degradation was attenuated when the disks were implanted subcutaneously. Our data showed that collagenases and gelatinases were present and that the collagenase MMP-13 and the gelatinase MMP-2 were predominantly in their active forms at both sites. In contrast, the major MMP inhibitor TIMP-1 was only observed in subcutaneous implants, which provides an explanation for why MMP-13 and MMP-2 cannot degrade the collagen scaffold at the subcutaneous implantation site. Remarkably, interleukin 10 (IL-10), a potent inducer of TIMP-1, was also detected and subcutaneously co-localised with giant cells. We surmise that IL-10 suppresses the degradation of implanted collagen scaffolds in the FBR via the regulation of the ratio of MMPs to TIMP-1. This finding indicates that the degradation of collagen scaffolds

can be regulated via the MMP network by modulating the micro-environment, for example, by modulating the expression levels of TIMP-1 and/or IL-10.

In **Chapter 3,** we investigated the fate of dermal sheep collagen disks at a single implantation site (subcutaneous), although the disks were different with respect chemical cross-linkers (glutaraldehyde = GDSC and hexamethylenediisocyanate = HDSC). GDSC was almost completely degraded after 28 days, whereas HDSC remained intact. Major differences in the presence of neutrophils inside the two disks were observed; in GDSC disks, neutrophils were present throughout the FBR, and massive infiltration of neutrophils was observed at day 2 and day 21, which coincided with high levels of IFN-γ and the phagocytosis of collagen bundles by macrophages. In contrast, only minor infiltration occurred at day 2 in HDSC, and no phagocytosis was observed. Degradation of GDSC occurred via collagenolytic activity and phagocytosis by macrophages. IL-13 was only observed in HDSC, which resulted in the formation of giant cells in HDSC. In agreement with **Chapter 2**, the giant cells produced IL-10, which promoted TIMP-1 expression and the subsequent inhibition of collagenolytic activity. We conclude the following: (a) the function of macrophages in mice is largely influenced by differences in the micro-environment, and the nature of the micro-environments was governed by the chemical features of the implanted collagen scaffold itself; and (b) the presence/absence of neutrophils plays a major role in the shaping of this micro-environment (high IFN-γ and low IL-10 levels in GDSC and low IFN-γ and high IL-10 levels in HDSC). This study provides insight into how the scaffold itself can regulate its own micro-environment.

Chapter 4 is a follow-up study to gain further insight into the role of molecular mediators in the micro-environment and, consequently, on phagocytosis in the FBR. As shown in **Chapter 3**, subcutaneously implanted HDSC or GDSC disks in mice incur significantly different degradation rates. Phagocytosis of collagen by macrophages occurred only in GDSC, although comparable numbers of macrophages were observed in HDSC and GDSC. This study aimed to discover the underlying molecular mechanisms of phagocytosis. Our data show that Endo180 was expressed in GDSC alone, which correlated with the expression

of IFN-γ. Endo180 co-localised with MMP-14 on F4/80-positive cells (murine macrophages), which is likely responsible for the phagocytosis in GDSC. *In vitro*, IFN-γ induced the expression of Endo180 and MMP-14 in murine macrophages cultured on type-I collagen (although excessive IFN-γ dampened the expression of Endo180 and MMP-14). Moreover, the expression of Endo180 and MMP-14 induced by IFN-γ was inhibited by IL-10. The differences in the micro-environments of GDSC and HDSC (high IFN-γ and low IL-10 levels in GDSC and low IFN-γ and high IL-10 levels in HDSC) provide an explanation for why the phagocytosis of collagen by macrophages was only observed in GDSC. In summary, we show for the first time that the IFN-γ-dependent co-expression of Endo180 and MMP-14 on macrophages coincides with the phagocytosis of collagen, thereby providing evidence that the mechanism of phagocytosis of collagen by macrophages in the FBR is similar to the mechanism of intracellular collagen degradation by fibroblasts observed under physiological tissue repair conditions. Based on these results, the regulation of the phagocytosis of collagen by macrophages through the regulation of the levels of IFN-γ or IL-10 (counterpart of IFN-γ) may be feasible.

In earlier chapters (**Chapters 2-4**), we investigated the molecular and cellular basis for the degradation of collagen scaffolds modified with chemical cross-linkers; however, little is known about the mechanisms of degradation of non-cross-linked collagen scaffolds *in vivo*. In **Chapter 5**, non-cross-linked dermal sheep collagen (NDSC) and non-cross-linked gelatin (denatured collagen) disks were implanted subcutaneously in mice. Gelatin disks were degraded quickly due to the efficient formation of large giant cells and the presence of MMP-13; the inhibitor TIMP-1 was absent. The DDR-2 receptor was not expressed in the gelatin disks. Endo180 and MMP-14 were expressed, but a lack of co-expression was primarily observed. In contrast, NDSC disks showed a very low rate of degradation despite the presence of high numbers of macrophages and the influx of neutrophils. This was attributed to the presence of the matrix metalloproteinase inhibitor TIMP-1. The limited degradation that occurred was mainly in the later stages of the FBR and could be attributed to (a) phagocytosis by macrophages due to the co-expression of

Endo180 and MMP-14 on these cells (intracellular degradation) and (b) the presence of MMP-13 due to the upregulation of the DDR-2 receptor (extracellular degradation). We conclude that the physical state of collagen (native or denatured) had a strong influence on the degradation rate and provoked a completely different FBR.

With respect to the degradation of collagen scaffolds, all studies (**Chapters 2-5**) focused on the role of matrix metalloproteinases. However, nothing is known about the role of cathepsin K, a strong collagenolytic enzyme, in the FBR. The study in **Chapter 6** reports for the first time that cathepsin K and TRAP, two enzymes that are highly expressed in osteoclasts, are present in the FBR to non-cross-linked collagen (NDSC), glutaraldehyde cross-linked collagen (GDSC) and hexamethylenediisocyanate cross-linked collagen (HDSC), but not in the FBR to denatured collagen (gelatin). Cathepsin K, which was absent, was not involved in the rapid degradation of gelatin. In the FBR to NDSC, the main cells that were positive for cathepsin K were the multinucleated cells, whereas in the FBR to GDSC, the main cells that were positive for cathepsin K were the mononucleated cells. The giant cells in the FBR to gelatin and NDSC showed different phenotypic properties because they were cathepsin K-negative and cathepsin K-positive, respectively. Further investigation is needed to gain further insight into the role of cathepsin K and giant cell heterogeneity in the FBR to the collagen scaffolds.

Taken together, we can conclude the following regarding the degradation of collagen disks in the FBR:

1) Enzymatic degradation of collagen scaffolds

Generally, collagen is degraded via the interplay between collagenases and gelatinases. MMPs are produced and secreted as inactive precursors (proMMP) by inflammatory cells such as macrophages. These cells also produce membrane-bound MMP-14. Together, these MMPs degrade collagen and gelatin to smaller products. This process is inhibited by the binding of, for example, TIMP-1 to MMPs. This thesis (**Chapter 2**) has increased our understanding of the molecular mechanisms and regulation

of the MMP-based proteolytic network in the degradation of collagen disks during the FBR. In the absence of TIMP-1, i.e., in epicardial implants, both collagenases (MMP-13) and gelatinases (MMP-2 and MMP-9) were present as active enzymes and acted sequentially to completely degrade the implanted disk. However, subcutaneously, the elevated expression of TIMP-1 prevented the collagenolytic activity of the various collagenases.

Besides MMPs, little attention has been paid to other proteinases, such as cathepsin K, in the FBR directed against implanted materials. Cathepsin K, a strong collagenolytic enzyme, was reported to be present in giant cells in the FBR to wear debris derived from the gliding surfaces of prostheses used in joint replacements. However, nothing is known about the involvement of cathepsin K in the FBR to collagen scaffolds. In this thesis (**Chapter 6**), we report for the first time the presence of cathepsin K in the FBR to subcutaneous collagen scaffolds in mice. Interestingly, cathepsin K was not present in gelatin (denatured collagen) scaffolds. Although we are unable to draw any conclusions about the precise roles of cathepsin K in the FBR at this stage, our pilot studies show that it is necessary to further explore the involvement of cathepsin K in the degradation of collagen scaffolds.

2) Phagocytosis of collagen scaffolds

In addition to enzymatic degradation, collagen scaffolds can be eliminated by phagocytosis, an intracellular process of collagen degradation. Knowledge has accumulated regarding the mechanisms of the phagocytosis of collagen by fibroblasts under physiological conditions, but virtually nothing is known about whether the inflammatory cells phagocytose fibrillar collagen in the FBR to collagen implants. This thesis shows for the first time that phagocytic cells, such as macrophages and giant cells, play a critical role in the breakdown of collagen scaffolds via phagocytosis.

The phagocytosis of collagen by macrophages was observed in

GDSC scaffolds at day 2 and 21 (**Chapter 3**), as well as in NDSC at day 21 and 28 (**Chapter 5**). Further study (**Chapter 4**) showed that the phagocytosis of collagen correlated with the interplay between the membrane-localised mediators Endo180 and MMP-14. It is logical that collagen phagocytosis by macrophages is achieved by the cleavage of collagen fibrils near the cell membrane via MMP-14 followed by the lysosomal delivery of cleaved collagen. However, in HDSC, there was a different type of macrophage present that did not express Endo180, and therefore, no phagocytic activity was associated with this type of macrophage.

Furthermore, the phagocytosis of collagen by giant cells was also observed in gelatin scaffolds and NDSC (**Chapters 5 and 6**). Interestingly, the presence of giant cells in these two biomaterials

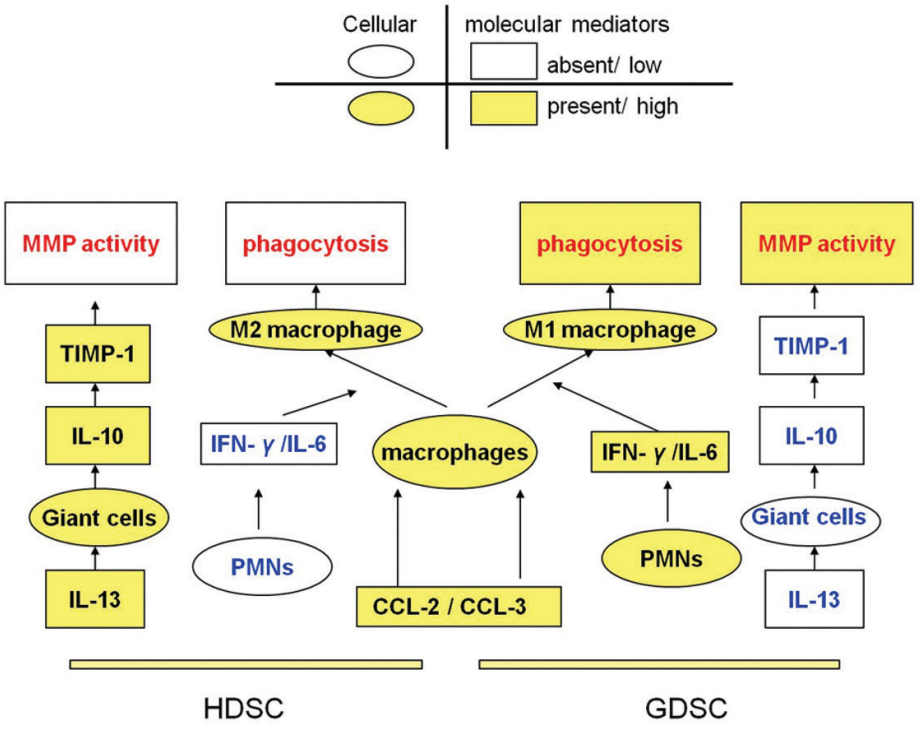

Figure 7.1 Schematic illustration of the different foreign body reactions in HDSC and GDSC

exhibited completely different characteristics. The giant cells in gelatin showed more nuclei and a greater surface area than the giant cells in NDSC. Endo180 and MMP-14 were expressed in both scaffolds; however, their distribution patterns differed. Endo180 and MMP-14 co-localised in NDSC, suggesting that the phagocytosis of collagen by giant cells utilised a comparable mechanism to that which has been observed in fibroblasts. In contrast, Endo180 and MMP-14 were not co-localised in gelatin, indicating that the phagocytosis of collagen by giant cells in gelatin may occur by a different mechanism. Further study is required to understand this process. Furthermore, the giant cells in NDSC were positive for cathepsin K and TRAP, whereas both enzymes were absent in giant cells in gelatin scaffolds. Taken together, our data clearly show two distinct sub-sets of giant cells in terms of size, morphology and biological behaviours during the FBR to non-cross-linked collagen and gelatin scaffolds.

The phagocytosis of collagen in GDSC strongly correlated with the presence of neutrophils (**Chapter 3**), but there is no evidence that neutrophils are directly involved in the phagocytosis of the collagen scaffold. The presence of neutrophils apparently induced the expression of pro-inflammatory cytokines, including IFN-γ, which is a major activator of phagocytosis by macrophages. Therefore, we conclude that neutrophils play a crucial regulatory role in the phagocytosis of collagen by macrophages via IFN-γ

3) Regulation of collagen degradation through changes in the molecular mediators in the FBR micro-environment

Extensive study of the roles of cytokines (IL-1β, IL-4, IL-6, IL-10, IL-13, TNF-α and IFN-γ) and chemokines (CCL-2 and CCL-3) in the regulation of proteolysis and cellular phagocytosis has been conducted in this thesis (**Chapters 2-5**).

We have shown that in proteolysis, the expression of TIMP-1 (a major regulator of MMP activity) depends on the presence of IL-10

(**Chapter 2**). IL-10 in HDSC was mainly produced by giant cells. One of the major mediators that drive the formation giant cells is IL-13, which was highly expressed in HDSC (**Chapter 3**). Interestingly, the collagen receptor DDR-2 contributes to the up-regulation of MMP-13 (**Chapter 5**). These findings provide indications and clues to modulating the enzymatic degradation of collagen scaffolds in future therapies in tissue engineering: a) to reduce the MMP-based enzymatic degradation of collagen by increasing of the expression of IL-10 and/or IL-13 and b) to accelerate enzymatic degradation by stimulating the expression of DDR-2.

Our data also show that the collagen receptor Endo180 is critical for the phagocytosis of collagen by macrophages (**Chapter 3**) and that the expression of Endo180 on macrophages is dependent upon the presence of IFN-γ but not upon the other pro-inflammatory factors such as IL-1β and TNF-α. Interestingly, the induction of Endo180 by IFN-γ can be blocked by IL-10 in a dose-dependent manner (**Chapter 4**). Therefore, IFN-γ produced by neutrophils appears to be the key regulator of the phagocytosis of collagen by macrophages. However, the same may be not true for the phagocytosis of collagen by giant cells in the gelatin scaffold where neutrophils and IFN-γ were virtually absent (**Chapter 5**). This suggests that the phagocytosis of collagen by giant cells in gelatin is regulated by other unknown pathways, which require further investigation.

4) Regulation of collagen degradation by the nature of chemical cross-linking

It is known that the FBR reaction differs between species, biomaterials and implantation sites. Our current studies extend this knowledge and show that the differences in the FBR are due to the different micro-environments created by the different types of implanted collagen scaffolds. A change in the chemical nature of the collagen scaffold, for example by cross-linking the native collagen

with different chemical compounds, causes a completely different FBR (Figure 7.1). A pro-inflammatory micro-environment was created with a glutaraldehyde cross-linker in GDSC, which led to the rapid degradation of the collagen scaffold by enzymatic degradation (due to the absence of TIMP-1 expression as a result of the absence of IL-10-expressing giant cells) and by phagocytosis by macrophages (due to the expression of IFN-γ by neutrophils). In contrast, the hexamethylenediisocyanate cross-linker created an anti-inflammatory micro-environment in HDSC, which blocked enzymatic degradation (due to the over-expression of TIMP-1) and phagocytosis (due to the absence of IFN-γ) (**Chapters 3 and 4**).

5) Regulation of collagen degradation by changing the physical nature of collagen

Our data further show that not only the chemical nature but also the physical status of collagen (native or denatured) has a profound effect on the degradation rate of the scaffold. Non-cross-linked native collagen scaffolds (NDSC) and denatured collagen scaffolds (gelatin) were implanted in mice subcutaneously. Gelatin scaffolds were completely degraded within 3 weeks, whereas only marginal degradation was observed in NDSC after 4 weeks. In contrast with the absence of TIMP-1 in gelatin, the elevated expression of TIMP-1 was observed in the NDSC micro-environment, which may explain the delay in the degradation of the NDSC scaffolds (**Chapter 5**).

Future perspectives

The aim of this thesis was to discover the molecular and cellular mechanisms of degradation of collagen scaffolds in the FBR. Our data have provided several striking findings regarding the nature and regulation of the enzymatic degradation and phagocytosis of collagen scaffolds. IL-10, IL-13, TIMP-1 and DDR-2 have been identified as potential therapeutic factors in the regulation of MMP-based proteolysis in the extracellular enzymatic degradation of collagen. IFN-γ appears to be the optimal activator for the phagocytosis of collagen by macrophages via the up-regulation of MMP-14 and Endo180. This effect can be neutralised by the addition of IL-10. Although our data have expanded our understanding of the regulation of collagen degradation, it is still a long way from concept to clinic. First, to apply these findings to clinical practice, additional laboratory studies with knock-out (of the targeting factor) animal models followed by well-designed randomised controlled clinical trials are needed. Second, the precise mechanisms underlying the phagocytosis of gelatin by giant cells must be considered. Third, further exploration of the role of cathepsin K and giant cell heterogeneity in the FBR to collagen scaffolds is necessary.

Taken together, it is tremendously important to choose an appropriate substrate and design the physical and chemical nature of the scaffolds so that its degradation can be tuned to the rate of tissue regeneration.

CHAPTER 8 / HOOFDSTUK 8

SUMMARY AND GENERAL DISCUSSION (DUTCH)

SAMENVATTING & ALGEMENE DISCUSSIE

De biopolymeer collageen wordt vaak gebruikt als biostellagemateriaal (*scaffold)* bij weefselengineering. Net als bij ieder ander biomateriaal, veroorzaakt de implantatie van collageen *scaffolds* een lokale ontstekingsreactie die bekend staat als "vreemdlichaamreactie" (*foreign body reaction, FBR*). Zoals aangevoerd in **Hoofdstuk 1**, is de interactie tussen de *scaffold* en het lokale weefsel in het algemeen diersoort-, biomateriaal-, en implantatielocatie-specifiek. De vreemdlichaamreactie op collageen *scaffolds* omvat een complexe cascade van spatiotemporeel gereguleerde en onderling verbonden processen waaronder cellulaire infiltratie, activering van ontstekingscellen, fagocytose en proteolyse. Dit resulteert uiteindelijk in de ontbinding en afbraak van de geïmplanteerde *scaffold*. Afbraak van de collageen *scaffold* is een belangrijk onderdeel van de vreemdlichaamreactie. Idealiter komt de afbraaksnelheid overeen met de snelheid van de weefselregeneratie. Er zijn twee belangrijke trajecten voor collageenafbraak: (a) fagocytose van collageenbundels door omliggende ontstekingscellen, oftewel macrofagen en reuscellen (gefuseerde macrofagen) en (b) enzymatische afbraak door uitgescheiden enzymen zoals matrix metalloproteinasen (MMP's). Hoewel verschillende cellulaire en moleculaire factoren betrokken blijken te zijn bij de afbraak van collageen, zijn de exacte mechanismen grotendeels onbekend. Derhalve werd een reeks experimenten uitgevoerd om dit onderwerp te onderzoeken.

In **Hoofdstuk 2**, bestudeerden we de aard en de regulering van op MMP's gebaseerde proteolytische afbraak van gecrosslinkt collageen *scaffolds* in subcutane en epicardiale implantatielocaties. Epicardiale collageenschijven werden snel afgebroken, terwijl de afbraak geremd was wanneer de schijven subcutaan geïmplanteerd waren. De gegevens toonden de aanwezigheid van collagenasen en gelatinasen aan en lieten zien dat zowel de collagenase MMP-13 als de gelatinase MMP-2 overwegend in actieve vorm aanwezig waren op beide locaties. De voornaamste MMP inhibitor TIMP-1 daarentegen, werd alleen waargenomen in subcutane implantaten, hetgeen verklaart waarom MMP-13 en MMP-2 de collageen *scaffold* niet kunnen afbreken op een subcutane implantatielocatie. Opmerkelijk genoeg werd ook interleukine 10 (IL-10), een krachtige inhibitor van TIMP-1, gedetecteerd en subcutaan *geco-lokaliseerd* met

reuscellen. Verwacht wordt dat IL-10 de afbraak van geïmplanteerde collageen *scaffolds* tijdens de vreemdlichaamreactie onderdrukt via regulering van de verhouding tussen MMP's en TIMP-1. Deze bevinding geeft aan dat de afbraak van collageen *scaffolds* gereguleerd kan worden via het MMP netwerk door de micro-omgeving te moduleren, bijvoorbeeld door het expressieniveau van TIMP-1 en/of IL-10 te variëren.

In **Hoofdstuk 3** onderzochten we het lot van schijven dermaal schapencollageen op één enkele implantatielocatie (subcutaan), ofschoon de schijven verschilden ten aanzien van chemische cross-linkers (glutaaraldehyde = GDSC en hexamethyleendiisocyanaat = HDSC). GDSC werd bijna volledig afgebroken binnen 28 dagen, terwijl HDSC intact bleef. Er werden belangrijke verschillen waargenomen wat betreft de aanwezigheid van neutrofielen in de twee schijven; bij GDSC-schijven, waren gedurende de gehele vreemdlichaamreactie neutrofielen aanwezig en werd er massale infiltratie van neutrofielen waargenomen op dag 2 en dag 21. Dit viel samen met hoge gehaltes IFN-γ en fagocytose van collageenbundels door de macrofagen. Bij HDSC-schijven daarentegen, vond slechts geringe infiltratie plaats op dag 2 en werd geen fagocytose waargenomen. Afbraak van GDSC vond plaats via collagenolytische activiteit en fagocytose door macrofagen. IL-13 werd alleen waargenomen bij HDSC, wat resulteerde in de vorming van reuscellen bij HDSC. In overeenstemming met **Hoofdstuk 2**, produceerden de reuscellen IL-10, wat TIMP-1 expressie en de daaropvolgende inhibitie van collagenolytische activiteit bevorderde. De volgende conclusie kan getrokken worden: (a) de functie van macrofagen in muizen wordt grotendeels beïnvloed door verschillen in de micro-omgeving en de aard van de micro-omgeving werd beheerst door de chemische eigenschappen van de geïmplanteerde collageen *scaffold* zelf en (b) de aanwezigheid/afwezigheid van neutrofielen speelt een belangrijke rol bij de vormgeving van deze micro-omgeving (hoge IFN-γ en lage IL-10 niveaus bij GDSC en lage IFN-γ en hoge IL-10 niveaus bij HDSC). Deze studie geeft inzicht in hoe de *scaffold* zelf zijn eigen micro-omgeving kan reguleren.

Hoofdstuk 4 is een vervolgonderzoek om meer inzicht te krijgen in de rol van moleculaire mediatoren in de micro-omgeving en daarmee in fagocytose tijdens de vreemdlichaamreactie. Zoals aangetoond in

Hoofdstuk 3, veroorzaken subcutaan geïmplanteerde HDSC- of GDSC-schijven in muizen significant verschillende afbraaksnelheden. Fagocytose van collageen door macrofagen deed zich alleen voor bij GDSC, hoewel vergelijkbare aantallen macrofagen werden waargenomen bij zowel HDSC als GDSC. Deze studie had als doel de onderliggende moleculaire mechanismen van fagocytose te ontdekken. De gegevens tonen aan dat Endo180 alleen bij GDSC tot expressie kwam, wat correleerde met de expressie van IFN-γ. Endo180 co-lokaliseerde met MMP-14 in F4/80-positieve cellen (murine macrofagen), hetgeen waarschijnlijk verantwoordelijk is voor de fagocytose bij GDSC. *In vitro* induceerde IFN-γ de expressie van Endo180 en MMP-14 in murine macrofagen gekweekt op collageen type I (hoewel excessieve hoeveelheden IFN-γ de expressie van Endo180 en MMP-14 deden afnemen). Bovendien werd de expressie van Endo180 en MMP-14, geïnduceerd door IFN-γ, geremd door IL-10. De verschillen in de micro-omgevingen van GDSC en HDSC (hoge IFN-γ en lage IL-10 niveaus bij GDSC en lage IFN-γ en hoge IL-10 niveaus bij HDSC) vormen een verklaring waarom fagocytose van collageen door macrofagen alleen wordt waargenomen bij GDSC. Samengevat, wordt er voor het eerst aangetoond dat IFN-γ-afhankelijke co-expressie van Endo180 en MMP-14 in macrofagen samenvalt met fagocytose van collageen, en leveren daarmee het bewijs dat het mechanisme van fagocytose van collageen door macrofagen tijdens de vreemdlichaamreactie overeenkomt met het mechanisme van intracellulaire collageenafbraak door fibroblasten, waargenomen onder fysiologische weefselherstel omstandigheden. Gebaseerd op deze resultaten, zou de regulering van fagocytose van collageen door macrofagen door middel van regulering van het IFN-γ of IL-10 niveau (tegenhanger van IFN-γ) mogelijk kunnen zijn.

In eerdere hoofdstukken **(Hoofdstukken 2-4)**, werd de de moleculaire en cellulaire basis voor de afbraak van collageen *scaffolds,* gemodificeerd met chemische cross-linkers onderzocht ; er is echter maar weinig bekend over de mechanismen *in vivo* van de afbraak van niet-gecrosslinkt collageen *scaffolds*. In **Hoofdstuk 5** werden schijven niet-gecrosslinkt dermaal schapencollageen (NDSC) en schijven niet-gecrosslinkt gelatine (gedenatureerd collageen) subcutaan geïmplanteerd in muizen. De

schijven gelatine werden snel afgebroken door de efficiënte vorming van grote reuscellen en de aanwezigheid van MMP-13; de inhibitor TIMP-1 was afwezig. De DDR-2 receptor kwam niet tot expressie bij de gelatineschijven. Endo180 en MMP-14 kwamen tot expressie, maar er werd voornamelijk een gebrek aan co-expressie waargenomen. In tegenstelling tot de gelatineschijven, toonden de NDSC schijven een zeer lage afbraaksnelheid, ondanks de aanwezigheid van grote aantallen macrofagen en de influx van neutrofielen. Dit werd toegeschreven aan de aanwezigheid van de matrix metalloproteinase inhibitor TIMP-1. De beperkte afbraak deed zich vooral in de latere stadia van de vreemdlichaamreactie voor en kon mogelijk worden toegeschreven aan (a) fagocytose door macrofagen vanwege co-expressie van Endo180 en MMP-14 in deze cellen (intracellulaire afbraak) en (b) de aanwezigheid van MMP-13 door de upregulatie van de DDR-2 receptor (extracellulaire degradatie). De conclusie kan getrokken worden dat de fysieke gesteldheid van het collageen (natief of gedenatureerd) een sterke invloed had op de afbraaksnelheid en een geheel verschillende vreemdlichaamreactie uitlokte.

Met betrekking tot de afbraak van collageen *scaffolds*, richtten alle studies (**Hoofdstukken 2-5**) zich op de rol van matrix metalloproteinasen. Er is echter niets bekend over de rol van cathepsine K, een sterk collagenolytische enzym, tijdens de vreemdlichaamreactie. Het onderzoek in **Hoofdstuk 6**, rapporteert voor het eerst dat cathepsine K en TRAP, twee enzymen die sterk tot expressie komen in osteoclasten, aanwezig zijn tijdens de vreemdlichaamreactie op niet-gecrosslinkt collageen (NDSC), glutaaraldehyde gecrosslinkt collageen (GDSC) en hexamethyleendiisocyanaat gecrosslinkt collageen (HDSC), maar niet tijdens de vreemdlichaamreactie op gedenatureerd collageen (gelatine). Cathepsine K, door zijn afwezigheid, was niet betrokken bij de versnelde afbraak van gelatine. Tijdens de vreemdlichaamreactie op NDSC, waren de belangrijkste cathepsine K-positieve cellen meerkernige cellen, terwijl tijdens de vreemdlichaamreactie op GDSC de belangrijkste cathepsine K-positieve cellen, mononucleaire cellen waren. De reuscellen tijdens de vreemdlichaamreactie op gelatine en NDSC toonden verschillende fenotypische eigenschappen, omdat ze respectievelijk cathepsine

K-negatief en cathepsine K-positief waren. Nader onderzoek is nodig om meer inzicht te verkrijgen in de rol van cathepsine K en reuscelheterogeniteit tijdens de vreemdlichaamreactie op collageen *scaffolds*.

Al met al kan het volgende geconcludeerd worden met betrekking tot de afbraak van collageenschijven tijdens de vreemdlichaamreactie:

1) Enzymatische afbraak van collageen scaffolds

In het algemeen, wordt collageen afgebroken via de wisselwerking tussen collagenasen en gelatinasen. MMP's worden geproduceerd en uitgescheiden als inactieve precursoren (pro-MMP) door inflammatoire cellen zoals macrofagen. Deze cellen produceren ook membraangebonden MMP-14. Samen breken deze MMP's collageen en gelatine af tot kleinere producten. Dit proces wordt geremd door de binding van bijvoorbeeld TIMP-1 aan MMP's. Dit proefschrift (**Hoofdstuk 2**) heeft ons begrip van de moleculaire mechanismen en regulering van het op MMP's gebaseerde proteolytische netwerk in de afbraak van collageenschijven tijdens de vreemdlichaamreactie doen toenemen. In afwezigheid van TIMP-1, dat wil zeggen in epicardiale implantaten, waren zowel collagenasen (MMP-13) en gelatinasen (MMP-2 en MMP-9) aanwezig in de vorm van actieve enzymen, die sequentieel optraden om de geïmplanteerde schijf volledig af te breken. Subcutaan echter, verhinderde de verhoogde expressie van TIMP-1 de collagenolytische activiteit van de verschillende collagenasen.

Naast de MMP's, is er weinig aandacht besteed aan andere proteinasen, zoals cathepsine K, in de vreemdlichaamreactie op geïmplanteerde materialen. Naar verluidt was cathepsine K, een sterk collagenolytisch enzym, aanwezig in reuscellen tijdens de vreemdlichaamreactie op slijtageprodukten van glijdende gewrichtsoppervlakken van prothesen die gebruikt worden voor gewrichtsvervanging. Er is echter niets bekend over de betrokkenheid van cathepsine K bij de vreemdlichaamreactie op collageen *scaffolds*. In dit proefschrift (**Hoofdstuk 6**), wordt voor het eerst de

aanwezigheid van cathepsine K tijdens de vreemdlichaamreactie op onderhuidse collageen *scaffolds* in muizen gemeld. Interessant is dat cathepsine K niet aanwezig was bij gelatine (gedenatureerd collageen) *scaffolds*. Het is niet mogelijk om in dit stadium over de exacte rol van cathepsine K tijdens de vreemdlichaamreactie. De pilotstudies tonen aan dat het noodzakelijk is om de betrokkenheid van cathepsine K bij de afbraak van collageen *scaffolds* nader te onderzoeken.

2) Fagocytose van collageen scaffolds

Behalve door enzymatische afbraak kunnen collageen *scaffolds* ook geëlimineerd worden door fagocytose, een intracellulair afbraakproces. Er is kennis opgebouwd met betrekking tot de mechanismen van fagocytose van collageen door fibroblasten onder fysiologische omstandigheden, maar er is vrijwel niets bekend over het fagocyteren van fibrillair collageen door inflammatoire cellen tijdens een vreemdlichaamreactie op collageenimplantaten. Dit proefschrift toont voor het eerst aan dat fagocyterende cellen, zoals macrofagen en reuscellen, een cruciale rol spelen bij de afbraak van collageen *scaffolds* via fagocytose.

Fagocytose van collageen door macrofagen werd zowel bij GDSC *scaffolds* op dag 2 en 21 (**Hoofdstuk 3**), als bij NDSC *scaffolds* op dag 21 en 28 waargenomen (**Hoofdstuk 5**). Nader onderzoek (**Hoofdstuk 4**) liet zien dat fagocytose van collageen gecorreleerd was aan de wisselwerking tussen de membraangebonden mediatoren Endo180 en MMP-14. Het spreekt voor zich dat collageen fagocytose door macrofagen bereikt wordt door de splitsing van collageenfibrillen dichtbij het celmembraan via MMP-14, gevolgd door lysosomale uitscheiding van gekliefd collageen. Bij HDSC echter, was een ander type macrofagen aanwezig die geen expressie van Endo180 vertoonden, waardoor er geen fagocytaire activiteit geassocieerd werd met dit type macrofagen.

Fagocytose van collageen door reuscellen werd tevens

waargenomen bij gelatine *scaffolds* en NDSC (**Hoofdstukken 5 en 6**). Interessant is dat de aanwezigheid van reuscellen in beide biomaterialen totaal verschillende eigenschappen vertoonden. In het geval van gelatine, toonden de reuscellen meer kernen en een groter oppervlak dan de reuscellen bij NDSC. Endo180 en MMP-14 kwamen tot expressie bij beide *scaffolds*; zij het dat hun distributiepatronen verschilden. Endo180 en MMP-14 co-lokaliseerden bij NDSC, hetgeen suggereert dat de fagocytose van collageen door reuscellen een vergelijkbaar mechanisme benutte als dat wat waargenomen is bij fibroblasten. In tegenstelling tot NDSC, waren Endo180 en MMP-14 bij gelatine niet geco-lokaliseerd, wat aangeeft dat fagocytose van collageen door reuscellen bij gelatine mogelijk plaats vindt via een ander mechanisme. Nader onderzoek is vereist om dit proces te begrijpen. Daarnaast waren de reuscellen bij NDSC cathepsine K- en TRAP-positief, terwijl beide enzymen afwezig waren in reuscellen bij gelatine *scaffolds*. Alles bijeen genomen tonen onze gegevens duidelijk twee verschillende sub-sets reuscellen in termen van grootte, morfologie en biologisch gedrag, tijdens de vreemdlichaamreactie op niet-gecrosslinkt collageen en gelatine *scaffolds*.

Fagocytose van collageen bij GDSC was sterk gecorreleerd met de aanwezigheid van neutrofielen (**Hoofdstuk 3**), maar er is geen bewijs dat neutrofielen direct betrokken zijn bij fagocytose van de collageen *scaffold*. Ogenschijnlijk induceerde de aanwezigheid van neutrofielen de expressie van pro-inflammatoire cytokines zoals IFN-γ, een belangrijke activator van fagocytose door macrofagen. Daarom kon de conclusie getrokken worden dat neutrofielen een cruciale regulerende rol spelen in de fagocytose van collageen door macrofagen via IFN-γ.

3) Regulering van collageenafbraak door veranderingen in de moleculaire mediatoren in de micro-omgeving van de vreemdlichaamreactie

In dit proefschrift is uitgebreid onderzoek verricht naar de rol van

cytokines (IL-1β, IL-4, IL-6, IL-10, IL-13, TNF-α en IFN-γ) en chemokines (CCL-2 en CCL-3) in de regulering van proteolyse en cellulaire fagocytose (Hoofdstukken 2-5).

Er is aangetoond dat de expressie van TIMP-1 (een belangrijke regulator van MMP activiteit) tijdens proteolyse, afhankelijk is van de aanwezigheid van IL-10 (**Hoofdstuk 2**). IL-10 werd bij HDSC voornamelijk geproduceerd door reuscellen. Eén van de belangrijkste mediatoren die de vorming van reuscellen stimuleert is IL-13, dat sterk tot expressie kwam bij HDSC (**Hoofdstuk 3**). Interessant is dat de collageenreceptor DDR-2 bijdraagt aan de upregulatie van MMP-13 (**Hoofdstuk 5**). Deze bevindingen leveren aanwijzingen en ideeën op voor het moduleren van de enzymatische afbraak van collageen *scaffolds* in toekomstige weefselengineering-therapieën: a) om de op MMP gebaseerde enzymatische afbraak van collageen te reduceren door de expressie van IL-10 en/of IL-13 te vergroten en b) om de enzymatische afbraak te versnellen door de expressie van DDR-2 te stimuleren.

De onderzochte gegevens tonen eveneens aan dat de collageenreceptor Endo180 essentieel is voor fagocytose van collageen door macrofagen (**Hoofdstuk 3**) en dat de expressie van Endo180 in macrofagen afhankelijk is van de aanwezigheid van IFN-γ maar niet van andere pro-inflammatoire factoren zoals IL-1β en TNF-α. Interessant is dat de inductie van Endo180 door IFN-γ op dosis-afhankelijke wijze geblokkeerd kan worden door IL-10 (**Hoofdstuk 4**). Derhalve lijkt het door neutrofielen geproduceerde IFN-γ de centrale regulator van fagocytose van collageen door macrofagen. Dit zou echter mogelijk niet opgaan voor fagocytose van collageen door reuscellen bij gelatine *scaffolds*, waarbij neutrofielen en IFN-γ vrijwel geheel afwezig waren (**Hoofdstuk 5**). Dit suggereert dat fagocytose van collageen door reuscellen bij gelatine gereguleerd wordt via andere onbekende routes, die nader onderzoek vereisen.

4) Regulering van collageenafbraak door de aard van de chemische crosslinking

Het is bekend dat de vreemdlichaamreactie verschilt tussen diersoorten, biomaterialen en implantatielocaties. Deze huidige onderzoeken breiden deze kennis uit en tonen aan dat de verschillen in vreemdlichaamreacties te wijten zijn aan de verschillende micro-omgevingen die door verschillende soorten geïmplanteerde collageen *scaffolds* gecreëerd worden. Een wijziging in de chemische aard van de collageen *scaffold*, bijvoorbeeld door het crosslinken van natief collageen met verschillende chemische verbindingen, veroorzaakt een geheel andere vreemdlichaamreactie (figuur 7.1). Een pro-inflammatoire micro-omgeving werd gecreëerd met een glutaaraldehyde crosslinker bij GDSC, wat leidde tot een snelle afbraak van de collageen *scaffold* door enzymatische afbraak (dankzij de afwezigheid van TIMP-1 expressie als gevolg van de afwezigheid van reuscellen met IL-10 expressie) en door fagocytose door macrofagen (dankzij de expressie van IFN-γ door neutrofielen). De hexamethyleendiisocyanaat crosslinker daarentegen, creëerde een anti-inflammatoire micro-omgeving bij HDSC, wat enzymatische afbraak (dankzij de over-expressie van TIMP-1) en fagocytose (dankzij de afwezigheid van IFN-γ) blokkeerde (**Hoofdstukken 3 en 4**).

5) Regulering van collageenafbraak door wijziging van de fysieke aard van collageen

De resultaten van deze studie laten verder zien dat niet alleen de chemische aard, maar ook de fysieke gesteldheid van het collageen (natief of gedenatureerd) een diepgaand effect heeft op de afbraaksnelheid van de *scaffold*. Niet-gecrosslinkt natief collageen *scaffolds* (NDSC) en gedenatureerd collageen *scaffolds* (gelatine) werden subcutaan geïmplanteerd in muizen. Gelatine *scaffolds* werden binnen 3 weken volledig afgebroken terwijl na 4 weken slechts marginale afbraak werd waargenomen bij NDSC.

In tegenstelling tot de afwezigheid van TIMP-1 bij gelatine, werd een verhoogde expressie van TIMP-1 waargenomen in de NDSC micro-omgeving, hetgeen de vertraging in de afbraak van de NDSC *scaffolds* kan verklaren (**Hoofdstuk 5**).

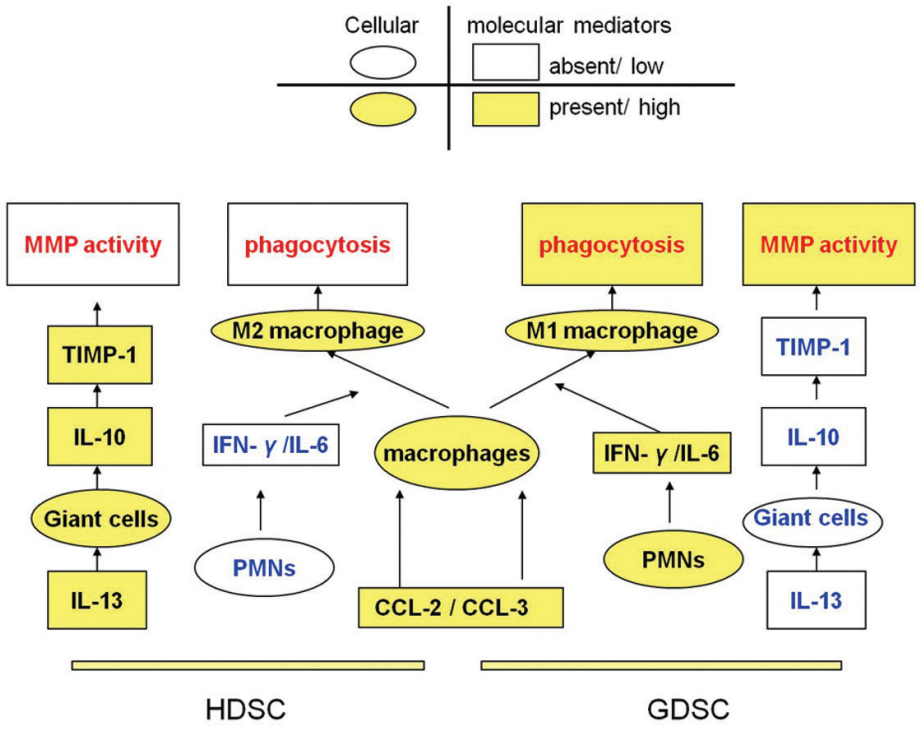

Figuur 7.1 Schematische weergave van de verschillende vreemdlichaamreacties op HDSC en GDSC

Toekomstperspectieven

Het doel van dit proefschrift was om de moleculaire en cellulaire mechanismen van afbraak van collageen *scaffolds* tijdens de vreemdlichaamreactie te ontdekken. Onze gegevens hebben een aantal opmerkelijke bevindingen met betrekking tot de aard en de regulatie van de enzymatische afbraak en fagocytose van collageen *scaffolds* opgeleverd. IL-10, IL-13, TIMP-1 en DDR-2 werden geïdentificeerd als potentiële therapeutische factoren in de regulatie van op MMP's gebaseerde proteolyse in de extracellulaire enzymatische afbraak van collageen. IFN-γ lijkt de optimale activator van fagocytose van collageen door macrofagen via de upregulering van MMP-14 en Endo180. Dit effect kan geneutraliseerd worden door toevoeging van IL-10. Hoewel deze gegevens het begrip van de regulering van collageenafbraak vergroot hebben, is er nog steeds een lange weg te gaan van concept tot kliniek. Om deze bevindingen toe te passen in de klinische praktijk, zijn ten eerste aanvullende laboratoriumonderzoeken met knock-out (van de doelwitfactor) diermodellen, gevolgd door goed opgezette gerandomiseerde gecontroleerde klinische onderzoeken nodig. Ten tweede moeten de precieze mechanismen die ten grondslag liggen aan fagocytose van gelatine door reuscellen overwogen worden. Ten derde is een verdere verkenning van de rol van cathepsine K en reuscelheterogeniteit tijdens de vreemdlichaamreactie op collageen *scaffolds* noodzakelijk.

Alles bij elkaar opgeteld, is het belangrijk om een geschikt substraat te kiezen en de fysische en chemische aard van de *scaffolds* zo te ontwerpen dat hun afbraak kan worden afgestemd op de snelheid van weefselregeneratie.

CHAPTER 9

Summary and general discussion (Chinese)

总结及讨论

在组织工程中，生物大分子胶原被广泛于制造生物支架材料。与其他生物材料一样，这类胶原支架材料的植入会引起局部组织的炎症反应，又称作异物反应(foreign body reaction, FBR)。

第一章主要介绍了支架材料与局部组织之间存在的相互关系，这种关系具有物种，生物材料及植入部位特异性。由胶原支架引起的异物反应是一个时空调控、交互连通复杂的联动 反应，涉及了细胞浸润，炎症细胞活化，以及吞噬作用和蛋白水解作用的激活等，最终导致植入的支架分解和降解。胶原支架的降解构成了异物反应重要的一部分。理想状态下，支架材料的降解速率应与组织的再生速度相匹配。胶原的降解主要有两个途径：一，周围的炎症细胞吞噬胶原束，例如，巨噬细胞和巨细胞（由多个巨噬细胞融合而来）；二，酶降解作用，例如基质金属蛋白酶(matrix metalloproteinases, MMPs)。尽管实验一些细胞及分子已经被证明参与了胶原降解，但是对于降解的确切机制仍缺乏充分的认识。

第二章，在皮下和心外膜植入交联胶原支架，旨在研究基质金属蛋白酶的蛋白水解的本质和调控过程。在心外膜区植入的胶原片降解较快，而皮下植入的胶原片却不完全降解（attenuated）。降解过程中，胶原酶和明胶酶发挥主要作用。其中，胶原酶MMP-13和白明胶酶MMP-2在两个植入区均呈活化的状态。主要基质金属蛋白酶抑制酶(the major MMP inhibitor, TIMP-1)仅出现在皮下植入区，这个现象解释了皮下植入的胶原片的不完全降解。此外，在皮下植入区检测到了主要基质金属蛋白酶抑制酶的诱导物白介素-10(IL-10)，且与巨细胞并存。小结：我们推测白介素-10通过调节基质金属蛋白酶/主要基质金属蛋白酶抑制酶比值（the ratio of MMPs/TIMP-1）来抑制异物反应中胶原支架的降解。此发现表明胶原支架的降解可以通过调节植入物周围的微环境，进而调控基质金属蛋白酶网络，比如，调节主要基质金属蛋白酶抑制酶和/或白介素-10的表达水平。

第三章集中研究了不同的绵羊真皮胶原片在单一植入区（皮下）的归宿。不同的胶原片的区别在于合成时其化学交联方式的不同：戊二醛交联(glutaraldehyde=GDSC)和六亚甲基二异氰酸酯交联(hexamethylenediisocyanate=HDSC)。皮下植入28天后，戊二醛交联的支架材料几乎全部降解，而六亚甲基二异氰酸酯交联的支架完整如初。二者的主要区别在于中性粒细胞出现与否。在戊二醛交联的支架中，伴随异物反应全程可见中性粒细胞。在植入第2天和第21天，支架材料中发现大量中性粒细胞浸润，与此同时γ -干扰素(IFN-γ)呈高表达，巨噬细胞吞噬胶原束活跃。然而，在六亚甲基二异氰酸酯交联的支架

中，仅在植入第2天见少量细胞浸润，未察及巨噬细胞吞噬胶原束的现象。戊二醛交联支架的降解通过胶原溶解和巨噬细胞吞噬来实现。白介素-13(IL-13)只出现在六亚甲基二异氰酸酯交联支架中，前者亦促进了巨细胞的形成。与第二章相呼应，巨细胞分泌白介素-10，后者促进了主要基质金属蛋白酶抑制酶的表达，因此胶原溶解的活性受到了抑制。小结：1.老鼠巨噬细胞的功能很大程度上被微环境的差异所影响，而微环境又受到胶原支架本身化学特性所左右；2.中性粒细胞的存在与否对构建微环境起着重要的作用。本研究揭示了胶原支架调节影响其自身周围微环境的过程。

第四章，进一步深入研究分子调节因子在微环境中扮演的角色，以及在异物反应中对细胞吞噬活动的影响。第三章通过小鼠模型揭示了两种交联支架皮下植入后截然不同的降解速率。尽管两种支架材料中均观察到巨噬细胞的存在，但是只在戊二醛交联支架中观察到巨噬细胞吞噬胶原的现象。因此，本章旨在研究此细胞吞噬背后的分子学机制。我们发现仅戊二醛交联支架中有Endo180表达，后者与γ -干扰素表达相关。在F4/80阳性细胞（鼠巨噬细胞）中，Endo180与基质金属蛋白酶-14共存。F4/80阳性细胞被认为参与介导了戊二醛交联支架的细胞吞噬过程。在对I型胶原培养的鼠巨噬细胞研究中发现γ -干扰素具有诱导Endo180和基质金属蛋白酶-14 的表达（但过量的γ -干扰素消减Endo180和基质金属蛋白酶-14 的表达）。同时，白介素-10具有抑制Endo180和基质金属蛋白酶-14 表达的作用。两种交联方式的支架（戊二醛交联支架和六亚甲基二异氰酸酯交联）具有不同的微环境：戊二醛交联支架形成高γ -干扰素和低白介素-10的微环境，六亚甲基二异氰酸酯交联支架形成相反的微环境。这为胶原的细胞吞噬现象只存在于戊二醛交联的支架中提供了一种解释。小结：本研究首次证实了在巨噬细胞内Endo180与基质金属蛋白酶-14的共表达是γ -干扰素依赖的，且与胶原的细胞吞噬活动相吻合。同时，本文还论证了异物反应中巨噬细胞吞噬胶原的机制与生理状态下机体组织修复时破纤维细胞降解细胞内胶原的机制相似。综上，通过调控γ-干扰素或白介素-10可能可以调节巨噬细胞的胶原吞噬活动。

前述章节（第二-四章）主要从分子和细胞水平介绍了不同化学修饰后胶原支架的降解机理。第五章将对非交联胶原支架在体内的降解机制展开探索。非交联的绵羊真皮胶原片(non-cross-linked dermal sheep collagen, NDSC)和非交联的明胶片（改性胶原）分别植入小鼠皮下。由于有足量巨细胞形成和基质金属蛋白酶-13的表达，且主要基质金属蛋白酶抑制酶的表达缺失，明胶片很快降解。明胶片上没有表达DDR-2受体。Endo180和基质金属蛋白酶-14虽然有表达，但是在植入的

最初期没有观察到二者的同时表达。与此相反的是尽管出现了大量巨噬细胞和中性粒细胞的聚集，非交联的绵羊真皮胶原片只有少量的降解。这应该归因于主要基质金属蛋白酶抑制酶的表达。这有限的降解主要发生在异物反应的后期。究其可能的原因如下：1.由于巨噬细胞通过表达Endo180和基质金属蛋白酶-14而介导细胞吞噬胶原活动，促成了细胞内降解；2.由于上调的DDR-2受体，导致基质金属蛋白酶-13的表达，促成了细胞外降解。小结：胶原自身的状态（天然或者改性）影响着胶原的降解速率，并且决定了截然不同的异物反应。

前文（第二-五章）着重于研究基质金属蛋白酶在胶原支架降解中的作用，第六章转移研究重点到胶原溶解酶方面。组织蛋白酶K (cathepsin K) 和抗酒石酸酸性磷酸酶(tartrate resistant acid phosphatase, TRAP) 在破骨细胞中呈高表达，是强胶原溶解酶。这两个酶存在于非交联胶原，戊二醛交联胶原和六亚甲基二异氰酸酯交联胶原诱导的异物反应中。但这两个酶不存在与改性胶原（明胶）诱导的异物反应中，其中组织蛋白酶K没有参与明胶的快速降解。在非交联胶原诱导的异物反应中，组织蛋白酶K阳性的细胞主要是多核细胞；在戊二醛交联胶原诱导的异物反应中，组织蛋白酶K阳性的细胞主要是单核细胞。在明胶和非交联胶原（即天然和改性非交联胶原）诱导的异物反应中，由于分属组织蛋白酶K阴性和阳性，导致巨细胞呈现不同表型。小结：异物反应中组织蛋白酶K和巨细胞的异质性对胶原支架降解的作用需要进一步深入的研究。

关于异物反应的胶原片降解，总结以下几点：

1）胶原支架的酶降解

一般，胶原的降解通过胶原酶与明胶酶的相互作用来实现。基质金属蛋白酶由炎症细胞，如巨噬细胞，以前体形式(proMMP)分泌形成。该类炎症细胞还合成膜结合蛋白，基质金属蛋白酶-14。这些基质金属蛋白酶将胶原和明胶降解为分子量较小的产物。这一降解过程可因主要基质金属蛋白酶抑制酶与基质金属蛋白酶的结合而遭到抑制。本论文（第二章）主要介绍了异物反应中的胶原片降解的分子机制和基质金属蛋白酶的蛋白水解网络的调节。例如，在心外膜种植体附近，当主要基质金属蛋白酶抑制酶缺失时，胶原溶解酶(MMP-13)和明胶酶(MMP-2和MMP-9)均以活化形式存在，最后胶原植入片发生完全降解。然而在皮下种植体附近，主要基质金属蛋白酶抑制酶呈高表达，广泛的抑制了各种胶原溶解酶的溶解活动。

此外，在排斥种植材料的异物反应中其他蛋白酶受到的重视并不

多。例如，组织蛋白酶K (cathepsin K)，一种强胶原溶解酶。有研究报道该酶存在于异物反应中的巨细胞内，与降解人工关节滑动面摩擦产生的碎屑有关。然而，该酶与异物反应中的胶原支架的关系尚未见研究报道。在本论文中（第六章），首次报道了小鼠皮下植入胶原支架诱导的炎症反应中存在组织蛋白酶K。但是，在明胶植入体（改性胶原）诱导的炎症反应中并未观察到组织蛋白酶K。尽管目前尚不能对组织蛋白酶K在异物炎症反应中扮演的角色给予定论，但是目前的预实验表明组织蛋白酶K在胶原支架降解过程的作用值得进一步深入研究。

2）胶原支架的细胞吞噬

除酶降+解作用之外，胶原支架的降解亦可通过细胞吞噬作用来实现。这是一个胞内降解胶原过程。过去的研究结果已经积累了不少对生理状态下破胶原细胞吞噬胶原现象的认识。然而，在胶原植入物诱导的异物炎症反应中，炎症细胞是否也吞噬纤维状的胶原束目前尚不清楚。在本论文中，首次通过体外实验证实了巨噬细胞和巨细胞的确存在细胞吞噬降解胶原支架的现象。

第三章介绍了在植入戊二醛交联合成的支架材料后第2天和21天，存在巨噬细胞吞噬胶原的证据；第五章研究发现该细胞吞噬作用发生在植入非交联的绵羊真皮胶原片后第21天和28天。第四章通过进一步研究揭示了胶原吞噬作用与位于胞膜调节Endo180 和基质金属蛋白酶-14相互作用相关。巨噬细胞的胶原吞噬作用通过靠近细胞膜的基质金属蛋白酶-14对胶原纤维束进行裂解，紧接着由溶酶体进一步降解。然而，在六亚甲基二异氰酸酯交联胶原诱导的异物炎症反应中，发现另一种巨噬细胞。后者不表达Endo 180，因而此类巨噬细胞没有吞噬胶原的功能。

再者，巨细胞吞噬胶原的现象也发生在明胶支架和非交联胶原支架中，见第五章和第六章。但是，这两种生物材料中的巨细胞表现出截然不同的特性。与非交联胶原诱导产生的巨细胞相比，在明胶支架实验中，巨细胞表现为多核及较大的表面积。两种巨细胞均表达Endo180 和基质金属蛋白酶-14，但分布有所不同。在非交联胶原的巨细胞中，Endo180 和基质金属蛋白酶-14共存，表明该巨细胞吞噬胶原的机制与破胶原细胞的作用机制类似；而在明胶的巨细胞中，Endo180 和基质金属蛋白酶-14(MMP-14)并未共存，表明该巨噬细胞通过其他机制吞噬胶原。对于这一情况，具体的机制还需要进一步研究才能明确。再者，在非交联胶原的巨细胞中，检测到了组织蛋白酶K和抗酒石酸酸性磷酸酶呈阳性表达；在明胶的巨细胞中，两种酶均未查见。总之，我们通过研究证实了巨细胞存在两种亚型。在非交联胶原和明胶诱导的异物炎症反

应中，这两种巨细胞的差异体现在大小，形态和生物学行为方面。

虽然戊二醛交联胶原中的细胞吞噬胶原现象与中性粒细胞的出现呈强相关，但是没有证据证明中性粒细胞与胶原支架的细胞吞噬直接相关。显然，中性粒细胞的出现诱导了炎症因子前体的表达。例如，γ -干扰素，它是巨噬细胞介导的细胞吞噬作用的主要活化剂。因此，我们认为中性粒细胞通过γ -干扰素在巨噬细胞介导的吞噬胶原活动中发挥了重要的调节作用。

3）异物反应微环境中影响胶原降解的分子调节因子

本论文（第二至五章）分析了调控酶降解和细胞吞噬降解的一些细胞因子（白介素-1β，白介素-4，白介素-6，白介素-10，肿瘤坏死因子-α和γ-干扰素）和趋化因子（CCL-2和CCL-3）的作用。

在酶降解过程中，发现主要基质金属蛋白酶抑制酶-1受白介素-10的影响（第二章）。在六亚甲基二异氰酸酯交联胶原诱导的异物反应中，白介素-10主要由巨细胞合成。而巨细胞的形成主要受白介素-13调节诱导。白介素-13 在六亚甲基二异氰酸酯交联胶原中呈高表达（第三章）。胶原受体DDR-2促进了基质金属蛋白酶-13的上调（第五章）。这些发现对于未来组织工程中调节胶原支架的酶降解提供解决方案：1）通过增加白介素-10和/或白介素-13的表达来减少基质金属蛋白酶的酶降解过程；2）通过促进DDR-2的表达加速酶降解。

通过我们的实验证实，胶原受体Endo180是巨噬细胞吞噬胶原的关键（第三章）以及巨噬细胞上Endo180的表达依赖于γ-干扰素。而非其他促炎症反应的细胞因子，如白介素-1β和肿瘤坏死因子-α。有趣的是，γ-干扰素诱导Endo180的反应可以被白介素-10阻断，且这一阻断作用呈剂量-效应关系（第四章）。因此，由中性粒细胞合成的γ-干扰素似乎是巨噬细胞吞噬胶原的关键调节因子。然而，这个机制并不存在于巨细胞吞噬明胶的过程中。因为在这个过程中几乎观察不到中性粒细胞和γ-干扰素的存在（第五章）。中巨细胞吞噬明胶的过程应该是通过其他未知的途径来调节的，这需要进一步的研究。

4）化学交联性质影响胶原降解

异物反应可因不同的物种，生物材料和植入部位而呈现出不同的炎症反应。我们的研究加深了对这一异相性的认识，各种异物反应的差异是由不同类型的植入胶原支架构建的微环境造成的。例如，经不同化合物交联的天然胶原在降解过程中可诱导截然不同的异物反应。戊二醛交

联的胶原支架形成了促炎症反应的微环境，借由酶降解和巨细胞吞噬活动将胶原支架迅速降解。酶降解活动的是由分泌白介素-10的巨细胞的出现和继发的主要基质金属蛋白酶抑制酶-1的表达缺失来实现，而细胞吞噬降解活动的实现归功于中性粒细胞表达的γ-干扰素。

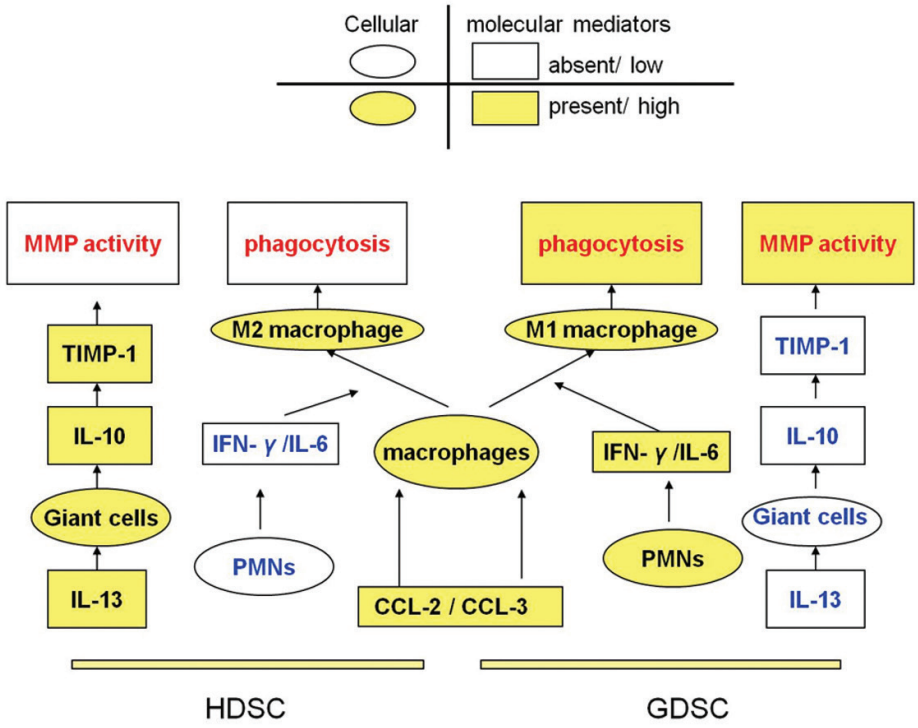

上图：戊二醛交联(GDSC)和六亚甲基二异氰酸酯交联(HDSC)的胶原支架中不同的异物反应简图。

1）胶原物理性质影响胶原降解

我们的研究发现，胶原支架材料的降解速率一方面受其化学性质影响，另一方面受到胶原自身的物理状态（天然或改性）的影响。将改性的胶原（明胶）和非交联胶原支架分别植入小鼠皮下，明胶支架在3周内完全降解，而非交联胶原支架在4周后仅发生边缘降解。在明胶支架中缺失主要基质金属蛋白酶抑制酶的表达，而在非交联胶原支架里可见

该酶的增高表达。这个种植体周围微环境的差异可能可以用来解释非交联胶原支架滞后（或译作：延迟）降解的现象（第五章）。

未来展望

本论文旨在揭示异物反应中胶原支架降解的分子学和细胞学机制。通过一系列发现丰富了对胶原支架的酶降解和细胞吞噬降解的作用机制和调节的认识。白介素-10、白介素-13、主要基质金属蛋白酶抑制酶和DDR-2已被当做为准治疗因子（原文：identified as potential therapeutic factors），以期调节胞外胶原酶降解活动中基质金属蛋白酶的蛋白溶解过程。γ -干扰素似乎可以成为理想的活化物，通过上调基质金属蛋白酶-14和Endo 180来影响巨噬细胞吞噬胶原的活动。γ -干扰素的这个作用可以被过量的白介素-10所中和抵消。尽管本论文对胶原降解的机制有所补充贡献，但是距离将实验结果应用于临床治疗尚远。因此首先，需要一系列动物实验以及接下来的临床随机对照试验。其次，巨细胞吞噬明胶的确切机制尚不明了。最后，组织蛋白酶K的作用和巨细胞的多相性在胶原支架诱导的异物反应中的地位需要进一步实验来明确。

总之，为了更好的匹配组织再生速度，支架材料的降解速度应该可控可调。这对选择支架材料的基质材料，物理化学性质的设计均提出了诸多苛刻要求。

CHAPTER 10

APPENDICES

ACKNOWLEDGEMENT
LIST OF PUBLICATIONS
CURRICULUM VITAE

ACKNOWLEDGEMENTS

The work described in this thesis has been carried out at the Department of Pathology and Medical Biology, University Medical Center Groningen (UMCG), during the years 2006-2010. I would like to express my sincere thanks to the people who have contributed to this thesis in one way or another:

Dear Prof. dr. Yijin Ren, thank you for your enthusiasm, understanding, patience and excellent mentorship throughout the study period in Groningen. Whenever I met a problem, you were always the one who gave me most encouragement and guided me through. I enjoyed every conversation we had and feel myself so lucky to have you as a respectful promoter of my research.

Dear Prof. dr. Ruud Bank, thanks a lot for your inspiration, dedication and mentorship of my scientific research. Though you got involved in the project during the second half of my PhD study, this thesis would not be possible without your generous contribution and I always admire you as a great scientist. I have also been impressed by your frankness in communication.

Dear Prof. dr. Andrew Sandham, thank you for inviting me to Groningen and providing me with the opportunity of doing a PhD at UMCG in January 2006. It has always been inspiring and pleasant to discuss science and practice orthodontics with you. Your enthusiasm and wisdom have had a profound impact on my career development. I am fortunate to have the chance to work together with you.

Sincere thanks also go to Dr. Marco Harmsen and Prof. dr. Marja van Luyn, for their initiation, inspiration and excellent supervision for this

project from 2006 to 2009. Thank you very much!

Prof. dr. Henk Busscher (the former director of Kolff institute) and Prof. dr. Sibrand Poppema (the former dean of UMCG) for providing me with the financial support for my research and living in Groningen for 4 years.

The member of the read committee: Prof. dr. ir. H. Busscher, Prof. dr. G. Molema and Pro.dr. R.R.M. Bos, for your time and expertise in carefully reviewing this manuscript.

Special thanks to my paranimfen: Drs Ee-Soo Lee and Drs Arjen Grotenhuis for your time and great effort in taking care of everything for the promotion.

Special thanks also go to my colleague at James Cook University Mr. Ian Harris for the layout of the thesis. You've done a great job, thanks so much!

I would like to express my greatest appreciation to all my fellow colleagues and good friends at the Medical Biology-Z lab: Post-Docs:Eliane (A/Prof), Paticia, Annemarie, Anna Rita, Jasper B and Barry;The PhD (AIO) team: Ee-Soo, Ewa, Mojtaba, Jan-Renier, Guido, Sander, Diana, Miriam, Nynke, Machteld, Martine, Maike, Caroline; and theTechnical support team: Marja B., Ben, Jasper K, José, Xavier, Lind@ and Martin, Saskia , Ali, Alice, Henriette, Jelle and Roelof-Jan. Thanks you all for your kindness and friendship which have made me feel at home during my stay in the Netherlands.

Mrs. Gea van der Bijl is highly appreciated for the continuous support for my study, clinics and life during my stay in Groningen. Gea, your kindness will never go unnoticed. Thank you very much!

My sincere thanks to Prof. dr. Henny van der Mei (Director of Kolff institute), Ms. Riekje Banus, Ms. Wya Kloppenburg for the solid support in my study and promotie.

All the colleagues at the Department of Orthodonitics, UMCG, University of Groningen for their friendship, hospitality and support during my clinical years.

Deparment of Orthodontics, Sichuan University: Sincere thanks Prof. dr. Zhao Zhihe, Prof dr. Zou Shujuan for establishing the "2+2" collaborative project with UMCG. Although it ended up as a 4 year project in the Netherlands, your kind support to my PhD project will be always remembered. I also appreciate the kind assistance from the staff and postgraduate students in the orthodontics department.

The School of Dentistry at James Cook University: all the staff members for supporting me in coming here for the promotie ceremony and sharing my responsibilities during the period of my absence.

It has been a great pleasure serving as the vice president of the Association of Chinese Students and Scholars in Groningen (ACSSG) and the representative of PhD students at UMCG for two years. I really enjoyed working with the ACSSG team, Ding Ning, Xiang Fei, Weiqi, Zilin, Renxuan and Gao Peng.

My sincere thanks go to my Chinese fellow students: Hongtao, Chunling, Liqiang (aka. Lao-da), Li Jing, Thomas, Jianhua, Zhang Ying, Xing Quan, Xiaoming, Chen Li, Luke, Hongyou, Wuchao, Zilin, He Tao, Xiaoyu, Mei Li, Qu Wenwen……

Sincere thanks also go to my good friends in the Netherlands: Ai-Hong (Lucy), Guojing, Chen-Feng, Arjen, Oleh, Yijun, Jing-kai, Mervyn, Dima, Kirsten and Helen……

I will always be indebted to my dear parents, dear sisters and dear Yan. Thank you for your love, your sacrifice, and for the endless support you have given me. This dissertation is dedicated to all of you.

PUBLICATIONS (2009-2012)

1 **Ye Q**, Harmsen MC, van Luyn MJA, Bank RA. The relationship between collagen scaffold cross-linking agents and neutrophils in the foreign body reaction. ***Biomaterials*** 2010; 31: 9192-9201.

2 **Ye Q**, Harmsen MC, Ren Y, Bank RA. The role of collagen receptors Endo180 and DDR-2 in the foreign body reaction against non-crosslinked collagen and gelatine. ***Biomaterials*** 2011; 32(5):1339-50.

3 **Ye Q**, Xing Q, Ren Y, Harmsen M C, Bank RA. Endo180 and MT1-MMP are involved in the phagocytosis of collagen scaffolds by macrophages and is regulated by interferon-gamma. **European *Cells and Materials*** 2010; 20: 197-209.

4 **Ye Q**, van Amerogen M, Sandham A, Bank R A, van Luyn M J A, Harmsen M C. Site-specific tissue inhibitor of metalloproteinase-1 governs the matrix metalloproteinases-dependent degradation of crosslinked collagen scaffolds and is correlated with interleukin-10. ***Journal of Tissue Engineering and Regenerative Medicine*** 2011; 5:264-274.

5 Xing Q*, **Ye Q***, Fan M, Zhou Y. (* Co-first author) Porphyromonas gingivalis Lipopolysaccharide inhibits osteoblastic differentiation in preosteoblasts via activating Notch1 signaling. ***Journal of Cellular Physiology*** 2010; 225(1): 106-114..

6 Xing Q, de Vos P, Faas MM, **Ye Q**, Ren Y. LPS promotes pre-osteoclast activity by up-regulating CXCR4 via TLR-4. ***Journal of Dental Research*** 2011; 90(2): 157-162.

7 Li F, Hu H, Chen J, Liu Z, Li G, He S, Zou S, **Ye Q**. Comparison of anchorage capacity between implant and headgear during anterior segment retraction. ***Angle Orthodontist*** 2011; 81(5):915-22.

8 Meng B,Chen J,Guo D,**Ye Q**, Liang X. The effect of titanium particles on rat bone marrow stem cells in vitro. ***Toxicology Mechanisms and Methods*** 2009, 1537-6524, 19(9):552 – 558.

9 Dvortsin D.P *,**Ye Q***, Pruim G. J., Dijkstra P.U.,Ren Y. (*Co-first author) Reliability of the intergrated radiograph-photograph method to obtain natural head position in cephalometric diagnosis. ***Angle Orthodontist*** 2011; 81(5):889-94.

10 Guo J, Li C, Zhang Q, Wu G, Deacon SA, Chen J, Hu H, Zou S, **Ye Q**. Secondary bone grafting for alveolar cleft in children with cleft lip or cleft lip and palate. ***Cochrane Database of Systematic Review*** 2011, Issue 6. Art. No.: CD008050. DOI: 10.1002/14651858.CD008050.pub2.

11 Xie H, Wan B, **Ye Q**, Wan C, Li L. Application of K/Sr co-doped calcium polyphosphoate boceramics as a scaffold for bone substitute. ***J Mater Sci Mater Med***. 2012; 23(4):1033-44.

CURRICULUM VITAE

Dr. Qingsong (Adam) Ye was born on March 7th, 1981 in Linhai, China. He obtained his bachelor (BDS) degree and the first orthodontic postgraduate training (2006) at West China College of Stomatology, followed by PhD study at the stem cell and tissue engineering research group and orthodontic department ,University Medical Centre Groningen, the Netherlands. In 2009, Dr. Ye received his first PhD degree in Orthodontics after completing a joint clinic research project between the Orthodontic departments of Sichuan University and University of Groningen. Dr. Ye has also succeeded in the diploma examination for the Membership in Orthodontics, Royal College of Surgeons of Edinburgh, UK.

Dr. Ye is an active scientist in the medical/oral biology field. He has published over 30 original scientific papers and review articles in various dental and medical journals. He also serves as an Associate Editor to the Journal of World Federation of Orthodontists, and as a reviewer for many leading biomedical journals such as Biomaterials, eCM Journal, Journal of Tissue Engineering and Regenerative Medicine, Biotechnology Progress, Australian Orthodontic Journal.etc. Dr. Ye has been invited to give numerous speeches at international conferences. Dr. Ye is also actively involved in the international society of Orthodontic specialists. He is a fellow of World Federation of Orthodontists, an international member of the American Association of Orthodontists, a member of the European Orthodontic Society, a member of the Chinese Orthodontic Society, a member of New Zealand Association of Orthodontics and an Executive member of the Australian Begg Orthodontic Society.

Dr. Ye has worked at the Dental School of James Cook University since October 2010 and is currently appointed as Associate Professor and the coordinator for the Orthodontic postgraduate program (D.Clin.Dent. Orthodontics). Dr. Ye is a grant referee for the Australian Research Council and has been awarded $460,000 in research grants since 2011.

NOTES